FINAL REPORT

Project I

March 2020

Freeway Management for Optimal Reliability

Dr. Jorge Laval | Georgia Institute of Technology

Dr. Nagui M. Rouphail | North Carolina State University

Dr. Rod Turochy | Auburn University

Dr. Yafeng Yin | University of Michigan

STRIDE | Southeastern Transportation Research, Innovation, Development and Education Center

UF | Transportation Institute UNIVERSITY of FLORIDA

TECHNICAL REPORT DOCUMENTATION PAGE

1. Report No. Project I	2. Government Accession No.	3. Recipient's Catalog No.
4. Title and Subtitle Freeway Management for Optimal Reliability		**5. Report Date** March 2020 **6. Performing Organization Code**
7. Author(s) Dr. Jorge Laval, Ph.D., Georgia Institute of Technology Dr. Nagui M. Rouphail, Ph. D., North Carolina State University Dr. Rod Turochy, Ph.D., Auburn University Dr. Yafeng Yin, Ph.D., University of Michigan		**8. Performing Organization Report No.** STRIDE Project I
9. Performing Organization Name and Address **Georgia Institute of Technology** 790 Atlantic Drive Atlanta, GA 30332 **North Carolina State University** 2501 Stinson Drive Raleigh, NC 27695 **Auburn University** 202 Ramsay Hall Auburn, AL36849 **University of Michigan** 2350 Hayward, 2120 GG Brown Ann Arbor, MI 48109		**10. Work Unit No.** **11. Contract or Grant No.** Funding Agreement Number 69A3551747104
12. Sponsoring Agency Name and Address University of Florida Transportation Institute Southeastern Transportation Research, Innovation, Development & Education Center 365 Weil Hall, P.O. Box 116580 Gainesville, FL 32611 U.S Department of Transportation/Office of Research, Development & Tech 1200 New Jersey Avenue, SE Washington, DC 20590 United States		**13. Type of Report and Period Covered** 01/19/2017 to 3/5/2020 **14. Sponsoring Agency Code**

15. Supplementary Notes

16. Abstract

Improving travel time reliability is at the core of battling traffic congestion. This report summarizes the findings from a multi-institutional effort for analyzing and improving freeway travel time reliability. It first investigates the effect of incidents on freeway segment capacity, enabling the calibration and validation of the emergent travel time distribution for a baseline condition of a freeway facility using the Highway Capacity Manual approach. The report then develops a unified framework for assessing the freeway travel time reliability, and then it proposes a new strategy of controlling the headways of cooperative connected vehicles to improve travel time reliability. It also presents a prototype micro-level simulation application, GTsim, which analyzes freeway network performance under various types of Active Traffic Management (ATM) strategies, including those aiming to improve travel time reliability. Lastly, the report reviews the safety benefits of ATM strategies.

17. Key Words	18. Distribution Statement		
Reliability; travel time distribution; active traffic management	No restrictions		
19. Security Classif. (of this report)	**20. Security Classif. (of this page)**	**21. No. of Pages** 124 pages	**22. Price**

Form DOT F 1700.7 (8-72) Reproduction of completed page authorized

DISCLAIMER

The contents of this report reflect the views of the authors, who are responsible for the facts and the accuracy of the information presented herein. This document is disseminated in the interest of information exchange. The report is funded, partially or entirely, by a grant from the U.S. Department of Transportation's University Transportation Centers Program. However, the U.S. Government assumes no liability for the contents or use thereof.

ACKNOWLEDGEMENT OF SPONSORSHIP AND STAKEHOLDERS

This work was sponsored by a contract from the Southeastern Transportation Research, Innovation, Development and Education Center (STRIDE), a Regional University Transportation Center sponsored by a grant from the U.S. Department of Transportation's University Transportation Centers Program.

Funding Agreement Number - 69A3551747104

LIST OF AUTHORS

Co-Principle Investigators:

Jorge Laval, Ph.D.
Georgia Institute of Technology
jorge.laval@ce.gatech.edu
ORCID 0000-0002-0986-4046

Nagui M. Rouphail, Ph.D.
North Carolina State University
rouphail@ncsu.edu
ORCID 0000-0002-2420-9517

Rod Turochy, Ph.D.
Auburn University
rodturochy@auburn.edu
ORCID 0000-0003-2294-7388

Yafeng Yin, Ph.D.
University of Michigan
yafeng@umich.edu
ORCID 0000-0003-3117-5463

Additional Researchers

Behzad Aghdashi, Ph.D.
North Carolina State University

Toru Seo, Ph.D.
University of Michigan

Mohammadali Shirazi, Ph.D.
University of Michigan

Tu Xu
Georgia Institute of Technology

TABLE OF CONTENTS

LIST OF FIGURES

LIST OF TABLES

ABSTRACT

Improving travel time reliability is at the core of battling traffic congestion. This report summarizes the findings from a multi-institutional effort for analyzing and improving freeway travel time reliability. It first investigates the effect of incidents on freeway segment capacity, enabling the calibration and validation of the emergent travel time distribution for a baseline condition of a freeway facility using the Highway Capacity Manual approach. The report then develops a unified framework for assessing the freeway travel time reliability, and then it proposes a new strategy of controlling the headways of cooperative connected vehicles to improve travel time reliability. It also presents a prototype micro-level simulation application, GTsim, which analyzes freeway network performance under various types of Active Traffic Management (ATM) strategies, including those aiming to improve travel time reliability. Lastly, the report reviews the safety benefits of ATM strategies.

Keywords: reliability, travel time distribution, active traffic management

EXECUTIVE SUMMARY

Maximizing reliability on freeways is very important given the economic impact of freeways to freight logistics as well as the time value for individual travelers. Quite a few active traffic management (ATM) strategies have been proposed to improve freeway reliability. These strategies include adaptive ramp metering, integrated ramp-metering and variable speed limit control, hard shoulder running, speed harmonization, dynamic pricing of express lanes, optimized traffic diversions and efficient incident response and management. However, there is a need to further enhance our capability of analyzing and optimizing these strategies to meet reliability goals.

This report represents a step in bridging this gap by a multi-institutional collaborative effort. We first investigated the effect of incidents on freeway segment capacity. The main objective was to develop methods to enable the calibration and validation of the emergent travel time distribution for a baseline condition of a freeway facility, using existing probe data sources. Currently, the Highway Capacity Manual provides a lookup table linking the remaining segment capacity fraction during an incident to the total and closed number of lanes on the segment. In reality, segment capacity during an incident will tend to vary over time, with the most severe effects felt early on before any type of response is initiated, with congestion progressively improving as the appropriate incident management actions are implemented. A portion of WB I-540 in Raleigh, NC, was selected as the study area. By applying a genetic algorithm calibration method on each incident day and calibrating the incident Capacity Adjustment Factors (CAFs), optimal time-dependent CAFs were derived that best represented the impact of incidents on the freeway segment capacity. By analyzing the optimal CAFs, the strongest relationship was revealed to be between the optimal time-dependent CAF and the temporal progression of the incident.

We further developed a unified framework based on a Lagrangian formulation of traffic flow model for assessing the freeway travel time reliability. We further suggested a control strategy, leveraging the connected vehicle technology to improve travel time reliability. This strategy controls the headways of cooperative connected vehicles. The effectiveness of the new strategy, as well as the conventional methods, was investigated by the proposed framework. It was found that the new strategy outperforms the conventional ones, even if the level of market penetration of cooperative connected vehicles is moderate. The potential impacts of this work are twofold. First, the proposed reliability assessment framework can be used to evaluate various ATM control strategies. Second, the proposed strategy is promising and can be implemented in the near future when connected vehicles are widely used. Still, one open question is how we can recruit drivers for such a participatory traffic control. We leave this question for future research.

In this study, we also investigated dynamic traffic assignment and enhanced a micro-level simulation application, GTsim. The ultimate goal of this effort is to offer a simulation-based platform, in contrast to the analytical approach, to conduct comprehensive analyses of the impacts of various ATM strategies on freeway reliability. Lastly, we also investigated the safety benefits of ATM strategies, given a lack of research regarding the specific safety effects of implementing these strategies.

1. INTRODUCTION

1.0. OBJECTIVE

Recent statistics show that while interstate miles constitute less than 1.6% of overall national road miles, they serve over 25% of the nation's total Vehicle Mile Traveled (VMT). More importantly, over 40% of all truck VMT is made on the Interstate highway system. While overall truck VMT comprises about 9% of total VMT, they are disproportionately represented on the freeway system at about 15.3%. These statistics, combined with the economic impacts of freight logistics and the time value of individual travelers, represent the importance of maximizing reliability on freeways.

Quite a few Active Traffic Management (ATM) strategies have been proposed to improve the freeway reliability. These strategies include adaptive ramp metering, integrated ramp-metering and variable speed limit control, hard shoulder running, speed harmonization, dynamic pricing of express lanes, optimized traffic diversions and efficient incident response and management. However, there is a lack of a systematic approach to analyze and optimize these strategies to meet reliability goals.

This project represents a step in enhancing our capability of analyzing and improving freeway travel time reliability. In this project, we investigate both analytical and simulation approaches to assess travel time reliability and develop strategies to further improve freeway travel time reliability.

1.1. SCOPE

This study is divided into four major portions.

The goal of the first portion of the study is to improve the freeway facility reliability method in the Highway Capacity Manual (HCM) and accompanying software, FREEVAL. One clear deficiency is the use of simple, untested, and uncalibrated capacity adjustment factors for incidents, which have not been evaluated for more than 30 years. Towards that goal, the main objective is to develop methods to enable the calibration and validation of the emergent travel time distribution for a baseline condition of a freeway facility using existing probe data sources. The second objective of the study is to provide background on the existing HCM methodology for calibration of capacity adjustment factors and compare and contrast this framework with a newly proposed calibration scheme; in particular, the new calibration allows for time-dependent estimation of capacity adjustment factors that mimic the process of incident occurrence and clearance in the field. The first portion is led by Professor ***Nagui Rouphail*** from North Carolina State University. The research findings are documented in Chapter 2.

The objectives of the second part of the study include (1) developing a unifying framework to assess the travel time reliability of the control strategies; and (2) investigating a new and modern scheme that improves the travel time reliability. This work is led by Professor ***Yafeng Yin*** from University of Michigan, and Chapter 3

documents the major findings. The unified framework is constructed upon a Lagrangian formulation of traffic flow model, and the new strategy for improving travel time reliability is via real-time control of the headways of cooperative connected vehicles.

The third part of the study aims to offer a simulation-based approach for assessing travel time reliability. This work is led by Professor ***Jorge Laval*** from Georgia Institute of Technology. Chapter 4 represents an early attempt towards this objective. A micro-level simulation application, GTsim, is developed to conduct simulation-based dynamic traffic assignment to analyze freeway system performance under various ATM strategies.

Lastly, there is limited research regarding the specific safety effects of implementing ATM strategies. A factor may be a lack of uniformity of how ATM strategies are used in many cases, and many of these methods are not commonplace in the United States. The objective of the fourth portion of the study, led by Professor ***Rod Turochy*** from Auburn University, is to review the safety benefits of ATM strategies. The literature review is documented in Chapter 5.

2. Calibration of Speed/ Travel Time Effects of Freeway Incidents

2.0. Introduction

The HCM is a widely used reference material in the United States for the operational analysis of transportation systems (Transportation Research Board 2016). The sixth edition of the HCM (HCM6) offers a new set of methodologies to account for the impact of non-recurring sources of congestion. There are three basic stochastic events that may affect travel time, namely (a) variability in traffic demand, (b) inclement weather events, and (c) incidents (Schroeder et al. 2013). Traffic demand level is not fixed and changes over time which results in variations in travel time. Similarly, inclement weather events are probabilistic events that result in drops in both free flow speed (FFS) and capacity of a roadway and consequently in travel time (Schroeder et al. 2013). Weather events that are considered in freeway travel time reliability analysis are taken from the HCM 2010 (Chase et al. 2013). Their impact on travel times is evaluated and reported as a series of reliability performance measures. Incidents are one of the most frequent and most impactful contributors to unreliable travel times on freeways. Their stochastic nature and unpredictability add to the complexity of modeling and measuring their impact on freeway travel times.

There is no clear-cut definition of incidents in the transportation literature. The Traffic Incident Management Handbook defines incidents as “any non-recurring event that causes a reduction of roadway capacity or an abnormal increase in demand” (Farradyne 2000). This definition classifies special non-recurring events (such as work zones or sports matches) as incidents. The HCM defines them as “any occurrence on a roadway that impedes normal traffic flow” (Transportation Research Board 2016). Finally, the Traffic Management Data Dictionary defines an incident as “an unplanned randomly occurring traffic event that adversely affects normal traffic operations” (Institute of Transportation Engineers, Undated). While these three definitions are similar, they do not exactly reflect the incident definition used in this study. We define an incident as an unscheduled and randomly occurring event that impedes normal traffic flow. This can result in the shoulder or some lane closures due to vehicle breakdowns, crashes, presence of disabled, stopped, or pulled-over vehicles on the roadway or on the shoulder, and the presence of debris on the roadway or on the shoulder. In addition, five incident severities are defined in the HCM as follows: a) shoulder closure, b) one lane closure, c) two lanes closure, d) three lanes closure, and e) four or more lanes closure.

HCM6 provides a lookup table to estimate the impact of an incident on the freeway segment capacity. Exhibit 11-23 of the sixth edition of HCM gives the Capacity Adjustment Factors (CAFs) for the *remaining open lanes* on freeway segments experiencing incidents (Transportation Research Board 2016), as depicted in Table 2-1 below. The closed lane capacity loss is not captured in these CAFs. As an example, for a freeway segment with three lanes, the overall capacity adjustment for a single lane closure incident would be $(⅔) \times 0.74=0.49$.

TABLE 2-1: CAFS BY INCIDENT TYPE AND NUMBER OF DIRECTIONAL LANES ON THE FACILITY

Directional Lanes	No Incident	Shoulder Closed	1 Lane Closed	2 Lanes Closed	3 Lanes Closed	4 Lanes Closed
2	1.00	0.81	0.70	N/A	N/A	N/A
3	1.00	0.83	0.74	0.51	N/A	N/A
4	1.00	0.85	0.77	0.50	0.52	N/A
5	1.00	0.87	0.81	0.67	0.50	0.50
6	1.00	0.89	0.85	0.75	0.52	0.52
7	1.00	0.91	0.88	0.80	0.63	0.63
8	1.00	0.93	0.89	0.84	0.66	0.66

Source: HCM6 Exhibit 11-23 (Zeeger et. al 2014)

As seen in Table 2-1, the incident's impact on capacity is assumed to be a fixed value throughout the duration of the incident. The only reported sensitivity of the incident capacity models in the HCM is to the “original” and “remaining open” lanes. Many real-world observations have resulted in disputing this capacity reduction model (North Carolina Department of Transportation – TIMS 2019). Most incidents follow a natural evolution from start to clearance, which is not accounted in the HCM models. This paper investigates this process and proposes a time-dependent adjustment factor consistent with field observations. Our investigation shows a significant relationship between the capacity impact of an incident and its evolution over time. The results of this research are incorporated in the unpublished version of FREEVAL software, the official computational engine for freeway facilities method in the HCM (Transportation Research Board 2016, Hall et al. 2000).

Following the introductory section, this chapter is organized as follows:1) we cover the relevant literature and cite the main contribution of this work to the state of practice and research; 2) the methodology employed is then presented followed by a discussion on how the data collection and model development took place; and 3)the updated models along with their implementation in a case study to demonstrate their impact on freeway capacity and reliability analyses are shown.

2.1. Literature Summary

2.1.1. Capacity Impact of Incidents

Recent federal rulemakings published by the Federal Highway Administration (FHWA) proposed that reliability performance measures be used as a basis for federal funding prioritization of road projects (Federal Register 2016), thus requiring a proper tool to simulate and evaluate this metric. The main source for evaluating the effects of both recurring and non-recurring congestion traffic remains the HCM6. The methodology is outlined in Chapter 11 of the HCM (Transportation Research Board 2016) and relies on Chapter 10 for facility-wide evaluation and Chapters 12 through 14 for a detailed segment by segment level assessment. The basis for these methods is the hydrodynamic theory of traffic,

often used numerically to approximate operational capabilities of freeway facilities (Transportation Research Board 2016, Daganzo 1994, and Daganzo 1995). HCM's travel time reliability method utilizes a deterministic model to measure the impact of non-recurring sources of congestion (Transportation Research Board 2016, Schroeder et al. 2013). The metrics of impact are represented by capacity adjustment factors (CAFs) for different severity incident types (Transportation Research Board 2016).

In the HCM's Travel Time Reliability analyses, the incident probabilities correspond to the fraction of time over a given month that an incident severity ranging from a shoulder closure and up to four lane closures is active anywhere along the freeway facility (Aghdashi et al. 2013). There has been extensive research on investigating the incident characteristics that are modeled within the HCM's reliability context.

Several agencies have tested the travel time reliability method on a number of facilities (Williges et al. 2014, Sobolewski et al. 2014, Hadi et al. 2014, Nisbet et al. 2014, and Karmakar et al. 2018). A study in North Carolina modeled three routes on I-40 in the Raleigh-Durham area and predicted the travel time indices (TTIs) reported by HCM modeling within the 80th percentile of true probe-based data (Karmakar et al. 2018). A major drawback of the HCM methods was that traffic demands were assumed to not be impacted by the occurrence of major incidents, in the process generating a longer tail of the travel time distribution than was warranted based on empirical observations.

Work by Samander and others investigated the use of reliability scenario generation in the HCM with respect to weather and incident cases (Samander et al. 2019). The scenario generation was validated under three data environments: 1) data-poor; 2) -moderate; and 3) -rich situations. The number of events in data-poor scenarios was wildly overestimated for both incident and weather-related cases. However, using site-specific data improved the generation of incidents to within 5% of the available empirical data.

In the current literature, the impact of incidents on capacity is only a function of the number of lanes closed and the total number of lanes available where incidents occur (see Table 2-1), in addition to the duration of the incident itself. This study investigates the capacity impact of incidents on freeway facilities considering all available influential factors. The main objective of this research is to update the HCM models to account for the incidents evolutionary impact on freeway capacity.

2.1.2. Freeway Facility Model Calibration

Calibration plays a crucial role in any traffic simulation (PTV Group 2019, Caliper 2019). HCM provides guidelines for calibrating freeway facilities; the flowchart in Figure 2-1 below shows the traditional steps in calibration, outlined in Exhibit 25-

26 of the HCM (Transportation Research Board 2016). It first starts with calibrating the free flow speed (FFS). The bottleneck segment is then identified through empirical observations and its capacity modified manually until its predicted performance measure matches actual traffic conditions. The manual approach towards calibration is time-consuming, does not guarantee the optimal adjustments to the speed and capacity and has strictly focused on (recurring) bottleneck calibration to the detriment of incident capacity modifications.

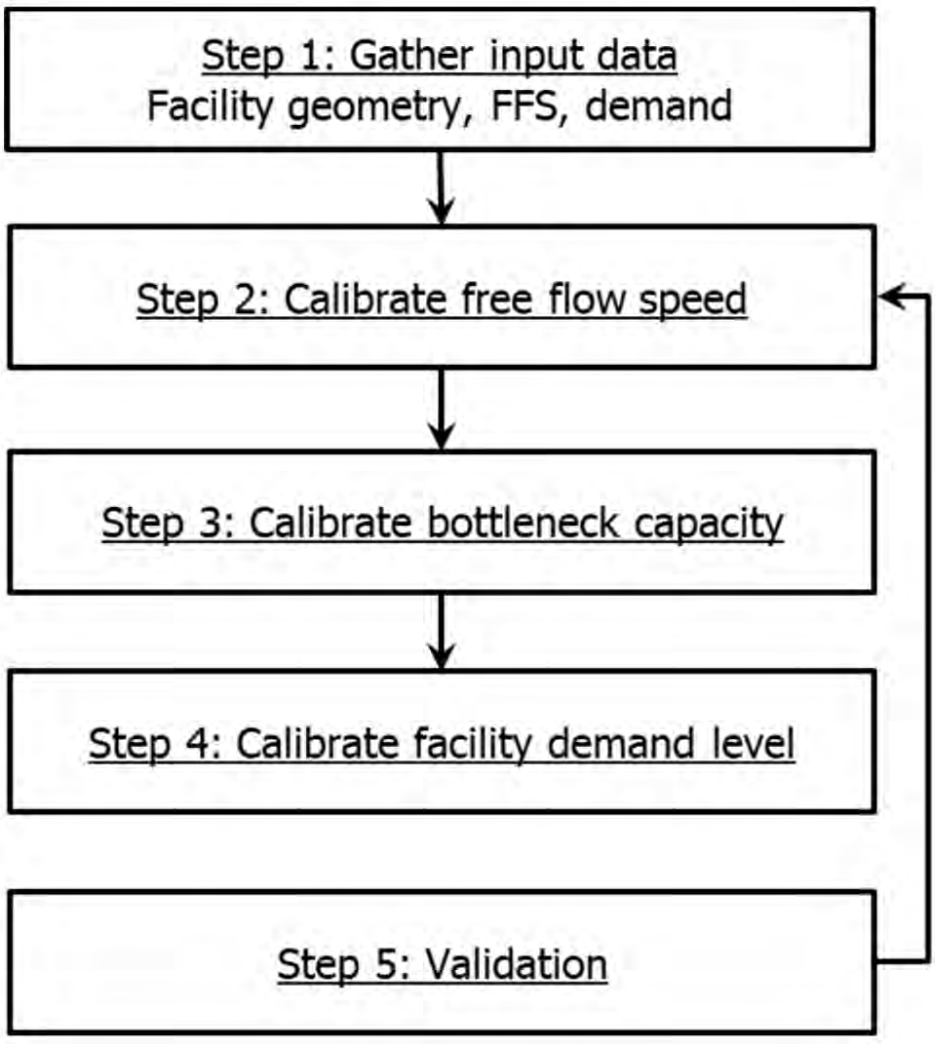

FIGURE 2-1: CALIBRATION STEPS FOR THE CORE FREEWAY FACILITY LEVELS

In lieu of a manual approach, Trask developed a metaheuristic that uses a genetic algorithm (GA) for freeway facility demand and capacity calibration (Trask 2017). GA is an evolutionary search metaheuristic that is generally applied to highly complex optimization problems where analytical solutions are difficult, such as in stochastic and non-linear cases (Holland 1975). Its objective is to

minimize the value of a fitness function that responds to changes in segment demand or capacity. As an evolutionary algorithm, GA begins with a randomly generated initial population of feasible solutions and the population "evolves" over iterations by simulating competition-based selection, elitism, preservation, and crossover (birth) operators as well as mutations applied to single organisms, thus simulating a sort of population evolution iteratively. The encoding scheme for an exact organism is a binary string (i.e., string of zeros and ones) whose corresponding integer value is projected onto an interval between a specified lower and upper bound for adjustment factors (projected from binary to standard base 10 integer system). Currently, the projection is a simple uniform distribution, but any probability distribution could ostensibly be used. Evaluation of organisms is done using a metric called a "fitness function" that the researcher specifies. Trask's function has been implemented in FREEVAL, which is simply a weighted sum of the absolute differences between ground truth speeds from probes and HCM/FREEVAL predicted speeds; as this is a minimization optimization, this fitness will be referred to as an "error function" for clarity in the remainder of the study. For given segments $i \in \{1,\ldots,I\}$ and time periods $j \in \{1,\ldots,J=96\}$, with probe speeds s_{ij} and HCM predicted speeds $\hat{s}_{ij}$ for segment i in time period j, the error function equation is as follows:

$$\sum_{i=1}^{I}\sum_{j=1}^{J} min(75 - s_{ij}, 20)\left|s_{ij} - \hat{s}_{ij}\right| \qquad (1)$$

Note that the weighting gives higher priority to fitting the lower speed cells in the HCM predicted model. Trask developed a two-stage approach to adjust demand and capacity while attempting to minimize the error function (Trask 2017, Trask et al. 2017). The first stage focused on demand volumes and queue discharge rates simultaneously, attempting to match travel times across the facility analysis periods (AP). The second stage focuses on pre-breakdown segment capacity adjustments and facility jam density, attempting to match speeds on individual segments for each analysis period. Utilizing the GA framework when using a speed composite from several typical recurring congestion days significantly improved the predictive speeds over the initial uncalibrated facility. It should be noted that Trask's work focused exclusively on calibrating the effect of segment demand and capacity to capture the recurring bottleneck (s) impact on speed and travel time. Furthermore, these adjustments were permeated throughout the analysis period, whether a one hour peak or a 24 hour period is considered. In other words the capacity adjustment time window was automatically set to the entire study period, which obviously will not apply to spatio-temporally confined incident location and duration.

In order to estimate the impact of incidents on capacity, certain modifications, and updates needed to be made to calibrate the capacity for the segment that is

experiencing the incident. This required modifications to the current GA approach used for calibration in FREEVAL.

2.2. Methodology

This section presents the methodology to determine the effect on capacity due to incidents as an evolutionary phenomenon. The starting point was the GA model developed by Trask (Trask 2017). The first part of the methodology section discusses the modifications made by this research to calibrate non-recurring sources of congestion's capacity impact. In the next section, we discuss how the incident calibration is performed considering the presence of the recurring and other non-recurring sources of congestion.

2.2.1. Enhanced GA Model for Incident Calibration

The main requirement to capture the impact of an incident is the ability to focus on the segments and time periods that are affected by the incident. More specifically, the queue formation and speed drop caused by an incident should be focused upon, while traffic conditions outside the analysis boundary should not be considered. This approach attempts to find optimal CAF sets that lead to queuing and congestion in FREEVAL that best match real-world conditions.

Furthermore, the original GA method was designed to calibrate recurring-congestion-only scenarios and returns a fixed time invariant CAF for each segment. This approach mimics the effect of geometric features of freeway segments that can cause lower capacities (e.g. grades or curvatures). However, to capture the variability in the incident capacity impact, the GA algorithm should be able to vary the CAFs for the selected incident segment in each 15-minute period. This is the second change required to record the evolutionary features of an incident on freeway operations.

The GA algorithm extended from Trask (Trask 2017) enabled the specification of spatio-temporal windows for analysis that approximately match when and where incidents occur (or generally congestion due to other non-recurring sources of congestion such as weather, work zones, etc.). Two contiguous time-space boxes are marked by specifying the most upstream and downstream segments impacted by the incident, as well as the first and last time period congestion prevails. The first box, one segment wide, is considered the *decision* box as this is where CAFs are generated that affect the HCM analysis speeds and other appropriate metrics. The second box is the *objective* box as this is where the error function values are calculated to evaluate the effectiveness of CAFs. This leads to the modification of equation (1) such that the segment set and time period sets are reduced; given the new segment set $i \in \{\underline{I},\ldots,\overline{I}\}$ where $\underline{I}$ is the first segment experiencing congestion and $\overline{I}$ the last and new time period set $j \in \{\underline{J},\ldots,\overline{J}\}$ where $\underline{J}$ is the first analysis period experiencing congestion and $\overline{J}$ the last, the error equation becomes:

$$\sum_{i=\underline{I}}^{\bar{I}} \sum_{j=\underline{J}}^{\bar{J}} min(75 - s_{ij}, 20)|s_{ij} - \widehat{s_{ij}}| \quad (2)$$

Figure 2-2 below shows an example of a one-lane incident. This speed contour shows congestion from 10:00am to 11:15pm on segment 7. Therefore, the black rectangle is the objective box (that needs to be matched with the real-world observations) while the blue rectangle is the decision box (the segment impacted by the incident).

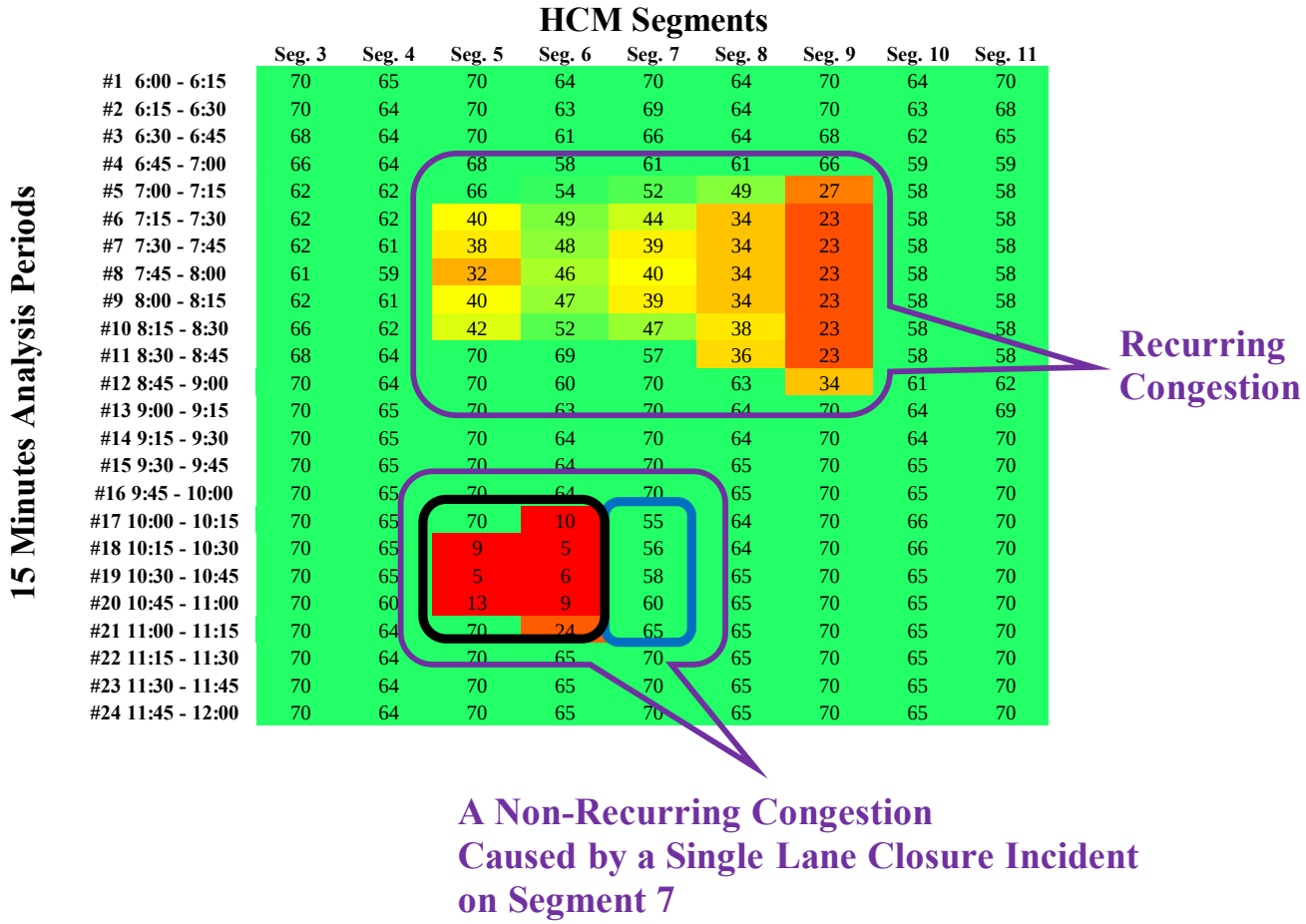

FIGURE 2-2: SPEED (MPH) CONTOUR WITH DECISION (BLUE) AND OBJECTIVE (BLACK) BOXES

Within the GA framework, the Lower Bound (LB) on CAF can be as close to zero as the bit string allows. This is quite different for the recurring congestion calibration case where a higher LB is considered (e.g., 0.85). For instance, some preliminary analysis used a lower bound of 0.01 and an upper bound of 1.0. Especially for the cases of one-lane incidents, the lower bound was rarely hit; this is likely a result of the fact that speeds were averaged over 15 minutes time periods while speeds with observation rates close to being continuous would

have more need for the lowest bound possible. In FREEVAL, the GA algorithm developed cannot account for the change in the net number of lanes. As such, the closed lanes capacity reduction is included in the CAFs. In other words, the one and two lanes closure will have CAFs equal to ⅔(0.74) = 0.49 and ⅓(0.51) = 0.17 respectively. In the final analysis, one-lane incidents were given an imposed lower bound of 0.1 and two-lane incidents a bound of 0.05. Four of sixteen one-lane incidents hit the 0.1 lower bound in the first time period while four out of six two-lane incidents hit the 0.05 lower bound.

2.2.2. Application of Enhanced GA to Data

Performing the CAF calibration requires determining where to place the decision and objective boxes. During calibration, empirical speed data are collected; these observed speeds are 15-minute averaged speeds usually collected via probe-based data sources such as INRIX or HERE (HERE 2019, INRIX 2019). As speed datasets use Traffic Message Channel (TMC) segments rather than HCM segments, the speeds are mapped and scaled automatically to each HCM segment inside the FREEVAL model. The user can then identify congested areas where speeds are reduced.

The decision box segment location is chosen as the segment *downstream* from the first slowdown segment where the incident queue begins; a slowdown is considered to occur when speeds drop below 55 mph (which is approximately the speed at capacity for high design freeway facilities). Time windows are applied for both decision and objective boxes that correspond to the time periods at the beginning of the slowdown. The objective box is subjectively determined as speed reductions follow a general pattern of tapering out leading to a triangle-pattern rather than a rectangle-pattern that our boxes require. The objective box is started at the furthest downstream queuing segment and ends at the upstream segment that still has a slowdown. The segment length is then modulated by looking across time to see where the bulk of the queuing has tapered out toward free flow speeds. A good rule of thumb is to consider the furthest upstream segment for a given time duration as the location where more than half of the speeds are beyond 55 mph.

All genetic algorithms used 100 as the number of maximum iterations, 100 as the population size, a mutation rate of 0.2, and the number of binary digits of five. The focus was on incidents occurring under good weather conditions during non-holiday weekdays. After reducing the incident dataset by eliminating weekend incidents and holidays, as described in the next section, further culling was done by flagging days in which visibility fell below ¼ mile or when any precipitation is encountered. By having this flagged database, incidents occurring on ideal days (no precipitation, visibility greater than ¼ mile) could easily be found. Some subjectivity is included in days where bad weather occurs before the incident as lasting impacts have different effects on freeway conditions in

different seasons (i.e., precipitation in winter likely has longer-lasting effects than in spring, summer, and fall). Incidents that occurred close to the recurring congestion period in a given day were also discarded to minimize any confounding effects in the calibration. Using these policies, a sample of incidents were identified for use in single incident calibration of CAFs.

2.3. Data Collection and Model Development

Incident Data was provided by the Traveler Information Management System (TIMS) of the North Carolina Department of Transportation (NCDOT). TIMS is a statewide traveler information database which includes incidents such as crashes and disabled vehicles as well as construction and maintenance projects which impact traffic (North Carolina Department of Transportation – TIMS 2019). The database is maintained by the three TMCs in North Carolina: the Statewide Traffic Operations Center in Raleigh and regional TMCs for the Triad and Metrolina regions. TIMS is used in real-time to provide driver information though the DriveNC website (North Carolina Department of Transportation – DriveNC 2019), on social media, as well as Dynamic Message Signs on major corridors.

In this research, the weather data was provided by the National Oceanic and Atmospheric Administration (NOAA) (US Department of Commerce 2018). Average annual daily traffic data (AADTs) were employed to determine demands for all entry and exit points on the facility from NCDOT GIS maps (North Carolina Department of Transportation – Connect NC 2019). Speed data were collected from the Regional Integrated Transportation Information System (RITIS), a national database maintained by the University of Maryland that aggregates a comprehensive set of data useful for transportation operations and analysis (The Center for Advanced Transportation Technology Laboratory 2018). The particular aggregated speed data used in the analysis came from two private companies working within transportation data analytics, notably HERE and INRIX (HERE 2019, INRIX 2019); both these companies collect data in similar ways, utilizing GPS-based probe data gathered through sources such as mobile phones and connected cars, road cameras and sensors, and government-provided data.

The study area selected for analysis is located in Raleigh, North Carolina, between US-401 and Aviation Parkway on Westbound I-540, a second beltline around the city. The exact geometry of each segment in the study area is depicted in Figure 2-3. Overall, there are 37 total HCM segments, corresponding to 18 TMC segments with a total length of 16.9 miles. The specific classes of the 37 total segments are 18 basic segments, nine on-ramps, nine off-ramps, and one weaving segment. The entire facility has a FFS of 70 mph and varies in the number of lanes from two to five lanes; incidents only occurred at three or four lane segments. The methods used to calibrate the initial seed file follow Chapters 10 and 11 of the 6th edition of the HCM, as shown in Figure 2-1.

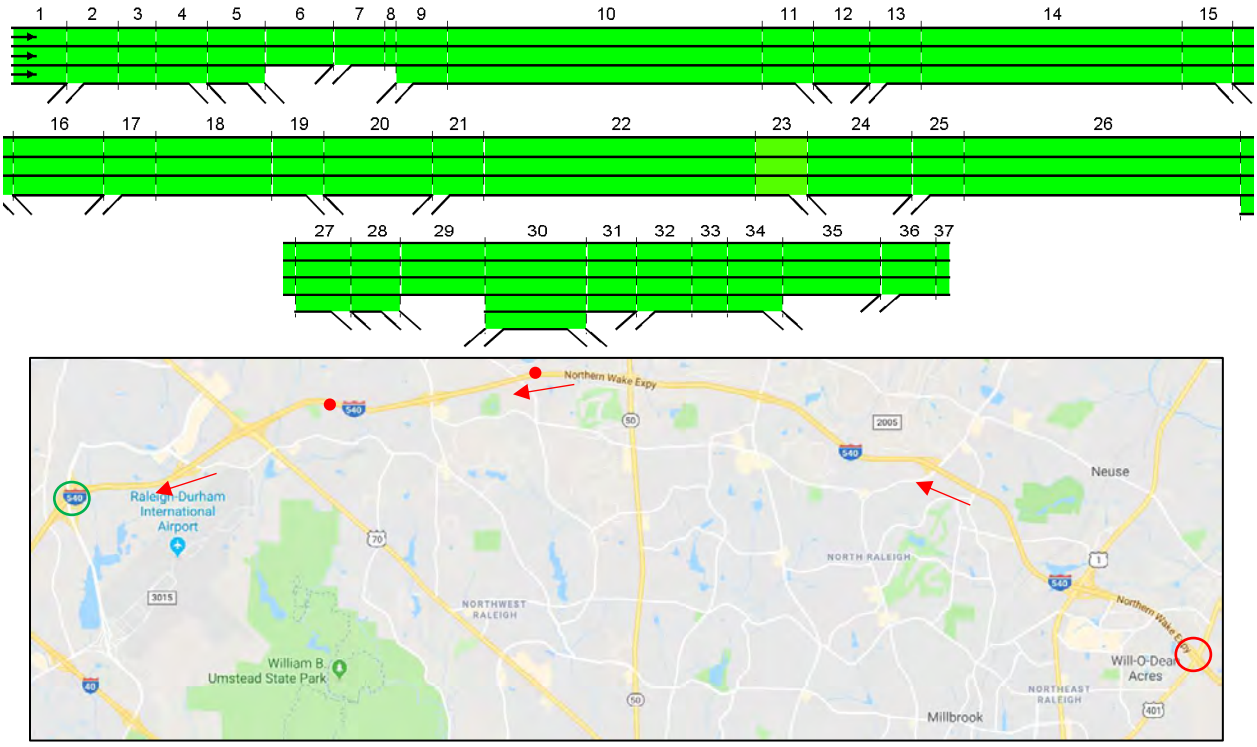

FIGURE 2-3: MAP AND MODELED I-540WB IN NORTH CAROLINA (US401 TO AVIATION PARKWAY)

The initial data collected from RITIS included true ground speed extracted from ideal weather Tuesdays, Wednesdays, and Thursdays in April 2017 that represented normal weekdays with peak hour congestion. After AADT and local hourly demand profile data were input into the FREEVAL tool, the demand calibration tool (also a GA algorithm) was used along with some manual input with the composite ideal speed data to further refine the demand. The rationale for adjusting the demand rather than the capacity to calibrate the base model was the fact that this facility has a high standard (e.g., wide lanes and good quality pavement). As such, the uncalibrated model in FREEVAL matched well with real-world observations. This left the research team to only fine-tune demands and not change the bottlenecks' capacities. This became the baseline file to be used in the analysis of incidents.

The incident days chosen for analysis met several requirements that were processed incrementally: weekday, non-holidays, incident days, weather, realized congestion, and distinct congestion. Dates were considered from 2014 to 2018 for a total of 1826 dates. The focus was on weekday traffic so the first filter applied reduced the initial set to 1565 weekday dates. Federal holidays with the exception of Washington's birthday, Martin Luther King Jr.'s birthday, and Columbus day were used to further filter days. Out of 41 total holidays, only 33 occurred on weekdays to reduce available days to 1532.

The prior filters were easy to apply, whereas the later filters required more significant data analysis. Incidents were first filtered to find authentic one up to four-lane incidents as the TIMS system contains data on other traffic impacts such as construction. Additionally, these incidents were reduced by only allowing reasonable incident durations to eliminate abnormally short or long duration incidents. HCM's default incident duration mean, min, and max values were utilized to carry out this filtration. The initial 766 entries in TIMS were categorized as 148 one lane incidents, 40 two-lane incidents, and only three three-lane incidents. As the sample size for three lanes was so limited, only the 188 one and two-lane incidents were considered for analysis.

Next, the weather was investigated to determine which days and their specific six-hour study period had either precipitation or low visibility. The NOAA weather database for the study area was used, providing hour by hour weather information (U.S. Department of Commerce 2018). In particular, any six-hour block with precipitation greater than zero or visibility under a quarter-mile was flagged. The exact number of adverse weather blocks was never calculated but used in the next step when cross-referencing with incident dates and available weekdays and non-holidays.

With 188 possible incidents and their start and end times, cross-referencing with the weather, weekdays/non-holiday flags, realized congestion, and having distinct congestion reduced the incident set to the final set. After initial reduction by weather, weekdays, and non-holidays, the speed contours corresponding to the remaining incident days were visually inspected to determine *realized* and *distinct* congestion. *Realized congestion* only occurred when an incident had a notable impact on speeds at its reported time, reducing speeds to imply true congestion. Otherwise, if congestion was not observed the incident was eliminated. *Distinct congestion* refers to the elimination of incidents that overlapped with recurring AM peak congestion (there is no PM peak for this facility), as recurring congestion would affect the independent analysis of incident-based congestion. After these final filters were applied, there remained 16 one-lane incidents and six two-lane incidents for analysis.

Table 2-2 depicts each individual incident remaining in the final database, the number of lanes on the incident bottleneck segment, segment numbers where the Queue Ends and Queue Starts, the maximum queue length from HCM segments reported by FREEVAL, and finally the Start and End Times of the incident, displayed in a 0-24 hour scale in units of hours. Table A-1 to Table A-22 in Appendix A provide additional details reported in TIMS for each incident date. An example of such a table is Table 2-3 below.

TABLE 2-2: FINAL LIST OF INCIDENTS USED FOR CAPACITY DETERMINATION

No. of Lanes Closed	Incident Date	Incident Segment	Number Lanes at Segment	Segment Type	Back of Queue Segment	Front of Queue Segment	FREEVAL Max Queue length (ft)	Start Time (hrs)	End Time (hrs)
1	2/27/2014	17	3	On Ramp	13	16	13,274	9.25	10.5
1	3/14/2014	13	3	On Ramp	6	12	17,717	16	17
1	5/5/2014	22	3	Basic	17	21	10,964	9.5	10
1	6/24/2014	20	3	Basic	16	19	8,984	9	9.75
1	7/15/2014	13	3	On Ramp	9	12	13,875	13.25	13.75
1	2/5/2015	29	3	Basic	26	28	10,809	17.5	18.25
1	3/27/2015	24	3	Basic	22	23	9,311	5.75	6.25
1	4/7/2015	29	3	Basic	26	28	10,809	17	17.5
1	8/5/2015	29	3	Basic	26	28	10,809	20.75	21
1	4/5/2016	14	3	Basic	10	13	13,875	17.5	18
1	4/26/2016	22	3	Basic	17	21	10,964	16.25	17
1	6/10/2016	10	3	Basic	3	9	9,680	6.25	8
1	9/6/2016	18	3	Basic	14	17	13,274	15	16.25
1	11/8/2016	14	3	Basic	10	13	13,875	8.5	9.25
1	9/11/2017	22	3	Basic	14	21	22,738	8.5	9.75
1	5/4/2018	14	3	Basic	3	13	23,555	6.5	7.5
1	6/18/2018	3	3	Basic	1	2	3,112	17	17.5
2	2/25/2015	31	4	Basic	25	30	17,387	7.5	8.75
2	4/22/2015	18	3	Basic	14	17	13,274	13	13.50
2	4/29/2015	13	3	On Ramp	10	12	12,375	20.5	21.25
2	12/15/2015	13	3	On Ramp	7	12	15,701	9.25	10.00
2	11/7/2016	18	3	Basic	3	17	36,829	9.75	10.50
2	6/19/2018	3	3	Basic	1	2	3,112	12.25	12.75

TABLE 2-3: SAMPLE INCIDENT DESCRIPTION ATTRIBUTES

Incident Date:	2/27/2014	Weekday:	Thursday
Incident Start Time:	9:19 EST	Incident End Time:	10:19 EST
Approx. Queue length:	13,274 ft	Weather Condition:	Clear/Normal
Incident Severity:	One Lane Closure	# of Freeway lanes:	3
Incident Description (from TIMS):	Left median reopened near Exit 11, Six Forks Road		

2.4. Results

The revised GA algorithm discussed in the Methodology section of this study was applied to the identified incidents described earlier. Table 2-3 shows an example day (Feb. 27, 2014, in Table 2-2) which experienced a single lane closure incident. More specifically, Table 2-4 outlines the GA optimal time-dependent CAFs and HCM CAFs across incidents duration (Transportation Research Board 2016). In this case, the calibrated CAFs varied from 0.1 in time block 9:15-9:30 up to 0.91 in 10:15-10:30. From the final error function row, it is obvious how much closer fitting the calibrated model is

when compared to the HCM model, with the error function reduced to almost a quarter of the HCM model (15,781 to 4,712). Additionally, the calibrated model with time-dependent CAFs performs much better than the average and HCM CAF. Interestingly, the *average* of the time-dependent CAF computed across all five time periods matched almost exactly the fixed HCM's CAF value. To further illustrate how well the calibration worked in this model, Table 2-4 shows the color-coded speed contours covering the area of congestion caused by the incident (the objective box). Speed contours for each incident are provided in Table A-23 to

Table A-44 of Appendix A. These tables contain two additional CAF scenarios beyond time-dependent CAFs and HCM CAF; these are the average CAF (a fixed average of a single incident's time-dependent CAFs) and an unadjusted capacity (all CAFs during incident equal to one). The average CAF scenario performed similarly to the HCM scenario while the unadjusted capacity performed poorly overall; neither provided a basis for further investigation.

TABLE 2-4: EMERGED TIME-DEPENDENT CAFS, COMPARISON TO THE HCM MODEL VIA ERROR FUNCTION VALUES AND EMERGED SPEED CONTOURS

Speed Contour Associated with	FREEVAL Seg #:	Time Dependent CAF used	Error Function Value	Seg. 13	Seg. 14	Seg. 15	Seg. 16
INRIX / TARGET Speeds	9:15 - 9:30	NA	NA	53.0	21.0	21.0	44.5
	9:30 - 9:45	NA		22.2	8.8	8.8	37.9
	9:45 - 10:00	NA		10.9	8.2	8.2	36.1
	10:00 - 10:15	NA		17.7	12.2	12.2	38.0
	10:15 - 10:30	NA		48.3	34.5	34.5	49.1
FREEVAL – Time-Dependent CAF Note: mean CAF =0.488	9:15 - 9:30	0.10	4,712	63.9	26.5	6.3	1.2
	9:30 - 9:45	0.10		27.7	1.6	1.2	1.0
	9:45 - 10:00	0.62		4.8	8.0	9.9	9.0
	10:00 - 10:15	0.71		16.1	14.2	14.1	11.4
	10:15 - 10:30	0.91		43.6	39.0	32.9	23.3
FREEVAL - HCM CAF	9:15 - 9:30	0.49	15,781	63.9	70.0	65.7	17.3
	9:30 - 9:45	0.49		64.4	70.0	66.1	13.7
	9:45 - 10:00	0.49		64.4	70.0	66.2	23.6
	10:00 - 10:15	0.49		64.6	70.0	66.6	60.2
	10:15 - 10:30	0.49		64.9	70.0	66.7	69.9

This table shows the speed contours for the two models mentioned above (Time-dependent, HCM) as well as showing the true ground speeds (from the probe) at the top across the four segments and five time periods chosen for the objective box. The time-

dependent CAF clearly most matches the target speeds even with some very low speeds, especially at segment 16 immediately upstream of the segment 17 bottleneck. The HCM model hovers around the free flow speed of 70 mph from segments 13 to 15, vastly different than the realized speed slowdowns.

Table 2-5 highlights the CAF results applied to all incident days. The CAF # columns are the raw CAFs generated by FREEVAL calibration while the average CAF column is the average of each incident's CAF across the time of the incident. HCM CAF is the adjustment factor provided by the HCM, derived from the relative remaining CAF from Table 2-1 of this study (Exhibit 11-23 in HCM). Note that the average CAFs are generally higher than the given HCM CAF, with the trend that CAFs increase in time as the incident clears; this is especially clear within two lane incidents. It is this trend of a clearing rate that ended up leading to the proposed model that described in detail in section 6. Additional Table A-45 to
Table A-66 in Appendix A outline CAFs and error functions for time-dependent and HCM CAFs as well as average and unadjusted CAFs.

TABLE 2-5: OPTIMAL TIME-DEPENDENT CAFS FOR ONE- AND TWO-LANE CLOSURE INCIDENTS

Incident Type	Incident Date	Optimal Time-Dependent CAFs							Average Time Depend CAFs	HCM CAF	Optimal CAF Error Function	HCM CAF Error Function
		AP1*	AP2	AP3	AP4	AP5	AP6	AP7				
One Lane Closure	2/27/2014	0.10	0.10	0.62	0.71	0.91			0.49	0.49	4,712	15,784
	3/14/2014	0.10	0.10	0.62	1.00				0.46	0.49	13,414	21,757
	5/5/2014	0.10	0.94						0.52	0.49	4,328	9,114
	6/24/2014	0.54	0.45	0.68					0.55	0.49	1,605	2,298
	7/15/2014	0.19	1.00						0.59	0.49	3,330	4,573
	2/5/2015	0.25	0.16	0.83					0.41	0.49	2,979	6,604
	3/27/2015	0.36	0.83						0.59	0.49	1,039	2,106
	4/7/2015	0.13	1.00						0.56	0.49	2,003	3,199
	8/5/2015	0.59							0.59	0.49	1,488	1,488
	4/5/2016	0.13	1.00						0.56	0.49	3,240	4,287
	4/26/2016	0.10	0.62	0.85					0.53	0.49	3,876	10,589
	6/10/2016	0.33	0.65	0.88	0.85	0.97	0.94	0.94	0.80	0.49	8,983	23,335
	9/6/2016	0.10	0.22	0.36	0.85	0.97			0.50	0.49	5,197	15,963
	11/8/2016	0.45	0.80	1.00					0.75	0.49	1,776	4,448
	5/4/2018	0.19	0.85	0.77	0.91				0.68	0.49	12,172	19,817
	6/18/2018	0.36	0.91						0.64	0.49	1,068	2,005
Two Lane Closure	2/25/2015	0.17	0.48	0.39	0.39	0.97			0.48	0.17	8,656	13,098
	4/22/2015	0.05	1.00						0.53	0.17	3,376	4,998
	4/29/2015	0.11	0.05	0.94					0.37	0.17	4,545	5,502
	12/15/2015	0.05	0.11	0.97					0.38	0.17	7,037	9,853

	11/7/2016	0.05	1.00	0.75					0.60	0.17	37,480	41,639
	6/19/2018	0.14	0.79						0.46	0.17	685	1,837
Average Error Function Value											**5,833**	**10,195**

**Analysis Period (15 minutes)*

Table 2-5 also presents the error function results associated with the above CAFs for one- and two-lane incidents, respectively; the optimal error function is calculated using the raw CAFs generated in FREEVAL. The technique developed in this study clearly results in time-dependent CAFs performing better overall than the HCM.

2.5. Proposed Model

Once it became apparent that the largest contribution to CAF calibration was the rate at which CAF changes during an incident, the need arose to determine which known data elements could be correlated with this rate of change. Intuitively, any duration-based metric will be correlated as the CAF should generally increase as time progress while first responders are effectively clearing the incident from the freeway.

Figure 2-4 below shows a correlation plot generated in R statistical software with potential predictors for CAFs for one lane incidents only, as the sample size for two lane incidents is fairly small. The larger and darker the color of the matrix element, the stronger the correlation between variables; red represents negative correlation and blue represents the positive correlation. The majority of variable names are self-explanatory, except for: HCM DAF represents HCM demand adjustment factor that is weekday-month AADT adjustment factor, the average incident CAF is the average of a single incident's optimal time-dependent CAFs, and the incident first and last time period CAFs are a single incident's first and last time period optimal time-dependent CAFs, respectively. While most high correlations derive from linear relationships that are expected such as duration and max queue lengths with error (the objective box is chosen accordingly), the incident duration variable had some mild positive correlation with both average incident CAF and incident last time period CAF This implies that the longer an incident, the higher the final CAF with the rate of clearing seen when comparing average CAF to final CAF. Therefore, we select the incident duration to become the model's predictor.

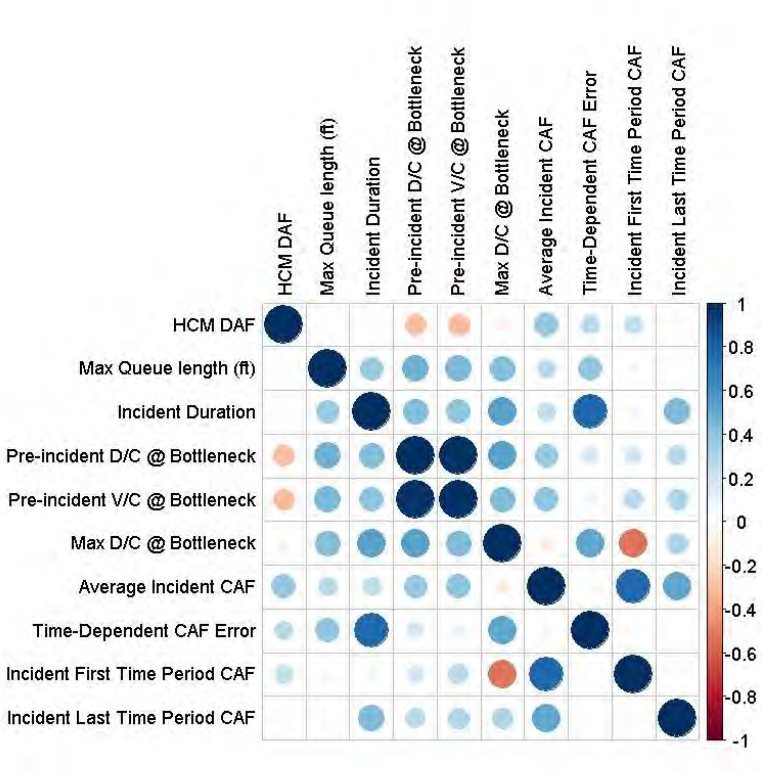

FIGURE 2-4: ONE LANE INCIDENT CORRELATION MATRIX

Rather than focusing on finding a single CAF, time-dependent CAFs could be applied to more accurately capture the true capacity change at a given time. To determine this clearing rate, incident time periods were reclassified from raw numbers to percentage duration elapsed for an incident. For instance, time period one of a four period incident became 25% while time period 1 of a five-period incident became 20%. Then, to fit the CAFs onto a similar scale the one lane CAFs were divided by the one lane CAF average of averages across incidents (0.583); similarly, the two lane CAFs were divided by the corresponding value (0.409). These data points were then plotted with percent duration elapsed on the x-axis and the adjusted CAFs on the y-axis. Figure 2-5 shows the linear regression for one-lane, two-lane, and a combined set when fixing the intercept at zero. The one lane has regression slope of 1.5595 and an R^2 of 0.5535, two lane has slope 1.8603 and R^2 0.5674; the combined dataset has slope 1.6371 and R^2 =0.5436. Therefore for every 10% duration of an incident elapsed, one lane incidents have a raw CAF increase of 0.1×0.583×1.5595=0.0909 and two lane incidents have increase of 0.1×0.409×1.8603=0.0761. As this model does require knowledge of the incident duration for prediction, the time-dependent CAF values can be assigned based on the overall incident duration distribution by severity, which is normally available as part of the HCM6 reliability analysis methodology based on a lognormal distribution of incident duration. An important limitation within the HCM context is that incident durations can only be specified in multiples of 15 minutes.

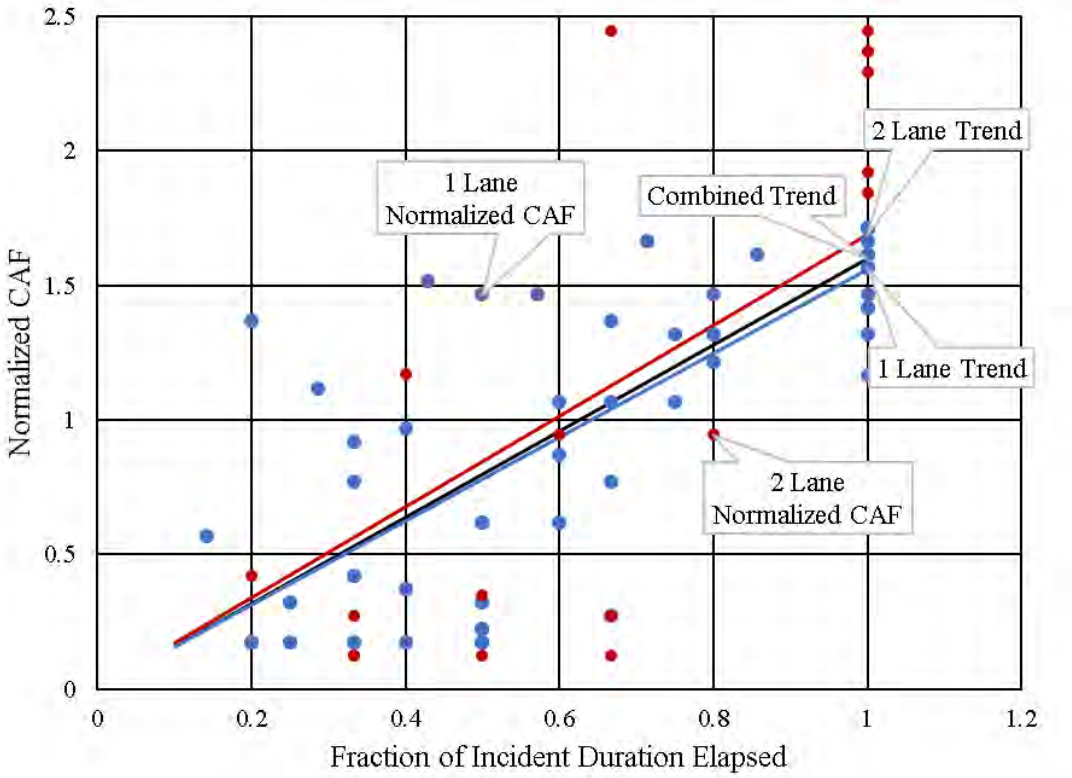

FIGURE 2-5: TREND AND MODEL OF CAF VS. ELAPSED INCIDENT DURATION

Note that the above graph suggests three models: one lane, two lane, and combined data models. Clearly, the combined data model results in approximately the same regression slope coefficient; there is further statistical justification to combine the data. To determine if the data should be combined and given that the intercept is fixed at zero, a hypothesis test for equal slopes is performed (Kleinbaum et. al 2008). The given models for one and two lane incidents are:

$$CAF_{(1)} = \beta_1 X_1 + \epsilon_1$$

$$CAF_{(2)} = \beta_2 X_2 + \epsilon_2$$

Where $\epsilon_1 \sim Normal(0, \sigma_1^2)$, $\epsilon_2 \sim Normal(0, \sigma_2^2)$ .The null hypothesis is $H_0 : \beta_1 = \beta_2$. To test for this slope parallelism a t-test is given as:

$$T = \frac{\widehat{\beta_1} - \widehat{\beta_2}}{S_{(\widehat{\beta_1} - \widehat{\beta_2})}} \sim t_{(n_1 - n_2 - 4, 1 - \frac{\propto}{2})}$$

where n_i is the sample size for group i and $\alpha = 0.05$ is the significance level. The denominator $S_{(\widehat{\beta_1} - \widehat{\beta_2})}$ is the estimated standard error of estimated difference between

slopes $(\widehat{\beta_1} - \widehat{\beta_2})$. In this case, evidence suggests different variances in errors (0.37 and 0.63 for one and two lanes, respectively), so the unpooled variance is used as

$$S_{(\widehat{\beta_1}-\widehat{\beta_2})} = \sqrt{s_{b_1}^2 + s_{b_2}^2}$$

with

$$s_{b_1}^2 = \frac{s_{res_1}^2}{s_{x_1}^2(n_1 - 1)}$$
$$s_{b_2}^2 = \frac{s_{res_2}^2}{s_{x_2}^2(n_2 - 1)}$$

where $s_{res_i}^2$ is the square of the residual standard deviations and $s_{x_i}^2$ is the standard deviation of the independent variable (duration percentage) for group i . The t-value was calculated as -0.523; as the critical value for t is 1.995 the null hypothesis cannot be rejected. Therefore, as the slopes are equal and the intercept is set to zero, these two regression lines are effectively coincident and justify combining the data into one final model.

The combined model is implemented using Equation (3), which shows the relationship between time-dependent CAFs as a function of HCM proposed constant CAF (in Table 2-1) and the time period i in which the incident is in the process:

$$CAF_i^n = 1.637\left(\frac{i}{n}\right)CAF_{HCM} \qquad (3)$$

Where CAF_i^n is the time-dependent CAF of an incident with duration n in the time period i. Both n and i correspond to the 15 minutes analysis period. CAF_{HCM} is the HCM proposed CAF depending on the number of lanes available in the given freeway segment. As an example, assume that a one lane closure incident is to be applied on a freeway segment with three lanes for 45 minutes. The 45 minutes will translate into three analysis periods. HCM proposes a fixed CAF of 0.74 for the remaining open lanes. The emerged CAFs to be used for modeling this incident will then be: $CAF_1^3 = 0.40$, $CAF_2^3 = 0.80$, and $CAF_3^3 = 1.2$ based on the *open lanes'* capacity. The corresponding *overall* segment capacity adjustments based on the *total number of segment lanes* are then CAF_1= 0.267; CAF_2= 0.53 and CAF_3= 0.80.

2.6. Enhanced GA Model Application to Recurring Congestion Events

While the focus of this study has been on non-recurring congestion events as a result of incidents, a similar analysis can be performed on recurring congestion periods arising from daily peak demands. Preliminary work on this recurring congestion showed some promise but could not resolve the issue that demand calibration of the FREEVAL seed (or average day) file cannot necessarily be separated from the congestion itself. Non-recurring congestions could effectively be treated independently from normal demand in off-peak hours, allowing for the calibration of CAFS, while the recurring congestion is

inevitably affected by the confounding demand variations. Additionally, peak traffic times have higher variability on the resulting capacity as will be shown.

In total, 26 daily congestion periods were investigated that satisfied the weekday, non-holiday, good weather, and distinct and realized congestion required by the methodology. Of those, 14 days corresponded to days in which incidents occurred (this data was already available from RITIS), and the remaining 12 days were used in the initial seed file demand calibration (ideal days in April 2017). The objective and decision boxes were chosen in the same manner and the GA algorithm used for incident congestion: 100 is the number of maximum iterations, 100 is the population size, 0.2 is the mutation rate of 0.2, the number of binary digits is five, 0.8 is the lower bound of CAFs, and 1.0 is the upper bound. No real temporal trend seemed to emerge with a clearing rate, so further analysis with a lower LB was not attempted; instead, the focus was on the average CAF during congestion, and how that compared to the "base" capacity of 2,400 pc/h/lane reported in the latest highway capacity manual.

Table 2-6 below describes the recurring congestion bottleneck, the start and end time of the recurring congestion events, and the duration of each congestion day tested. Except for one case, all bottlenecks occurred on basic segments; additionally, the average CAF for each day and the value of the error functions for optimal time-dependent CAFs and unadjusted CAFs are presented. The time-dependent CAF scenario performed slightly better overall as seen in the average with six days of the 26 leading to equal or worse errors (4/13/2017, 4/21/2017, 4/21/2017,4/27/2017, 3/26/18, and 5/4/18). Overall, the emerged average CAF of 0.92 will yield a base capacity of about 2,200 pc/hr/lane, which is in line with more recent research findings in Florida (Kondyli et al. 2017). For individual time-dependent CAFs, the reader can consult Table A0-67 in Appendix A.

Another interesting fact is that every congestion day in our sample, with the exception of 6/10/2016, had the bottleneck located on either segment 22 or segment 26. Segment 22 is located between Creedmoor Road and Leesvile Road, and segment 26 is between Leesville Road and Glenwood road; these locations are highlighted as red filled dots on the map in Figure 2-3. Figure 2-6 below shows that these two segments have differing time-dependent CAFs with segment 26 having slightly higher overall capacity than segment 22 (2,228 vs. 2,184 vph/lane, respectively) and slightly lower variability (144 vs. 132 veph/lane respectively).

TABLE 2-6: RECURRING CONGESTION DESCRIPTIONS AND RESULTS

Congestion Date	Bottleneck Segment	Bottleneck Segment Type	Start Time (hrs)	End Time (hrs)	Duration (hrs)	Average CAF	Optimal CAF Error Function	Unadjusted CAF Error Function
2/27/2014	22	Basic	7.75	9.25	1.5	0.89	5243	15711
5/5/2014	22	Basic	7.75	9	1.25	0.81	8611	28224
6/24/2014	22	Basic	7.75	8.5	0.75	0.97	1769	2505
4/22/2015	22	Basic	7.5	9	1.5	0.92	6886	8986
8/5/2015	22	Basic	7.5	9	1.5	0.91	7675	9774
8/11/2015	22	Basic	7.75	9	1.25	0.96	4735	5247
4/5/2016	26	Basic	7.75	9	1.25	0.88	10695	17096
4/26/2016	26	Basic	7.25	9	1.75	0.90	22500	40586
6/10/2016	23	Off Ramp	7.25	8.5	1.25	0.87	5839	9295
9/6/2016	26	Basic	7.75	9	1.25	0.89	15170	31340
4/3/2017	26	Basic	7.25	8.75	1.5	0.98	5770	10871
4/5/2017	26	Basic	7.25	9	1.75	0.92	5299	6562
4/6/2017	26	Basic	7.5	9.25	1.75	0.94	13797	18105
4/7/2017	26	Basic	7.5	8.25	0.75	1.00	11175	12273
4/10/2017	26	Basic	7.25	8.75	1.5	0.94	13876	13972
4/11/2017	26	Basic	7.5	8.5	1	0.87	22960	32508
4/12/2017	22	Basic	7.25	8.5	1.25	0.98	16080	21212
4/13/2017	22	Basic	7.5	8	0.5	0.94	8095	8095
4/17/2017	26	Basic	7.25	8.75	1.5	0.94	19885	15667
4/21/2017	22	Basic	7.5	8	0.5	0.86	19912	12319
4/26/2017	22	Basic	7.25	9.25	2	0.85	5377	6092
4/27/2017	26	Basic	7.25	9.25	2	0.93	5623	5054
3/26/2018	22	Basic	7.5	9	1.5	0.90	12231	8148
5/4/2018	22	Basic	7.5	8.75	1.25	0.94	3640	2005
6/18/2018	26	Basic	7.5	9	1.5	0.92	15578	38054
6/19/2018	26	Basic	7.75	9	1.25	0.95	31739	41148
Average					**1.34**	**0.92**	**11,545**	**16,186**

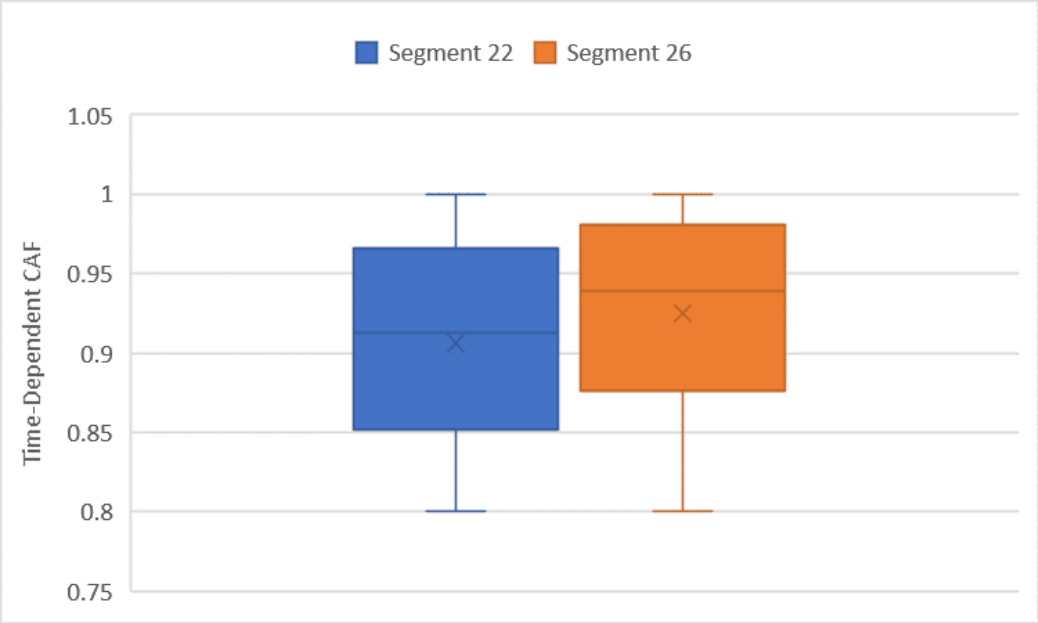

FIGURE 2-6: BOX AND WHISKER PLOT OF AVERAGE CAFS

Lastly, when sorting by date, it appears that there is no evident time trend in the average CAFs from 2014 to 2018 as shown in Figure 2-7, with values reaching no lower than 0.8 (1,920 pc/hr/lane) and not exceeding 2,400.

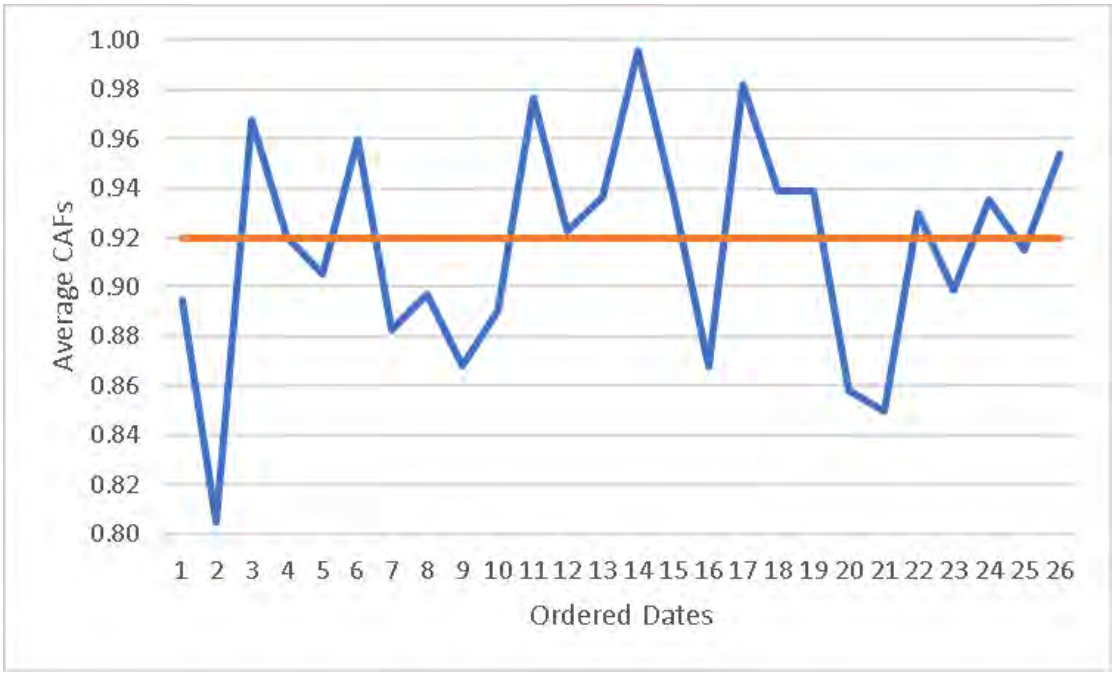

FIGURE 2-7: AVERAGE CAFS ACROSS IDENTIFIED DATES

2.7. Conclusion and Recommendations for Future Work

This study investigates the effect of incidents on freeway segment capacity. Past work has focused almost exclusively on the development of and updates to look-up tables linking the remaining segment capacity fraction during an incident to the total and closed number of lanes on the segment. HCM6 Chapter 11 contains such a table. In reality, segment capacity during an incident will tend to vary over time, with the most severe effects felt early on before any type of response is initiated, followed by congestion progressively improving as the appropriate incident management actions are implemented. The state of practice, however, continues to assume that incident capacity reduction effects are fixed throughout its duration.

Individual incident scenarios on I-540 in Raleigh, North Carolina, consisting of 22 one and two lane closures, were selected for analysis. All the analyzed incidents occurred outside the recurring congestion periods. Using an enhanced Genetic Algorithm developed in this study, which focused on the spatio-temporal domain of the incident, time-dependent calibration of capacity adjustments using probe data as the target speeds were carried out. The objective was to minimize the differences in speeds predicted by the HCM6 freeway facility method (implemented in FREEVAL) and the target speeds.

As expected, the emergent trends of the resultant (optimal) temporal adjustment factors showed strong association with the progression time of the incident, with low values towards the start of the incident gradually increasing toward the end of the incident. This pattern was used to develop a predictive linear model of a standardized *CAF temporal adjustment factor*. This multiplicative factor to the fixed HCM CAF adjusts it to be lower in the early stages of the incident and higher later. The difference in the fit between the fixed and time-dependent factor was quite significant, reducing the error function from the target speeds by more than 43%. Due to its simple format, the proposed temporal adjustment factor can be readily implemented in the HCM6 methodology and adjoining software, once the duration of the incident has been established.

Finally, an initial analysis of the recurring congestion domain over 26 days, using the enhanced GA method and carried for the same facility yielded capacity adjustment factors slightly lower than 1.0. This indicates that even after the demand calibration, there was still a need to slightly reduce capacity to match the empirical speed observations from probe data. The capacity reduction averaged about 8% but varied from day to day from 0 to 20%. This is consistent with recent research findings elsewhere.

3. Development of a unifying modeling framework

3.1 Travel time reliability assessment methods based on traffic flow model

In this section, a unified framework is proposed to assess the travel time reliability. The proposed framework is based on a stochastic traffic flow model.

3.1.1 Deterministic Lighthill–Whitham–Richards (LWR) model

The standard Lighthill–Whitham–Richards (LWR) model in a spatiotemporal (i.e., Eulerian) coordinates system is expressed as follows (Lighthill and Whitham 1955; Richards 1956):

$$\partial_t k + \partial_x Q(k) = 0 \tag{1}$$

where the variable k represents the value of density at the time t and location x, the function $Q(k)$ denote the flow at density k given the flow–density fundamental (FD) diagram, and $\partial_t k$ and $\partial_x Q(k)$ denote the partial derivative of *k* and $Q(k)$ with respect to t *and* x respectively. Equation (1) is equivalent to the following Hamilton–Jacobi partial differential equation (PDE) (Newell 1993a,b,c):

$$\partial_t N = Q(-\partial_x N) \tag{2}$$

where *N* represents the cumulative flow. Variational Theory (VT) solves Eq. (2) by reducing the equation to the following minimization problem (Daganzo 2006):

$$N_p = \inf_{p \epsilon V_p} \{N_B(p) + \Delta(p)\} \tag{3a}$$

$$\Delta(p) = \int_{t_{B(p)}}^{t_p} R(v,t,x)dt \tag{3b}$$

$$R(v,t,x) = sup_{k\epsilon[0,k_j]}\{Q(k,t,x) - kv(t,x)\} \tag{3c}$$

where N_P represents the cumulative flow at the time–space point *P*, V_p represents the so-called valid path set to the point *P*, *B(P)* represents a boundary point associated with the path *P*, $B(\mathcal{P})$ represents the cost of path $\mathcal{P}$, and *R* is the Legendre transformation of FD *Q*.

Let us assume a triangular FD where the free-flow speed is denoted by *u*, the reaction time is denoted by τ, and the minimum spacing (i.e.: the inverse of the jam density κ) is denoted by δ. In this case, Eq. (3) is equivalent to a shortest path search problem in the time–space diagram where the cost of each link is determined by the FD parameters as shown in Figure 3-1.

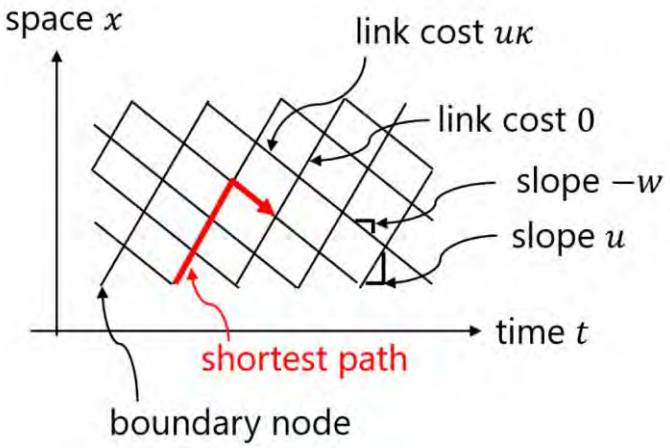

FIGURE 3-1: SHORTEST PATH SEARCH PROBLEM REPRESENTING VT IN EULERIAN COORDINATES SYSTEM. FW STANDS FOR FORWARD WAVE, BW STANDS FOR BACKWARD WAVE, AND W REPRESENTS BW SPEED.

The LWR model can also be formulated based on the vehicle-based (i.e., Lagrangian) coordinates system (Newell 2002; Leclercq et al. 2007; Laval and Leclercq 2013). In this case, the LWR model in Eqs. (1–3) is formulated based on spatiotemporal (i.e., Eulerian) coordinates system. As it will be explained later in this report in more detail, we found that the vehicle-space Lagrangian coordinates system is more useful to answer our research question. The LWR model is often referred to as T-model (Laval and Leclercq 2013) which is expressed as:

$$\partial_n T = H(-\partial_x T), \tag{4}$$

where *T* represents the travel time of vehicle *n* to the location *x*, and *H* represents the pace–headway FD. The parameters of the pace–headway FD are: the free-flow pace (the inverse of the free-flow speed *u*), *p*, the reaction time, τ, and the vehicle size δ. The VT form of T-model is

$$T_p = \sup_{p \in V_p^T} \left\{ T_{B(p)} + \Delta^T(p) \right\} \tag{5a}$$

$$\Delta^T(p) = \int_{n_{B(p)}}^{n_p} R^T(-s, n, x)\, dn \tag{5b}$$

$$R^T(-s, n, x) = inf_{p \in [1/u, \infty]} \{ H(p, t, n) - ps(n, x) \} \tag{5c}$$

In the case of a triangular FD, Eq. (5) is reduced to searching the longest path problem in vehicle–space diagram as shown in Figure 3-2.

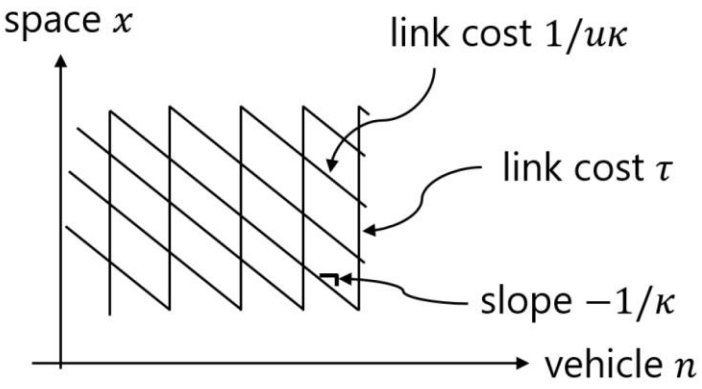

FIGURE 3-2: T-MODEL AND ITS VT AS A LONGEST PATH SEARCH PROBLEM.

3.1.2 Proposed stochastic LWR model in Lagrangian coordinates and structured stochasticity

Wada et al. (2018) proposed a novel stochastic LWR model in Eulerian coordinates system based on variational theory. Specifically, in the Eulerian VT network (Figure 1), a link associated with time–space point (*t, x)* has a cost of $u \times \kappa$. In the deterministic model, these variables, namely the FD parameters including *u* and κ, are assumed to be constant (i.e., spatiotemporally homogeneous). However, it is possible to assume that they are stochastic variables, for example, defined as $u(t,x) \sim \mathcal{N}(\bar{u}(t,x), \sigma_u(t,x))$, where $\mathcal{N}$ represents a normal distribution with a mean and variance of $\bar{u}$ and σ_u respectively. Under this specification, the LWR in Model (1) and (2) represent a stochastic traffic flow model in which the FD parameters are stochastic. In this case, the VT (3) is equivalent to a stochastic shortest path search problem. For further details, the interested readers are referred to Wada et al. (2018) and Takayasu et al. (2016).

This study formulates a stochastic extension of the T-model, by applying the idea of Wada et al. (2018). Specifically, we assume that the reaction time $\tau(n, x)$ and free-flow pace *p(n, x)* of vehicle *n* at location *x* are stochastic variables following the normal distributions. The stochasticity is structured as follows:

$$\tau(n,x) \sim N(\bar{\tau}_n, \sigma_n) \quad (6a)$$

$$p(n,x) \sim N(\bar{p}_n, \sigma_n) \quad (6b)$$

$$\bar{\tau}_n \sim N(\tau_0, \sigma_{\tau_0}) \quad (6c)$$

$$p_n \sim N(p_0, \sigma_{p_0}) \quad (6d)$$

Equation (6) ensures that each vehicle has its own mean reaction time $\bar{\tau}_n$ and free-flow pace $\bar{p}_n$. The parameters of each vehicle are randomly perturbated at each

location, and this perturbation is characterized by the standard deviations σ_τ and σ_p. The mean parameters $\bar{\tau}_n$ and $\bar{p}_n$ follow global distributions with mean of τ_0 and p_0, and standard deviations of $\sigma_{\tau 0}$ and σ_{p0}. Moreover, the boundary conditions *T(0, x)* and *T(n, 0)* are also given stochastically; specifically, they are defined as

$$T(0,0) = 0, \tag{7a}$$
$$T(n + \Delta n, 0) = T(n, 0) + \Delta T(n, 0), \tag{7b}$$
$$T(0, x + \Delta x) = T(0, x) + \Delta T(0, x), \tag{7c}$$
$$\Delta T(n, 0) \sim N\left(\overline{\Delta T}(n, 0), \sigma_{\Delta T}(n, 0)\right), \tag{7d}$$

where Δn and Δx represent the vehicle and space discretization widths, $\overline{\Delta T}$ represents the mean difference in the boundary condition, and $\sigma_{\Delta T}$ represents the standard deviation of the difference in the boundary condition. Note that although the normal distribution is employed in Eqs. (6) and (7), other distributions can be employed as well without substantially altering the framework.

Based on the framework of VT (5), the proposed model is reduced into a stochastic longest path search problem in the VT network (Figure 2). This can be solved by a Monte Carlo simulation.

3.1.3 Discussion

The proposed model captures the vehicle specific characteristics. In fact, the structured stochastic terms (6) represents vehicle specific characteristic themselves, namely, vehicle-specific desired speed $1/p(n,\cdot)$ and vehicle-specific reaction time $\tau(n,\cdot)$. This feature of Lagrangian coordinates system is discussed by Leclercq and Laval (2009) based on the vehicle-time-based coordinates system, which is different from the proposed model. Sophistication and theoretical analyses on this model is being investigated by Wada et al. (in preparation). This feature allows us to investigate how the macroscopic traffic pattern can be improved by controlling the vehicle-specific characteristics. Specifically, by properly setting the value of $\sigma_\tau, \sigma_p, \sigma_{\tau 0}, \sigma_{p0}, \overline{\Delta T}$ and $\sigma_{\Delta T}$, we can assess the effectiveness of various traffic control schemes that will affect these elements.

The T-model is also useful to represent the location-specific phenomena, because distribution of $p(\cdot, x)$ and $\tau(\cdot, x)$ can be directly specified. This is a very useful feature to model traffic on freeways, in which bottlenecks that are fixed on specific locations play a significant role. This is an advantage of this model compared to X-based Lagrangian coordinates used by, for example, Yuan et al. (2012) and Jabari et al. (2018).

The proposed model can directly evaluate the travel time reliability. This is because of the fact that the output of the proposed model is the distribution of $T(n, x)$, which is travel time of vehicle *n* to the location *x*. Distribution of travel time from a specific location to another location indicates travel time reliability itself.

For these reasons, the proposed model is an efficient framework to evaluate the freeway travel time reliability and identify how the control measures can improve the case. Moreover, since the model is a macroscopic traffic flow model, this model is a more computationally efficient alternative to the microscopic traffic flow simulator that is also able to evaluate these factors.

3.2 Control policy

In this section, a new strategy to improve the travel time reliability is proposed. Additionally, we incorporate the proposed strategy as well as conventional strategies into the assessment framework proposed for travel time reliability.

3.2.1 Conventional strategies

Conventional strategies to improve the travel time reliability can be represented in the proposed framework. Specifically, two strategies, the travel demand management and the variable speed limit are considered in this study.

Travel demand management

In this study, the travel demand management is broadly defined as any strategies that control the traffic demand so that the quality of service can be maintained high. These strategies include but are not limited to ramp metering, information provision to encourage travelers to make smarter travel decisions (e.g., route choice, departure time choice) to avoid potential congestion, and tolling in order to alleviate congestion. As a result of a proper travel demand management that aims to improve the travel time reliability, inflow to a highway segment could be stabilized. The outcome of travel demand management can be represented in the proposed framework as a small fluctuation in the boundary condition, namely, small $\sigma_{\Delta t}(n, 0)$.

Variable speed limit

The variable speed limit strategy is used in order to suppress stop-and-go waves in congestion and increase traffic safety (Papageorgiou et al. 2008). This strategy limits the maximum speed of vehicles with different approaches such as the variable message sign. Variable speed limit can be represented in the proposed framework as follows. First, the mean of the vehicle-specific maximum speed, $1/p_0$, is decreased. At the same time, the variance of the vehicle-specific maximum speed, $1/\sigma_{p0}$, is decreased.

3.2.2 Proposed headway normalization strategy

This study proposes a new strategy to improve the travel time reliability. This strategy is referred to as the headway normalization strategy.

Estimation method

In this section, a method of estimating dynamic delay externality of individual vehicle is developed. Two sources of input data are used in the proposed method: the trajectories of connected vehicles and a detector data. The output of the proposed methodology includes the reconstructed trajectories of all vehicles which are used to derive the dynamic delay externality. The trajectory reconstruction method follows the conservation law of traffic. The notable feature of the proposed method is that this method does not need the FD information, as opposed to the most of existing trajectory reconstruction methods (Seo et al. 2017). It makes the method free from a pre-calibrated headway–speed relation.

More specifically, the traffic flow on a link is considered. The traffic may be congested due to a fixed bottleneck. It is assumed that the following input data are available:

- Spatiotemporal trajectories of CVs with sufficiently high resolution, and
- One detector that records the passage time of all the vehicles at its location.

The estimation procedure can be described as follows:

1. Computation of cumulative flow of CVs
2. Reconstruction of virtual CV trajectories
3. Reconstruction of trajectories of all the vehicles
4. Detection of congestion and a bottleneck
5. Computation of individual headway in congestion
6. Computation of dynamic delay externality

In the paragraphs below, each of these steps is explained in detail.

Computation of cumulative flow of CVs: In this step, the cumulative flow of CVs is computed by the definition. The cumulative flow of connected vehicles, denoted by $\widehat{N}(t,x)$, is defined as the number of CVs that passed from location *x* by the time t. Since the CV trajectories are given, $\widehat{N}(t,x)\ \forall t,x$ can be directly computed.

Reconstruction of virtual CV trajectories: In this step, trajectories of what we call "virtual CVs" are reconstructed from the cumulative flow of CVs. The virtual CVs are defined as contour lines of the cumulative flow of CVs. The "height" of these contour lines indicates the cumulative flow of CVs at the detector location. Therefore, the virtual CVs can be considered as a representative trajectories of actual traffic, and they satisfy the first-in first-out principle.

Reconstruction of trajectories of all vehicles: In this step, trajectories of all vehicles are reconstructed from the virtual CV trajectories. First, the virtual CV trajectories in Eulerian coordinates, $\widehat{N}(t,x)\ \forall t,x$, are converted into the one in time-based Lagrangian coordinates, $\widehat{T}(n,x)\ \forall n \in P,x$, where *P* denotes a set of CVs. Note that $\widehat{T}(n,x)\ \forall n \in P,x$ is only defined on the CV trajectories. By interpolating

$\hat{T}(n,x)\ \forall n,x$ based on $\hat{T}(n,x)\ \forall n \in P,x$, we can reconstruct the trajectories of all the vehicles. In order to perform this procedure, we employ a simple linear interpolation method. Specifically, the value of $\hat{T}(n,x)\ \forall n \in (n_0,n_1)$ where n_0 and n_1 indicate two CVs that are next to each other, is linearly interpolated by the values of $\hat{T}(n_0,x)$ and $\hat{T}(n_1,x)$. This interpolation method was proposed by Seo and Kusakabe (2015), and fairly good accuracy was reported.

As a result of these steps, trajectories of all the individual vehicles are reconstructed. This can be considered as a traffic state estimation method in Lagrangian coordinates system without a fundamental diagram. The most notable feature is that, as mentioned earlier, the method does not use any fundamental diagrams (or related concepts) or pre-calibrated parameters. This is essentially important for the proposed traffic control strategy because the method is intended to estimate individual headways in congested traffic; if a fundamental diagram was assumed in an estimation procedure, it affects to its estimation results, causing an undesirable bias (for the details, see Seo et al. (2017). From traffic state estimation methodological point of view, the proposed method is similar to those proposed by Astarita et al. (2006); Seo and Kusakabe (2015); Bekiaris-Liberis et al. (2016), in the sense that these methods use CV (or probe vehicles) data, but not fundamental diagrams. The difference, however, is that, in comparison to Astarita et al. (2006); Bekiaris-Liberis et al. (2016), the proposed method is formulated in Lagrangian coordinates so that trajectories of each individual vehicle can be reconstructed, and in comparison to Seo and Kusakabe (2015), the proposed method employs the conventional CV and detector data.

Detection of congestion and a bottleneck: In this step, traffic congestion is detected based on the reconstructed trajectories and a given speed threshold. First, traffic speed in the entire spatiotemporal domain with a given resolution is calculated by applying Edie's definition (Edie 1963) to the reconstructed trajectories $\hat{T}$. Second, cells with a speed lower than a given threshold are determined as congested. Third, a spatiotemporal domain that consists of congested cells that are connected to each other is determined as a congested queue, and its downstream end is considered as a bottleneck that is causing this queue. Alternatively, in case of recurrent congestion, the location of a bottleneck can be specified by detailed analysis on CV trajectories.

Computation of individual headway in congestion: In this step, the individual headway in congestion is computed based on the reconstructed trajectories and the determined congested queue. Theoretically, each vehicle's contribution to the queue can be measured by its headway at the bottleneck location (the details will be explained in the next step). However, the application of this definition to the reconstructed trajectories would be erroneous due to the following reasons. First, the estimated headway at a location might be volatile, since it is a mere estimate. Second, the vehicle order might be different between the reconstructed trajectories and the actual ones, especially when the location is far from the

reference detector. To account for this issue, the proposed method computes each vehicle's contribution to the queue as its mean headway in congested queue. This can be directly computed from the reconstructed trajectories $\hat{T}$.

Computation of dynamic delay externality: In this step, dynamic delay externality (DDE) of each vehicle is computed based on the individual headway and reconstructed trajectories. Kuwahara (2007) introduced the concept of dynamic marginal cost in time-dependent queue at a bottleneck with homogeneous traffic. By extending his work, this study describes the concept of DDE in time-dependent queue at a bottleneck with *heterogeneous* traffic. The DDE is conceptually defined as each vehicle's externality imposed to the other vehicles in the form of delay in a queue. Mathematically, by assuming a point queue model, the externality is expressed as

$$d(n,m) = \bar{h}(n,m)N^{+}(n,m), \tag{8}$$

where *d(n,m)* represents the DDE of vehicle *n* in queue *m*, $\bar{h}(n)$ represents the mean headway of vehicle *n* in queue *m*, and $N^{+}(n)$ represents the number of vehicles following vehicle *n* in queue *m*. The DDE means a vehicle's contribution to total delay in a queue; thus, if the vehicle does not make a trip. the total delay is decreased by its DDE. Since the externality and marginal cost is also an important concept in traffic congestion theory (Yang and Huang 2005; Kuwahara 2007; Ozbay et al. 2007), the proposed DDE would be also useful for congestion management.

Possible control strategies

Once vehicles with excessive headway are identified by the estimation method. their behavior could be corrected by some policy interventions exploiting vehicle connectivity (c.f., connected vehicles). The most naive control scheme would be a psychological measure that simply notifies drivers with long headway to decrease their headway. A more advanced way is a particular congestion charge that charges a fee to drivers with long headway depending on the estimated DDE. By leveraging the vehicle connectivity in the near future, such individualized pricing might be practically possible.

The outcome of the headway normalization scheme can be represented in the proposed traffic flow framework as follows. The variance of the vehicle-specific reaction time ($\sigma_{\tau 0}$) is decreased. Note that in order to predict how the policy interventions, change the value of $\sigma_{\tau 0}$, we need to evaluate the behavioral response models of each individual driver. However, analysis and clarification of detailed behavioral mechanisms regarding this point are out of the scope of this study; it is left for future studies.

3.3 Evaluation of the control schemes

In this section, the effectiveness of the travel time reliability control schemes is evaluated by using the proposed framework.

3.3.1 Simulation setting

The effectiveness of each management strategy is evaluated by conducting numerical simulations based on the proposed framework. We consider a traffic flow that includes 100 vehicles on 300 m length of highway segment. Note that although the scale of the simulation study is small, the implication of the results will not be altered qualitatively when larger scale traffic is considered. The mean of FD parameters except at a bottleneck location is as follows: 80 km/h of the free-flow speed, 200 veh/km of the jam density, and 10 km/h of the backward wave speed; which represents a traffic capacity of 1777.78 veh/h. A bottleneck is located in the middle of the section, and its capacity is 1185.19 veh/h (= the standard capacity times 2/3). The discretization widths are specified as follows: Δn= 1 (veh) and Δx = 5 (m).

Following performance criteria are employed to evaluate the quality of services of the considered highway traffic:

- Mean travel time (TT) of all vehicles (T_M),
- Standard deviation (SD) of TT of all vehicles (T_{SD}), and
- Effective TT (T_E), which is defined as $T_M + \alpha T_{SD}$.

Among these measures, T_{SD} and T_E indicate the TT reliability, whereas T_M indicates the usual mean performance. The effective TT (also known as TT budget, Lo et al. 2006) considers the impact of both of the mean TT and the TT reliability, meaning that it represents the overall performance of a highway. The underlying behavioral assumption of the effective TT is that travelers dislike late arrivals than early arrivals, and thus their perceived (i.e., effective) TT takes the SD into account (Fosgerau and Karlström 2010). The parameter α is called mean–variance ratio, and large if travelers are risk-averse. In this study, we assume α = 1 because observational studies found that α was roughly one (e.g., Lam and Small 2001).

3.3.2 Reference scenarios

Travel time reliability of reference scenarios (i.e., without control) is evaluated first. These results will be used as a benchmark in later sections.

Deterministic case

The deterministic case, namely traffic with $\sigma_\tau = \sigma_p = \sigma_{\tau 0} = \sigma_{p0} = \sigma_{\Delta T} = 0$, is simulated and will be used as a benchmark for the performance evaluation. In the deterministic case, all of the boundary conditions and FD parameters are deterministic; thus, it is identical to the conventional LWR model.

Figure 3-3 shows the generated traffic flow in time–space diagrams. In a time-space diagram, the horizontal axis represents the time (the right is the future), and the vertical axis represents the space. A plot color indicates the value of the traffic state variable. According to the mean traffic states, propagation and diminishing of a traffic jam caused by the bottleneck can be observed. Obviously, the SDs are zero. Figure 3-4 shows the TT dynamics over vehicles, namely, the experienced travel time of each vehicle where vehicles are numbered according to their entrance time. It can be confirmed that the TT changes over time as a result of the propagation and diminishing of the traffic jam. The mean TT was 20.785 unit.

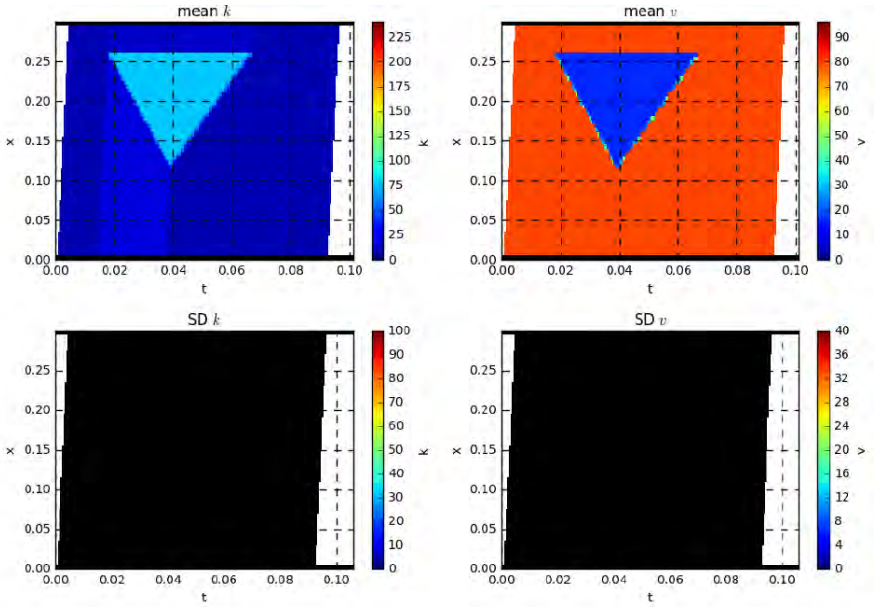

FIGURE 3-3: : TIME–SPACE DIAGRAMS IN THE DETERMINISTIC CASE.

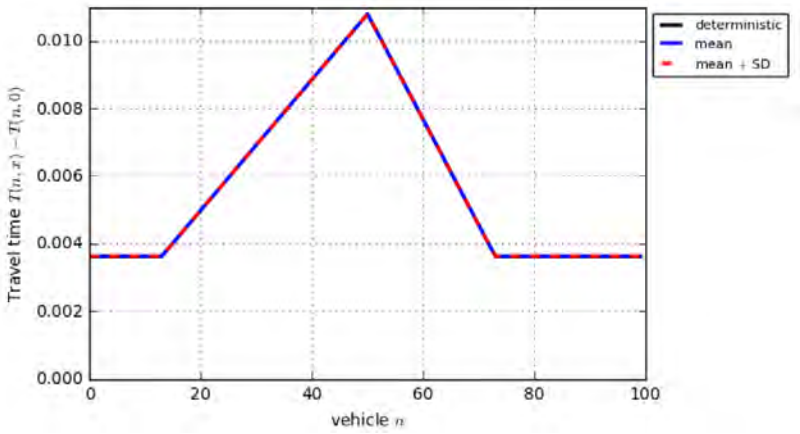

FIGURE 3-4: TT DYNAMICS IN THE DETERMINISTIC CASE.

Stochastic case without traffic management

A stochastic case without traffic management is simulated and will be used as a benchmark for the performance evaluation. The parameter settings are as follows:

$$\sigma_\tau = 0.2\tau_0$$

$$\sigma_p = 0.2p_0$$

$$\sigma_{\tau 0} = 0.05\tau_0$$

$$\sigma_{p0} = 0.05p_0$$

$$\sigma_{\Delta T}(n,0) = 0.2\overline{\Delta T}(n,0)$$

The mean TT and SD were 21.672 unit and 4.736, respectively, resulting in effective TT of 26.408. Compared with the deterministic case, the effective TT was greatly increased due to the stochasticity. This suggests traffic management to improve TT reliability is important.

Figure 3-5 shows the generated traffic flow in time–space diagrams. According to the mean traffic states, a traffic jam similar to the deterministic case can be observed. However, the border between the congested flow and free-flowing flow is blurred. This is because of the stochasticity. According to the SD traffic states, it can be confirmed that traffic fluctuated especially near the shock wave. Figure 3-6 shows the TT dynamics over vehicles. It can be confirmed that the effective TT of the no management case is always larger than that of the deterministic case. The statistics of these two reference cases are summarized in Table 3-1.

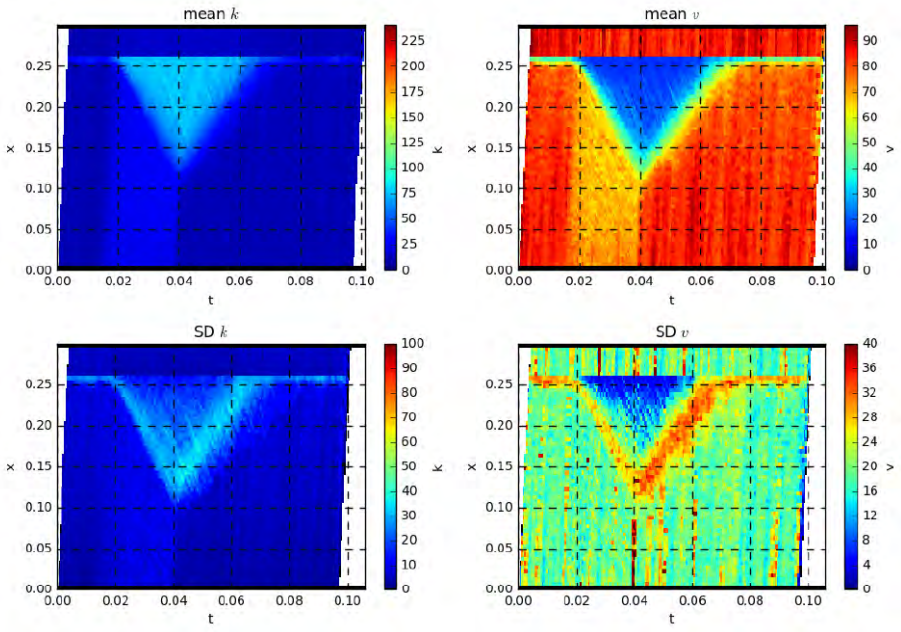

FIGURE 3-5: TIME–SPACE DIAGRAMS IN THE NO MANAGEMENT CASE.

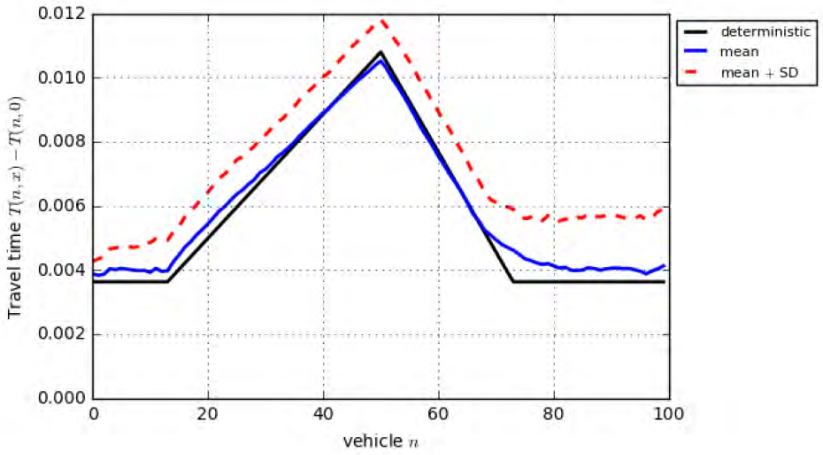

FIGURE 3-6: TT DYNAMICS IN THE NO MANAGEMENT CASE.

TABLE 3-1: STATISTICS OF THE REFERENCE CASES.

	Deterministic	No Management
Mean TT	20.785	21.672
SD TT	0.000	4.736
Effective TT	20.785	26.408

3.3.3 Demand management

In this section, the effectiveness of demand management is investigated. We consider three levels of management: moderate ($\sigma_{\Delta T}(n,0) = 0.05\overline{\Delta T}(n,0)$), gentle ($\sigma_{\Delta T}(n,0) = 0.1\overline{\Delta T}(n,0)$), and strict ($\sigma_{\Delta T}(n,0) = 0.01\overline{\Delta T}(n,0)$). First, the moderate case is investigated in detail; and then other cases are briefly presented and compared with the moderate case.

In the moderate case, the mean TT and SD were considered as 22.320 and 2.728 units respectively, resulting in effective TT of 25.048 unit. Compared to the no management case, the SD is greatly decreased, whereas the mean is slightly increased; the effective TT is improved.

Figure 3-7 shows the generated traffic flow when the moderate management case is used in time–space diagrams. According to the figure, the traffic state is mostly similar to that of the no management case. Figure 3-8 shows the TT dynamics over vehicles in the moderate management. It can be found that the TT dynamics, in this case, is slightly different from that of the no management case. Specifically, the difference between the deterministic TT and mean TT is almost always constant in this case. Additionally, the effective TT after the (mean) congestion is greatly improved.

The statistics of the gently, moderate, and strict management cases are summarized in Table 3-2. According to the table, the SD is decreased as the level of management increased. On the other hand, the mean is somewhat indifferent to the level of management.

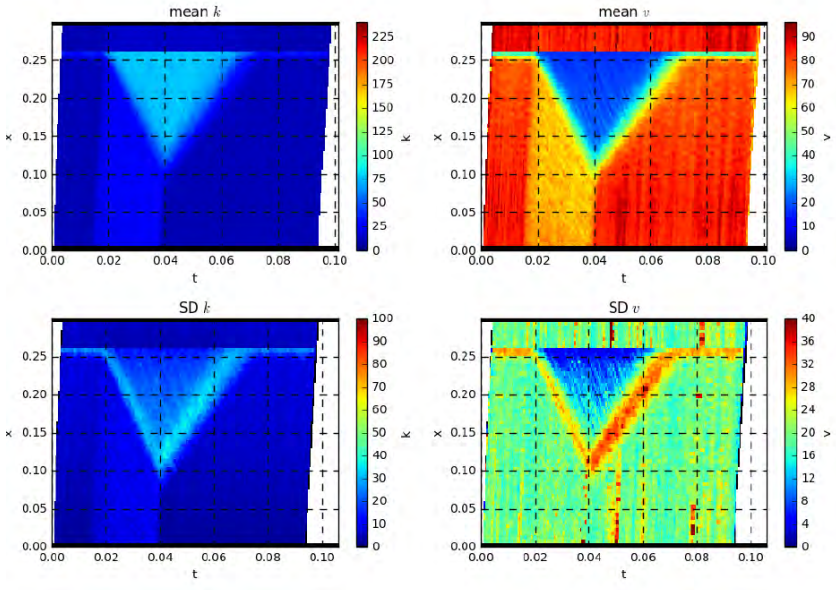

FIGURE 3-7: TIME–SPACE DIAGRAMS IN THE MODERATE DEMAND MANAGEMENT CASE.

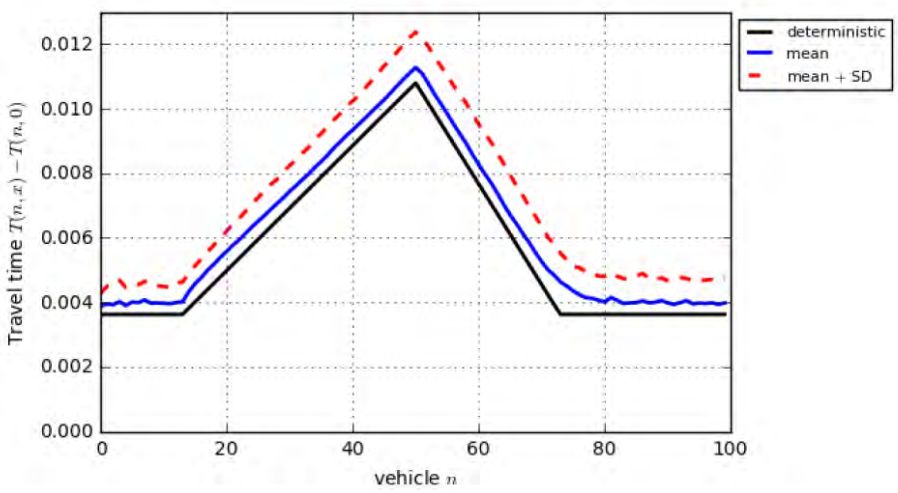

FIGURE 3-8: TT DYNAMICS IN THE MODERATE DEMAND MANAGEMENT CASE.

TABLE 3-2: STATISTICS OF THE TRAVEL DEMAND MANAGEMENT (TDM) CASES.

	TDM (0.1)	TDM (0.05)	TDM (0.01)
Mean TT	22.461	22.320	22.815
SD TT	3.315	2.728	2.690
Effective TT	25.776	25.048	25.505

3.3.4 Variable speed limit

In this section, the effectiveness of the variable speed limit is investigated. We consider three levels of management: moderate ($\sigma_{p0} = 0.05p_0$ and $p_0 := 1.15p_0$), gentle ($\sigma_{p0} = 0.1p_0$ and $p_0 := 1.1p_0$), and strict ($\sigma_{p0} = 0.01p_0$ and $p_0 := 1.19p_0$). First, the moderate case is investigated in detail, and then other cases are briefly presented and compared with the moderate case.

In the moderate case, the mean TT and SD were considered as 22.000 and 4.191 units respectively, resulting in an effective TT of 26.191 unit. Compared to the no management case, the SD is decreased, whereas the mean is slightly increased; the effective TT is slightly improved. This is an expected result, as the variable speed limit generally slows down vehicles with fast speed and thus harmonizes the traffic.

Figure 3-9 shows the generated traffic flow in the moderate management case in time–space diagrams. According to the figure, the speed is different from the no management case. Specifically, the mean speed is slightly slower than that of no management case and the SD of speed is greatly smaller than that of the no management case. Figure 3-10 shows the TT dynamics over vehicles in the

moderate management. This is also most similar to that of the no management case.

The statistics of the gently, moderate, and strict management cases are summarized in Table 3-3. According to the table, the SD is decreased as the level of management increased. On the other hand, the mean and the effective TT are increased to the level of management. This is due to that the variable speed limit decreases the mean free-flow speed. It suggests that there might be the optimal level of variable speed limit. However, it does not necessarily mean strict variable speed limit is always useless because of the following reasons. First, the effective travel time will be improved if the value of α is larger (i.e., travelers are more risk-averse). Second, it is known that the variable speed limit greatly improves traffic safety.

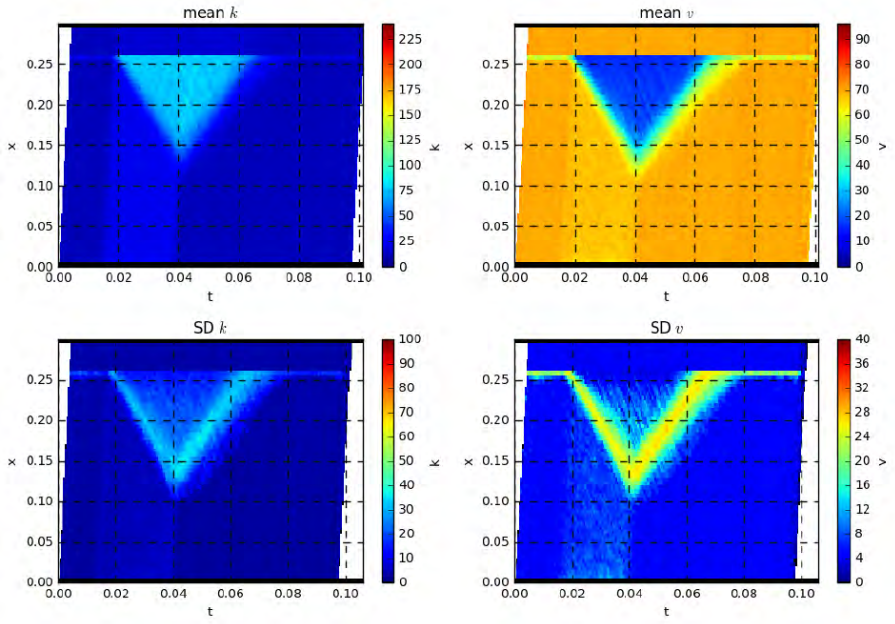

FIGURE 3-9: TIME–SPACE DIAGRAMS IN THE MODERATE VARIABLE SPEED LIMIT CASE.

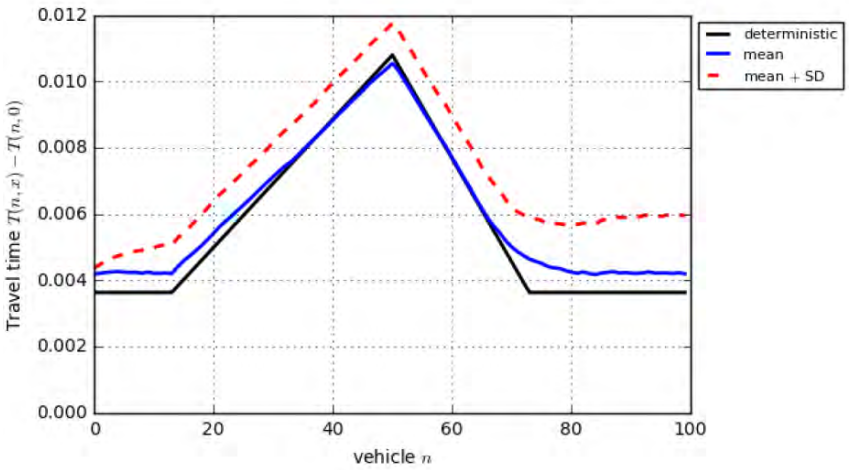

FIGURE 3-10: TT DYNAMICS IN THE MODERATE VARIABLE SPEED LIMIT CASE.

TABLE 3-3: STATISTICS OF THE VARIABLE SPEED LIMIT (VSL) CASES.

	VSL (0.1)	VSL (0.05)	VSL (0.01)
Mean TT	21.910	22.000	22.982
SD TT	4.256	4.191	3.902
Effective TT	26.166	26.191	26.884

3.3.5 Headway normalization

This evaluation consists of two parts. The first part is an evaluation of the mean headway estimation method in section 3.2.2 based on *actual* traffic data. The second part is an evaluation of the travel time reliability improvement scheme based on simulation with the proposed framework of Section 3.1.2.

Estimation accuracy evaluation by NGSIM dataset

In this section, the accuracy of the headway estimation method is evaluated based on actual traffic data. To do so, NGSIM dataset (USDOT 2006) is employed. This dataset includes complete vehicle trajectories on highway segments collected by image recognition. Specifically, we used the data from US-101; in this data, the section length is 650m, the time duration was 15 minutes, and the number of total vehicles was approximately 1800. The schematics of the highway segment is shown in Figure 3-11, and the ground truth traffic speed and vehicle trajectories are shown in Figure 3-12 in time–space diagrams. Several shockwaves and stop-and-go waves were observed due to traffic concentration. As references, the ground truth DDE and the distribution of each vehicle's mean headway in congested traffic are calculated from all the vehicles' trajectories and shown in Figure 3-13. The horizontal axis of Figure 3-13 (left) indicates the order

of vehicles sorted by exit time from the segment. It can be confirmed that DDE largely vary among vehicles due to headway heterogeneity.

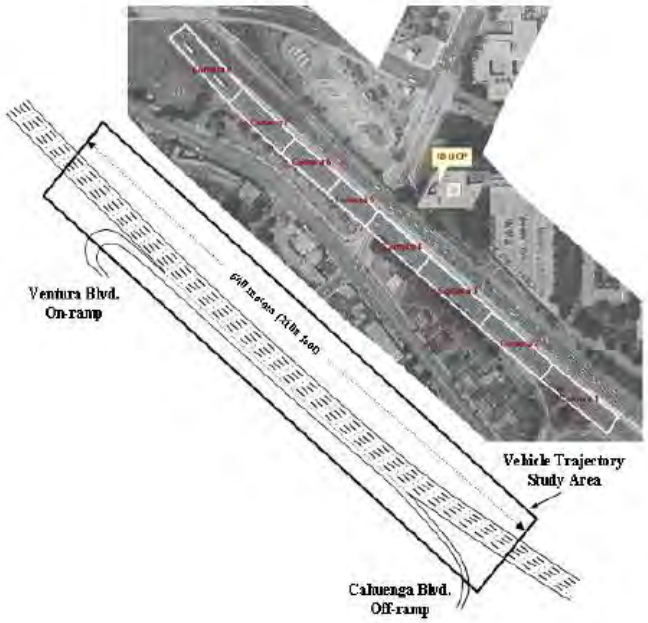

FIGURE 3-11: US-101 (ADOPTED FROM USDOT (2006)).

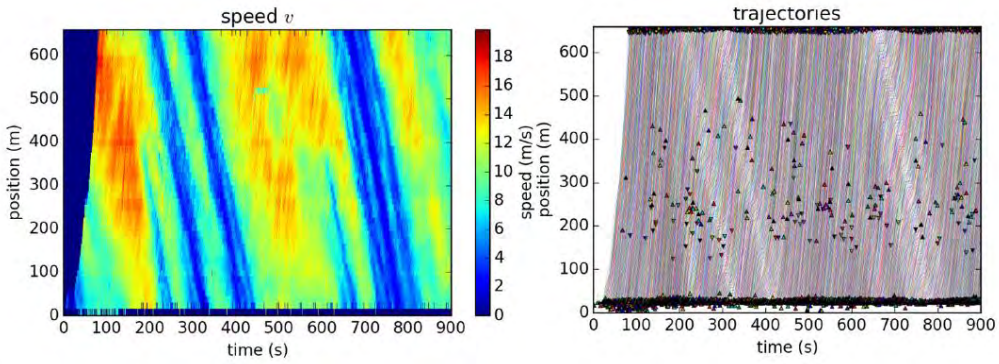

FIGURE 3-12: THE GROUND TRUTH TRAFFIC SPEED (LEFT) AND VEHICLE TRAJECTORIES (RIGHT). DOTS IN THE TRAJECTORIES PLOT INDICATE VEHICLE EXITING/ENTERING VIA OFF/ON-RAMPS.

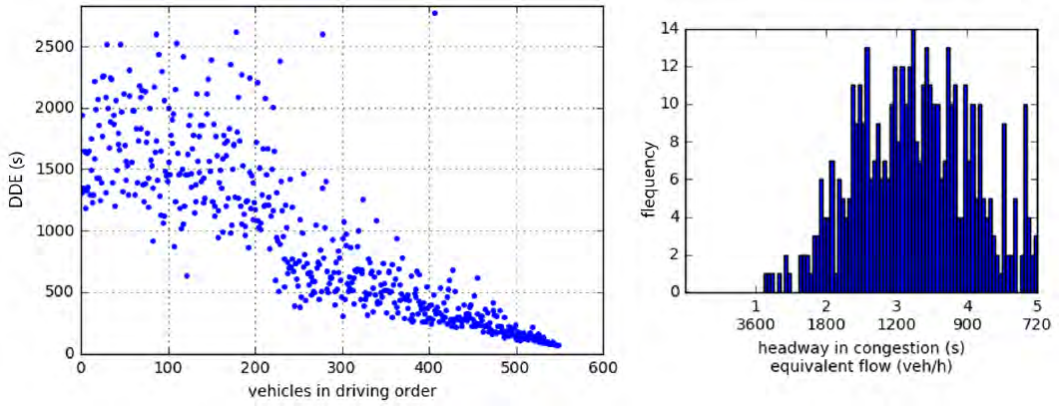

FIGURE 3-13: THE GROUND TRUTH DDE (LEFT) AND THE DISTRIBUTION OF EACH VEHICLE'S MEAN HEADWAY IN CONGESTED TRAFFIC (RIGHT).

The method explained in Section 3.2.2 was applied to the dataset by assuming several penetration rates of CVs to evaluate its estimation accuracy. Figure 3-14 shows the accuracy of the mean headway estimation depending on the penetration rate of CVs, ranging P from 5% to 20%. As an error index, the mean absolute percentage error (MAPE), defined as $\sum_{i=1}^{N}|\hat{x}_i - x_i|/x_i/N \times 100\%$ where $\hat{x}_i$ represents *i*-th estimate, x_i represents its ground truth value, and *N* represents the total number of estimates, is employed and shown in Figure 3-14. According to the figure, it is clear that the accuracy improves as the penetration rate of CVs increases; this is a reasonable behavior.

Figure 3-15 (left) shows the accuracy of the DDE estimation with 15% of CV penetration rate. By comparing to the ground truth (right), it can be confirmed that the general tendency of estimates is similar to that of the ground truth. However, unlike the ground truth, an estimated DDE of a vehicle tends to be similar to that of its neighborhood vehicles. This is an expected result because a mean estimated headway of a vehicle is almost identical to that of a platoon to which the vehicle belongs.

From these results, we conclude that the proposed estimation method can estimate the tendency of DDE fairly accurately when the penetration rate of CVs is sufficiently high, such as more than 15%; thus, the method can provide sufficient information to implement the proposed headway normalization strategy.

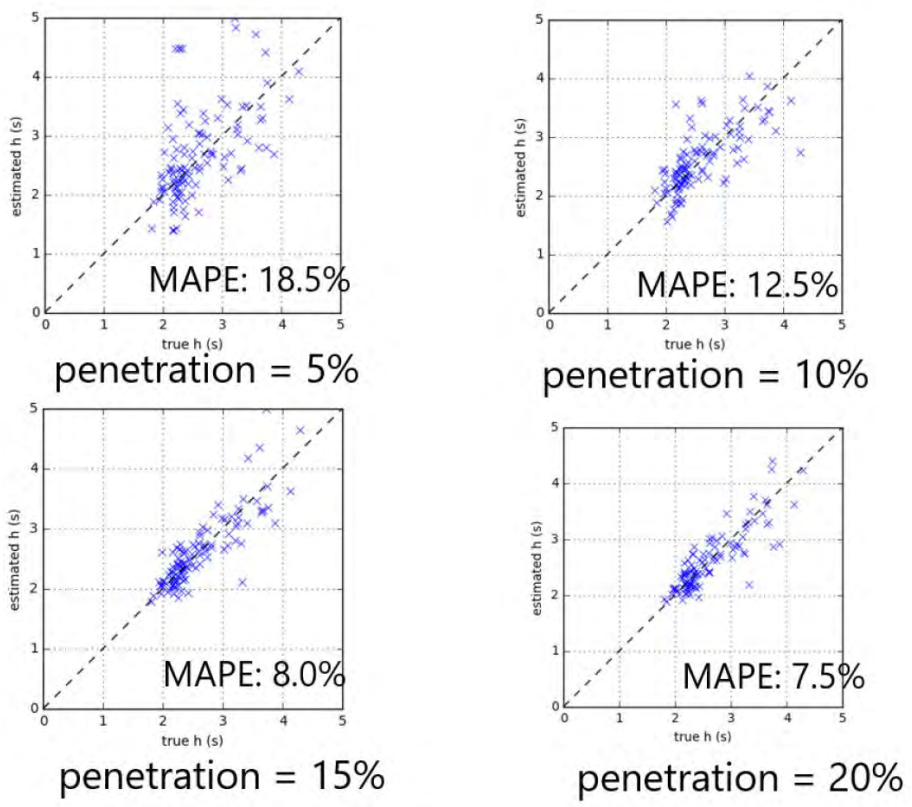

FIGURE 3-14: THE ACCURACY OF MEAN HEADWAY ESTIMATION.

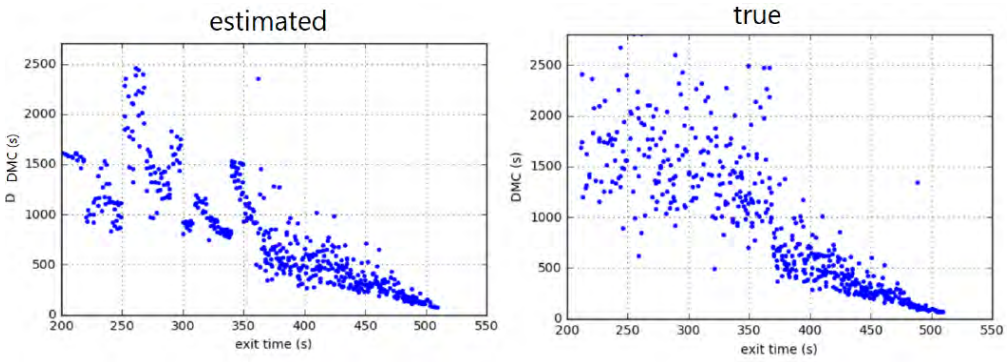

FIGURE 3-15: THE ACCURACY OF DDE ESTIMATION: ESTIMATES (LEFT) AND GROUND TRUTH (RIGHT).

Effectiveness evaluation by simulation

The effectiveness of headway normalization is investigated by assuming that the headway can be properly controlled. We consider three levels of management: moderate ($\sigma_{\tau 0} = 0.05\tau_0$), gentle ($\sigma_{\tau 0} = 0.1\tau_0$), and strict ($\sigma_{\tau 0} = 0.01\tau_0$). In the

following, the moderate case is investigated in detail, and then other cases are briefly presented and compared with the moderate case.

In the moderate case, the mean TT and SD were 21.051 unit and 3.767 unit, respectively, resulting in effective TT of 24.818 unit. Compared to the no management case, both of the mean and SD are decreased; thus, effective TT is also improved. This is an expected result, as the headway normalization generally slows down vehicles with fast speed and thus harmonizes the traffic.

Figure 3-16 shows the generated traffic flow in the moderate management case as time–space diagrams. According to the figure, the traffic state is mostly similar to that of the no management case. Figure 3-17 shows the TT dynamics over vehicles in the moderate management. This is also similar to that of the no management case. However, the mean and effective TT at the peak period of the congestion is remarkably smaller than that of no management case. This may be due to the stabilized capacity due to the headway normalization.

The statistics of the gently, moderate, and strict management cases are summarized in Table 3-4. According to the table, the level of the management is somewhat insensitive to the traffic performance. This suggests that we do not need to implement strict headway normalization scheme; only gentle schemes are sufficient. Moreover, it also suggests that the scheme is robust against the headway estimation error, meaning that the scheme would work well even if CV penetration rate is low.

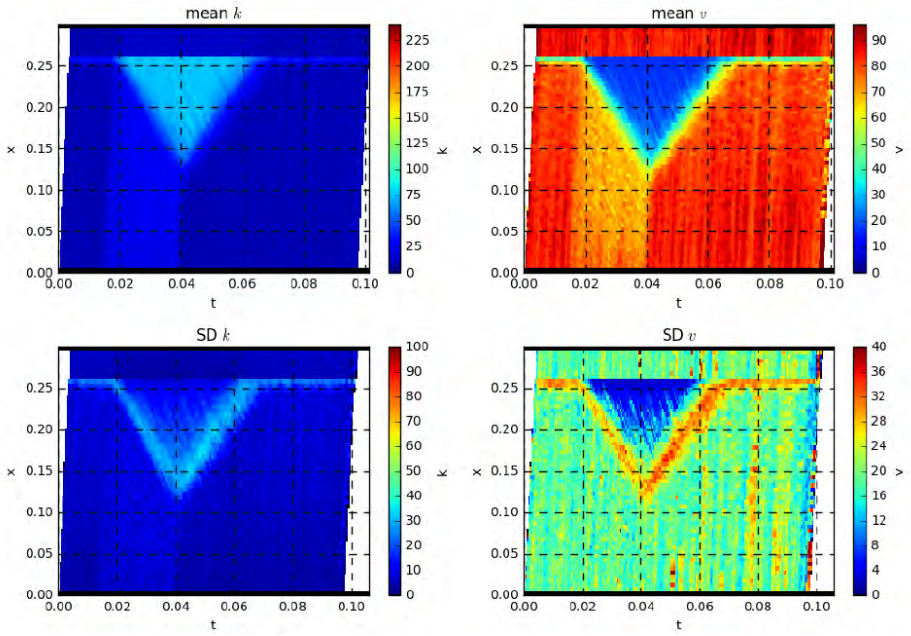

FIGURE 3-16: TIME–SPACE DIAGRAMS IN THE MODERATE HEADWAY NORMALIZATION CASE.

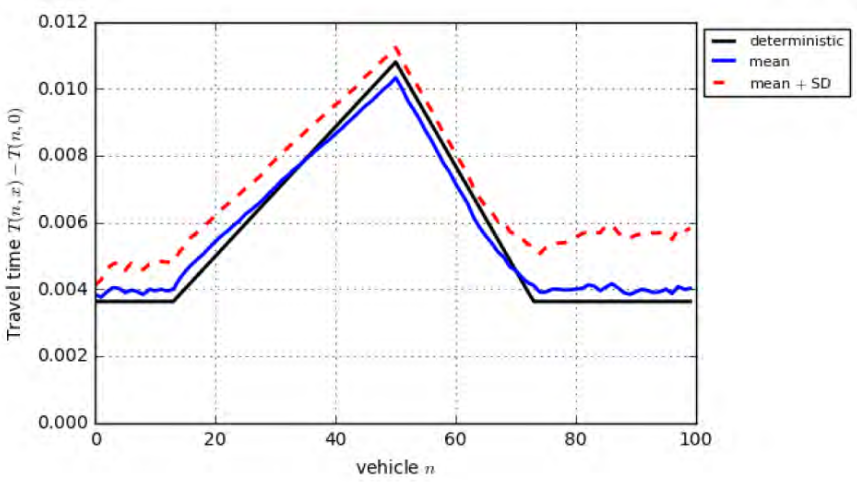

FIGURE 3-17: TT DYNAMICS IN THE MODERATE HEADWAY NORMALIZATION CASE.

TABLE 3-4: STATISTICS OF THE HEADWAY NORMALIZATION (HN) CASES.

	HN (0.1)	HN (0.05)	HN (0.01)
Mean TT	21.303	21.051	21.359
SD TT	3.921	3.767	3.839
Effective TT	25.224	24.818	25.198

3.3.6 Comparison and discussion

The statistics of all of the schemes as well as the reference cases are summarized in Table 5. Given this table, it can be found that the headway normalization strategy tends to realize the smallest effective travel time. The second best option is the travel demand management method. The variable speed limit strategy has the lowest performance in terms of travel time reliability; the effective TT of this strategy is slightly larger than the no management case.

TABLE 3-5: STATISTICS OF ALL THE CASES.

	Deterministic	No Management	TDM (0.1)	TDM (0.05)	TDM (0.01)	VSL (0.1)	VSL (0.05)	VSL (0.01)	HN (0.1)	HN (0.05)	HN (0.01)
Mean TT	20.785	21.672	22.461	22.320	22.815	21.910	22.000	22.982	21.303	21.051	21.359
SD TT	0.000	4.736	3.315	2.728	2.690	4.256	4.191	3.902	3.921	3.767	3.839
Effective TT	20.785	26.408	25.776	25.048	25.505	26.166	26.191	26.884	25.224	24.818	25.198

4. Simulation-based dynamic traffic assignment

4.0. Introduction

Trip assignment is an important step in the four-step travel demand model. User equilibrium model and system optimum model are the two commonly used methods to assign traffic. This study provides dynamic traffic assignment (DTA) solutions. First, an analytical solution is given for a simple road network with dynamic traffic input. Then, for a more complex network, we use a traffic simulation application, GTsim, to provide the simulation solution of DTA.

4.1. Analytical DTA solution for a freeway segment with a detour

In this section, we present an analytical DTA solution for a road network with dynamic traffic inflow.

4.1.1. Description of the system

The road network consists of a freeway segment with a bottleneck of capacity μ0 = 4000 vehicles per hour (vph). Upstream of the bottleneck there is one off-ramp per kilometer, each with a capacity of 1000 vph. The average speed on the arterials is 30 kilometers per hour (kph).

The road network has a demand such that the first 30 minutes the arrival flow is 10,000 vph and then decreases to 2000 vph.

4.1.2. User equilibrium solution

The analytical method to solve the user equilibrium assignment is provided in (Laval 2009). Under user equilibrium, five off-ramps need to be used. The condition of the traffic can be divided into 12 periods. A graphical solution is presented in Figure 4-1. In Figure 4-1, X-axis represents time and Y-axis represents the count of vehicles, A(t) is the arrival curve and D(t) is the departure curve.

Let Δ_r^* be the free flow travel time on off-ramp r

So $\Delta_0^* = 0$, $\Delta_1^* = \frac{1\text{km}}{30\text{km/hr}} = 2\text{min}$, $\Delta_2^* = 4\text{min}$, ..., $\Delta_r^* = 2r$ min. Δ_r^*s are shown in

Figure 4-1 as black dashed lines.

Let $\Delta_r(t)$ be the predictive trip time in route r at time t

(1) $t_0 < t < t_1$

Because $\Delta_0(t) < \Delta_1^*$, all vehicles take the freeway

The slope of $\mathrm{D}(t)$ for $t_0 < t < t_1 + \Delta_1^*$ is 4000veh/hr.

(2) $t_1 < t < t_2$

Because $\Delta_1^* < \Delta_0(t) = \Delta_1(t) < \Delta_2^*$, vehicles begin to take off-ramp 1

The slope of $\mathrm{D}(t)$ for $t_1 + \Delta_1^* < t < t_2 + \Delta_2^*$ is 5000veh/hr.

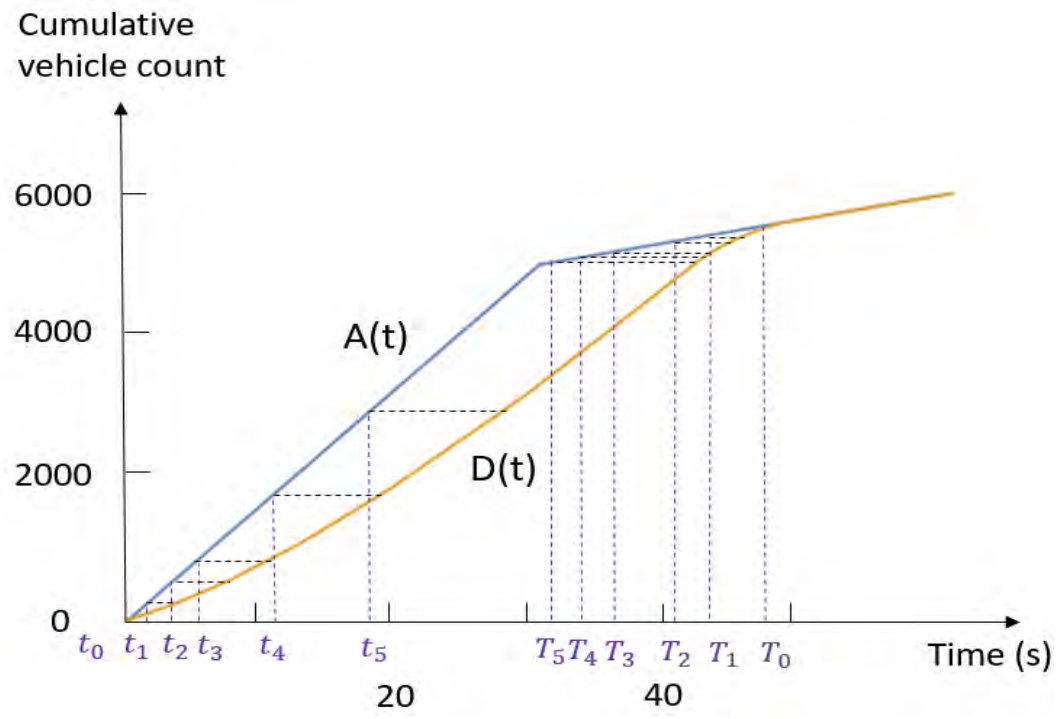

FIGURE 4-1: SIMPLIFIED GRAPHIC SOLUTION METHOD FOR THE USER EQUILIBRIUM.

(3) $t_2 < t < t_3$

Because $\Delta_2^* < \Delta_0(t) = \Delta_1(t) = \Delta_2(t) < \Delta_3^*$, vehicles begin to take off-ramp 2

The slope of $\mathrm{D}(t)$ for $t_2 + \Delta_2^* < t < t_3 + \Delta_3^*$ is 6000veh/hr.

(4) $t_3 < t < t_4$

Because $\Delta_3^* < \Delta_0(t) = \Delta_1(t) = \Delta_2(t) = \Delta_3(t) < \Delta_4^*$, vehicles begin to take off-ramp 3

The slope of $\mathrm{D}(t)$ for $t_3 + \Delta_3^* < t < t_4 + \Delta_4^*$ is 7000veh/hr.

(5) $t_4 < t < t_5$

Because $\Delta_4^* < \Delta_0(t) = \cdots = \Delta_4(t) < \Delta_5^*$, vehicles begin to take off-ramp 4

The slope of $\mathrm{D}(t)$ for $t_4 + \Delta_4^* < t < t_5 + \Delta_5^*$ is 8000veh/hr.

(6) $t_5 < t < T_5$

Because $\Delta_5^* < \Delta_0(t) = \cdots = \Delta_5(t) < \Delta_6^*$, vehicles begin to take off-ramp 5

The slope of $\mathrm{D}(t)$ for $t_5 + \Delta_5^* < t < T_5 + \Delta_5^*$ is 9000veh/hr.

(7) $T_5 < t < T_4$

Because $\Delta_4^* < \Delta_0(t) = \cdots = \Delta_4(t) < \Delta_5^*$, vehicles will no longer take off-ramp 5

The slope of $\mathrm{D}(t)$ for $T_5 + \Delta_5^* < t < T_4 + \Delta_4^*$ is 8000veh/hr.

(8) $T_4 < t < T_3$

Because $\Delta_3^* < \Delta_0(t) = \cdots = \Delta_3(t) < \Delta_4^*$, vehicles will no longer take off-ramp 4

The slope of $\mathrm{D}(t)$ for $T_4 + \Delta_4^* < t < T_3 + \Delta_3^*$ is 7000veh/hr.

(9) $T_3 < t < T_2$

Because $\Delta_2^* < \Delta_0(t) = \Delta_1(t) = \Delta_2(t) < \Delta_3^*$, vehicles will no longer take off-ramp 3

The slope of $\mathrm{D}(t)$ for $T_3 + \Delta_3^* < t < T_2 + \Delta_2^*$ is 6000veh/hr.

(10) $T_2 < t < T_1$

Because $\Delta_1^* < \Delta_0(t) = \Delta_1(t) < \Delta_2^*$, vehicles will no longer take off-ramp 2

The slope of $\mathrm{D}(t)$ for $T_2 + \Delta_2^* < t < T_1 + \Delta_1^*$ is 5000veh/hr.

(11) $T_1 < t < T_0$

Because $\Delta_0(t) < \Delta_1^*$, vehicles will no longer take off-ramp 1, all vehicles take the freeway

The slope of $\mathrm{D}(t)$ for $T_1 + \Delta_1^* < t < T_0$ is 4000veh/hr.

(12) $t > T_0$

There will be no queue because $\mathrm{A}(t)$ is smaller than the capacity of the freeway

The slope of $\mathrm{D}(t)$ for $t > T_0$ is 2000veh/hr.

4.1.3. System optimum solution

The analytical method to solve the system optimum assignment is provided in (Muñoz and Laval 2006). Under system optimum, six off-ramps are used, and the traffic condition of the system can be divided into eight periods. The graphical solution is presented in Figure 4-2 and Figure 4-3.

Let T_r be the time at which the last driver leaves off-ramp r

Let Δ_r be the free flow travel time on off-ramp r

So $\Delta_0 = 0$, $\Delta_1 = \frac{1\mathrm{km}}{30\mathrm{km/hr}} = 2\mathrm{min}$, $\Delta_2 = 4\mathrm{min}$, ..., $\Delta_r = 2r$ min

"We assume that

1. If an off-ramp is used, it is used at maximum throughput
2. All demand must be served
3. Arrival curves are non-decreasing functions
4. After the queue on off-ramp r is cleared, no vehicle will take it
5. The queue on ramp r ends $\Delta_r - \Delta_{r-1}$ times units earlier than on $r-1$:

$$T_r = T_{r-1} - (\Delta_r - \Delta_{r-1})$$

If we know T_0, we can draw $\mathrm{D}(t)$ backward in time. In this case,

$(10000 - 4000)/1000 = 6$ is the highest number of off-ramps p that could possibly be used.

$$\mathrm{D}(t) = \mathrm{A}(T_0) - \sum_{j=0}^{i} \mu_j (T_0 - t) + \sum_{j=1}^{i} \mu_j \begin{cases} \forall t \in [t_p, T_0 - \Delta_p], & \text{if } i = p \\ \forall t \in [T_0 - \Delta_k, T_0 - \Delta_{k-1}], & \text{if } i = k-1 \end{cases}$$

To identify T_0, we first assume T_0 is very large. So $\mathrm{D}(t)$ and $\mathrm{A}(t)$ should only intersect at $t = T_0$. Then we reduce T_0 and move $\mathrm{D}(t)$ along $\mathrm{A}(t)$ until the two curves first touch." (Munoz and Laval, 2006)

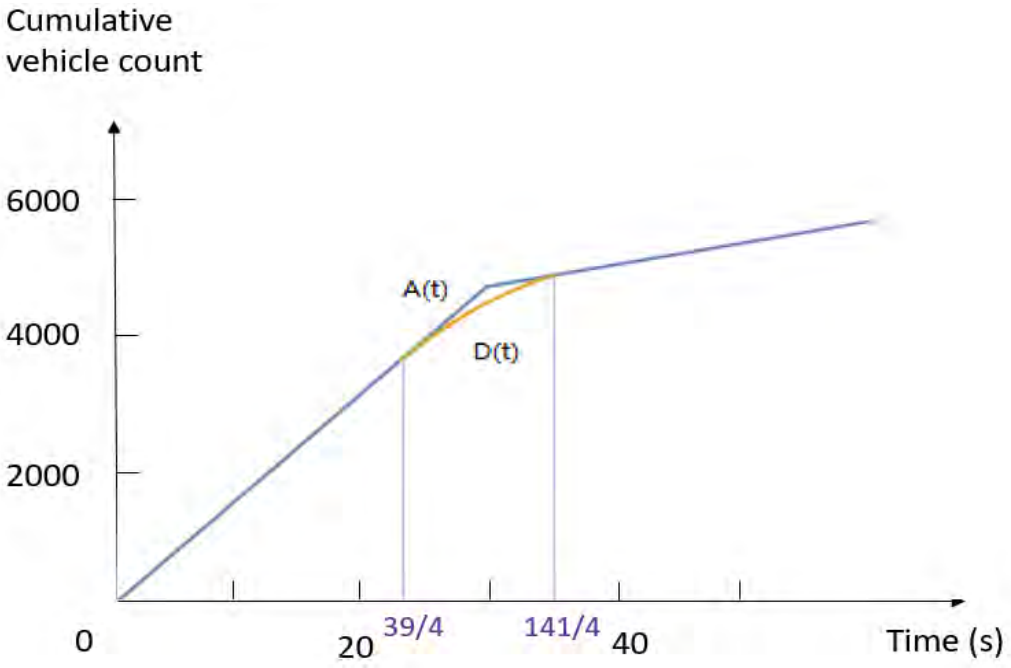

FIGURE 4-2: SIMPLIFIED GRAPHIC SOLUTION METHOD FOR THE SYSTEM OPTIMUM.

(1) $0 < t < 93/4$ Cars departs from freeway and off-ramp 1-6, $\mu = 10000\text{vph}$
(2) $93/4 < t < 101/4$ Cars departs from freeway and off-ramp 1-5, $\mu = 9000\text{vph}$
(3) $101/4 < t < 109/4$ Cars departs from freeway and off-ramp 1-4, $\mu = 8000\text{vph}$
(4) $109/4 < t < 117/4$ Cars departs from freeway and off-ramp 1-3, $\mu = 7000\text{vph}$
(5) $117/4 < t < 125/4$ Cars departs from freeway and off-ramp 1-2, $\mu = 6000\text{vph}$
(6) $125/4 < t < 133/4$ Cars departs from freeway and off-ramp 1, $\mu = 5000\text{vph}$
(7) $133/4 < t < 141/4$ Cars departs only from the freeway, $\mu = 4000\text{vph}$, $q = 4000\text{vph}$
(8) $t > 141/4$ Cars departs only from the freeway, $\mu = 4000\text{vph}$, $q = 2000\text{vph}$

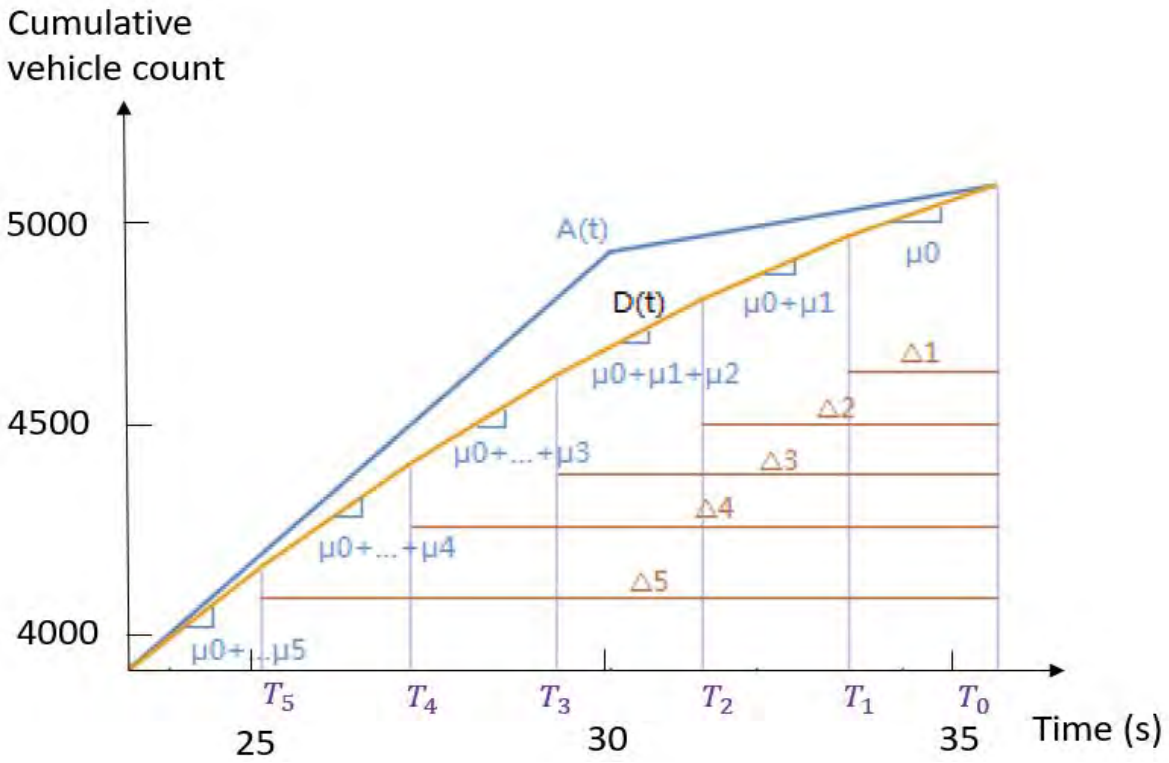

FIGURE 4-3: CLOSE UP OF SIMPLIFIED GRAPHIC SOLUTION METHOD FOR THE SYSTEM OPTIMUM

4.1.4. Comparison

The delays for the two assignments are:

$$\mathrm{TD}_{UE} = 43596.2 \text{ min and } \mathrm{TD}_{SO} = 18608.3\text{min}$$

Therefore, we can conclude that the total cost of the system optimum is much less than that of the use equilibrium. In real life, we can apply ways such as congestion cost in dynamic traffic assignment to move the system from user equilibrium toward system optimum.

4.2. DTA solution for a network based on simulation

In this section, we present a simulation DTA solution for a road network with traffic signal and ramp metering devices.

4.2.1. Description of the system

The transportation system consists of a three-lane freeway and a one-lane urban street. There is a one-direction connection from the city street to the freeway. The free-flow speed is 100 km/hr on freeway and on-ramp. On the city streets, the free-flow speed is 60 km/hr.

There are two traffic control devices in the system. One traffic signal is located on the urban street with a cycle of 60 seconds and an even split into green and red. A ramp metering device is located on the on-ramp to the freeway, whose rate is calculated based on the ALINEA algorithm.

There are two origins and one destination in the system. The inflow rate of vehicles at the city street (CS) origin is 1200 vehicles/hr and the inflow rate at the freeway (FW) origin can vary. All vehicles go to a single destination. The vehicles from the CS origin can take either the FW route or the CS route. The vehicles from the FW origin go to the destination all the way through the freeway.

The objective is assigning the vehicles from the CS origin to the two possible routes with DTA methods. It would be hard for us to perform an analytical analysis for such a network with multiple control devices. Therefore, we perform simulations in GTsim to get assignment solutions.

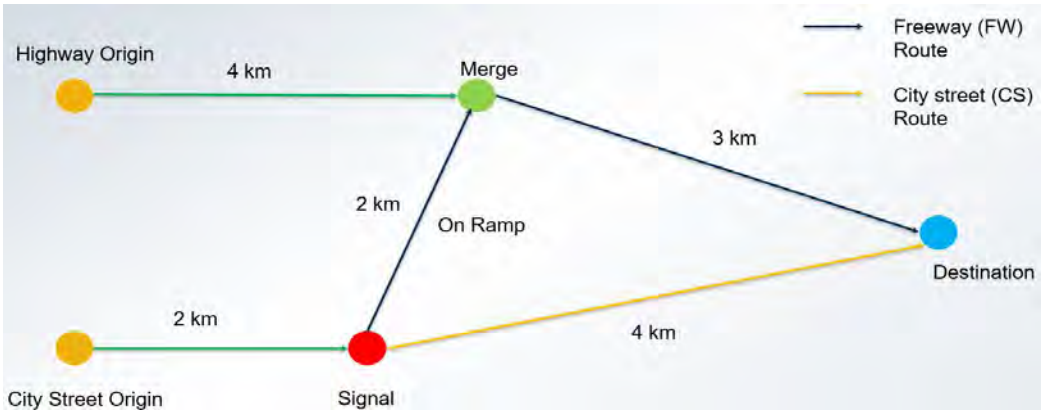

FIGURE 4-4: THE NETWORK TO BE STUDIED

4.2.2. GTsim

GTsim is a micro-simulation application to accurately model real-world conditions. This application includes the latest advancements in lane changing models that can explain congestion dynamics such as capacity drop. It also has several driver behavioral models for mandatory lane changes to replicate real-world behavior during congested traffic conditions. The application has been written in JAVA using the NetBeans IDE. Users can design a road network and input traffic into the system. The program can then update each vehicle's velocity, location, and animation every time-step.

The application can record the travel time of all users in the network and the cars are able to adjust their routes dynamically based on the average travel time.

We have the network modeled in GTsim as in Figure 4-5.

FIGURE 4-5: THE NETWORK OF THE TRANSPORTATION SYSTEM MODELED IN GTSIM.

4.2.3. User equilibrium solution

As shown in Section 4.2.1, the vehicles from the CS origin can choose either the FW route or the CS route. Under the user equilibrium scenario, every vehicle in the simulation select the route with current lower travel time. The travel time time on each route in the simulation is calculated based on the space-mean travel time of the last 20 vehicles on that route.

We set different scenarios which vary on the freeway traffic flow: (i) low flow: 1500 vehicles/hr, (ii) medium flow: 4000 vehicles/hr and (iii) 6500 vehicles/hr. For each scenario, we can get its results directly from the simulation output.

Under the user equilibrium traffic assignment, the route choice and travel time results are listed in Table 4-1. Here is the explanation of routes: (i) Route 1: city street origin to destination through local streets, (ii) Route 2: city street origin to destination through freeway, and (iii) freeway origin to destination.

TABLE 4-1: USER EQUILIBRIUM ROUTE CHOICE AND TRAVEL TIME RESULTS

Freeway flow	Route 1		Route 2		Route 3		Avg TT (s)
	Veh count	Avg TT	Veh count	Avg TT	Veh count	Avg TT	
Low	0	N/A	981	480.0	1395	258.9	350.2
Medium	0	N/A	978	481.8	4698	255.7	302.8
High	824	465.6	174	444.6	6045	255.7	284.9

When the freeway flow is low, the average speed on the freeway is close to free-flow speed, such that the travel time of Route 2 is less then Route 1. Therefore, all vehicles choose the freeway route under this scenario. When the freeway flow is high enough, vehicles start to take Route 1 to avoid freeway congestion.

4.2.4. System optimum solution

Under the system optimum scenario, the goal is to minimize the total travel time of all vehicles in simulation. The method in this study used is binary search to find the best route assisnment ratio.

We set different scenarios which vary on the freeway traffic flow: (i) low flow: 1500 vehicles/hr, (ii) medium flow: 4000 vehicles/hr and (iii) high flow: 6500 vehicles/hr. For each scenario, we compare different assignment strategies based on the average travel time metric and get the best route assignment policy.

Under the system optimum traffic assignment, the route choice and travel time results are listed in Table 4-2.

TABLE 4-2: SYSTEM OPTIMUM ROUTE CHOICE AND TRAVEL TIME RESULTS.

Freeway flow	Route 1		Route 2		Route 3		Avg TT (s)
	Veh count	Avg TT	Veh count	Avg TT	Veh count	Avg TT	
Low	814	426.5	182	458.2	1395	258.2	330.7
Medium	929	428.4	67	472.4	3720	253.7	291.2
High	998	433.8	0	N/A	6045	252.5	278.2

4.2.5 Comparison

Obviously, under system optimum, the average travel time of the network is less than that under user equilibrium. Notice that, more vehicles take Route 2 (freeway) under user equilibrium because the free-flow travel time through Route 2 is less than that through Route 1. However, this costs a higher network average travel time.

5. SAFETY BENEFITS OF ATM STRATEGIES

5.0. Introduction

In developing methods to optimize the efficiency and safety of a roadway, a common and relatively low-cost solution is to implement ATM strategies, which are capable of actively or automatically adapting to current traffic conditions to create noticeable improvements, primarily to travel times and congestion levels. ATM is defined by the ability to dynamically manage recurrent and non-recurrent congestion conditions based either on real-time or pre-planned parameters. ATM strategies can include such methods as speed harmonization, variable speed limits, hard shoulder running, adaptive ramp metering, dynamic signing, dynamic pricing of express lanes, optimized traffic diversions such as lane use control, and queue warning systems. It is important to note that typically methods such as high-occupancy vehicle or toll lanes, bus only lanes, and other managed lane types are not included as active traffic management (NCHRP, 2014). While ATM strategies have been proven to increase freeway reliability and decrease travel times as a whole, there is a relative lack of research regarding the specific safety effects of implementing these strategies. A factor may be a lack of uniformity of how ATM strategies are used in many cases, and many of these methods are not commonplace in the United States.

Additionally, directly measuring the impact of ATM strategies on safety along a roadway is difficult or even impossible in many cases. For instance, many studies on the effects of active traffic management focus solely on the benefits to roadway capacity and travel time, relying on more anecdotal evidence regarding safety conditions. ATM strategies are also commonly used in conjunction with other safety measures, so isolating the effect of one in particular out of a system of traffic management methods becomes unfeasible. In many studies, active traffic management is assumed to correlate to a direct benefit to roadway safety, but due to the nature of these devices, the degree to which they benefit safety is more difficult to determine. That is not to say there are no accounts of how ATM approaches directly affect safety, as many studies have been able to analyze either isolated systems or combined systems through means such as modeling or before-after analysis to demonstrate how conditions are made safer.

5.1. Speed Harmonization and Variable Speed Limits

One such ATM method that studies have shown a degree of success in determining its impact on safety is speed harmonization. Speed harmonization, simply speaking, is an attempt to reduce the speed variance between and within travel lanes, and as such create a more uniform and acceptable headway distribution that should reduce the potential for primary collisions. It reduces the amount of “stop and go” traffic, leading to a more stable flow along the roadway, as well as improved travel times (Nezamuddin et al. 2011). Similarly, variable speed limits (VSLs) can be used to this effect, which performs by altering the speeds of vehicles based on current volume and congestion

conditions in an attempt to reduce overall delay. While determining the safety effects of VSLs may difficult, as with speed harmonization, there are some studies that do determine their effect based on data.

For example, as a broad measure of what kind of effect speed harmonization and VSLs can have, a case study in Germany that analyzed traffic along the A9 Autobahn found that with these methods of traffic control, the roadway saw a 14% to 37% lower injury crash rate per vehicle-km (Metz et al. 1997). Similarly, a study included within a report from the NCHRP in 2014 concluded that across the spectrum of deployments in Europe, VSLs tended to reduce collision rate between 10% and 50% after deployment. This same study showed an analysis of a VSL deployment, as well as dynamic lane assignments, in Seattle, Washington using before-after analysis, finding that the total crash rate due to these methods decreased by 11% along the analyzed corridor (Sorrell, 2014). Another set of studies looked at the effects of VSLs on the M25 Motorway in the UK. This motorway was equipped with dual looped detectors every 0.3 miles, which provided volume data that automatically lowered speed limits when volumes reached specified thresholds. A preliminary study of this roadway saw that with VSLs, the number of collisions reduced by 10% (Harbord and Jones, 1996). Later, a pilot test of a new algorithm was performed, set to detect queues and slow-moving traffic. This system would lower speed limits in sections immediately prior to the end of the queue, and raise them again once the queue had progressed. Overall, with this system injury type crashes were reduced by 28%, found at a 95% confidence level, though the study did claim part of this figure may have been directly influenced by roadwork. Along with this crash reduction, the roadway saw a 5% increase in traffic demand, which was able to be accommodated without increasing congestion (Harbord 1998).

As an example of potential shortcomings studies can see when analyzing ATM methods, a study based in Michigan during summer 2002 analyzed Interstate-96, noting the effects of VSLs. Ultimately, this study produced very little usable data regarding safety, due to the highly limited time frame of the project. Their crash analysis did show a general trend of safety improvement in corridors where VSLs were deployed compared to others but showed a striking lack of data with total crash counts differing by almost negligible amounts. The ultimate conclusion of this crash analysis was that the installation of VSLs did not appear to cause any safety issues, but whether it increased safety “was not clear” (FHWA 2004). In an effort to somewhat mitigate other shortcomings, when direct analysis is not necessarily feasible, estimation or simulation modeling becomes a preferred method to determine ATM safety effects. One such study utilized a log-linear based microsimulation model to predict crash rates in relation to VSLs. Their ultimate findings based on the developed model predict that with VSLs active, they could reduce crash potential between 5% and 17%, by temporarily reducing speed limits during risky traffic conditions, which were specified by a pre-determined threshold (Lee et al. 2006).

5.2. Hard Shoulder Running

According to a compilation of information from reports by the FHWA, an estimated 40% of congestion in the United States is a result of insufficient capacity (Nezamuddin et al. 2011). Hard shoulder running primarily is a method to temporarily increase the capacity of a roadway when conditions warrant it, inherently reducing the potential of congestion conditions. Oftentimes shoulder-running lanes are opened during pre-specified hours, such as regular peak or rush-hour times, or subjectively when congestion levels have reached a certain threshold. In general, hard shoulder running is treated as a temporary measure, since road maintenance cost and time limitations can be imposed by frequent shoulder use. Shoulder running's safety benefit lies in this congestion reduction, as the improvement to speeds and travel times seen along the roadway should also decrease the potential for rear-end crashes. Additionally, this is a modification that often does not require any major infrastructure changes or expansion. Such a change, however, does potentially require relatively intense intelligent transportation system (ITS) deployments such as message signs to adequately indicate drivers to times that the shoulder is open for use (Nezamuddin et al. 2011).

When focusing the steps necessary to open hard shoulders to traffic, a study in Germany analyzed the purpose and safety effects of hard shoulder running, citing that the main functions of hard shoulders were to serve as an area to leave damaged vehicles, lateral space for avoiding obstacles on the roadway, a temporary traffic lane, or a place where maintenance crews or emergency vehicles can operate. Generally, this study found that roadways without hard shoulders showed a 25% higher collision rate and during testing found that when hard shoulders were opened as permanent lanes, congestion levels decreased between 68 and 82%, with a 9% increase in average speed. For temporarily opened shoulders lanes, they found that overall collision rates were reduced by half as a whole when considering approach and exit segments as well as the main highway segment. However, they found that when temporary shoulder lanes were opened during such times as heavy congestion periods, they did not have a significant effect on crash rates, as the number of congestion-induced or related crashes decreased but lane-change collisions increased at the same time (Kellermann, 2000). A separate study of sites in Germany was able to determine a significant improvement to safety and crash rates, however, citing that the data found a reduction in overall congestion of 30%, and a reduction in crashes due to traffic jams of 25% (Jones et al. 2011).

A significant risk when implementing hard shoulder running is that it may pose a tendency to worsen conditions for downstream traffic. One such study noted that a project that implemented hard shoulder running with the intent of reducing the "bottleneck" effect of peak-period traffic did achieve its overall goal, an increase in capacity of 16% and a 25% increase in speed along the portion of the roadway where shoulder running was implemented, but the additional flow created and then

discharged by this section actually caused worse congestion levels downstream (Cohen 2004). Additionally, similar to research work on methods such as speed harmonization, much of the research that has been done on hard shoulder running primarily focuses on congestion levels and travel times that are improved by ATM implementation rather than explicit safety effects. Another Germany-based study, for instance, cited specifically that roadway capacity increased by 20% with shoulder use, but was unable to provide anything but anecdotal evidence regarding safety effects, claiming only "significant accident and congestion reduction" (Riegelhuth and Pilz, 2007).

5.3. Ramp Metering and Junction Control

Another method used primarily to reduce congestion along a freeway is ramp metering and junction control. This method consists of traffic signals used at freeway on-ramps to reduce the rate at which vehicles enter the freeway. This has significant positive effects on the traffic stream, as it divides up platoons of merging vehicles, which minimizes their impact and disruption to the freeway, and can reduce the total number of merging vehicles as well, keeping the freeway at higher travel speeds without other disruptions (Nezamuddin et al. 2011). In many cases, this strategy is also seen to increase vehicle throughput, and actively decrease travel times and crash rates as a result (Taylor and Meldrum, 2000). Similarly, dynamic junction control, in response to high traffic demands, allocates lane access on mainline and ramp lanes in interchanges, particularly near high-volume entrance ramps. These can dictate traffic upstream of the entrance ramp, assigning lanes as through-exit, or exit only depending on demand (Nuedorff and McCabe, 2015). Additionally, while many other ATM strategies are more frequently seen in European countries, ATM strategies like ramp metering have seen significant use in the United States as well.

For example, a study performed for the Minnesota Department of Transportation analyzed the effects before and after shutting down an extensive ramp metering system near Minneapolis-St. Paul for a 6 week evaluation period. In a summary of their findings, they determined that without ramp meters, the freeway volume saw an overall reduction of freeway volume of 9% and a 14% reduction in peak period throughput, as well as a 7% reduction in freeway speed and an overall 26% increase in crashes. In terms of the cost due to implementing this ramp metering system and the overall benefits it provided, they determined that without ramp metering, the benefit/cost ratio is 5:1, while when ramp metering is in effect, the benefit/cost ratio was found to be 15:1, approximately 3 time more cost effective for the safety and efficiency benefits it provides (Levinson et al. 2005). Other safety statistics found in a report from the NCHRP in 2014 show that adaptive ramp metering, when compared with no ramp metering has shown a decrease in collisions in areas such as Portland, OR, by 43% during the peak period, Seattle, WA, by 39% overall, Minneapolis, MN, by 24% during the peak period, and Long Island, NY, by 15% overall (NCHRP, 2014).

A further collection of studies across the United States helps to demonstrate how effective ramp metering can be in improving safety conditions for drivers. Firstly, one such study that analyzed 5 ramps along I-25 in Denver, Colorado, performed in 1981 and 1982, found that with ramp metering in place, average speeds typically decreased by 58% and reduced the overall crash rate by 5%. A similar study in Portland, Oregon, in 1981 analyzed 16 metered ramps along I-5, finding that while metering was in effect, there was an approximate reduction in peak period collisions of 43%. This crash reduction occurred while average peak-period speeds increased in the northbound direction from 16 to 41 mph and in the southbound direction from 40 to 43 mph (Nezamuddin et al. 2011). Another study that analyzed 9 ramp metering stations along the Superstition Freeway in Arizona, using before-after analysis of 3 years each, found that when ramp metering was in use, rear-end and sideswipe crashes reduced by 10%, while crash rate overall increased by about 33% when ramp metering was not in use. However, the total crashes occurring just on the ramps themselves did see an increase in the after case, as traffic was required to stop during metered periods. Another notable factor in this study was that it found that during the after period, crashes increased by 24% overall on both the mainline road and ramps when metering was in effect but increased by 43% while ramp metering was not in effect. They concluded that this still demonstrates how the ramp meter system increased safety overall, and the overall increase in crash rate was likely due to large increases in traffic volume between the before and after cases. A study that analyzed six ramps along I-94 in Detroit, Michigan, also noted an increase in traffic volume, increasing from approximately 5600 to 6400 vehicles per hour, though with ramp metering in effect the total number of crashes decreased by nearly 50%, while the number of injury crashes dropped by 71%. Finally, a study based in Seattle, Washington, implemented ramp metering over a 6-year evaluation period, noting a crash rate decrease of approximately 39%, along with mainline volume increases of 86% in the northbound direction and 62% southbound (Nezamuddin et al. 2011).

Specifically pertaining to junction control, one study in Los Angeles along state route 110 utilized blank-out signs. These allowed the lane adjacent to the exit-only lane to be used as either an exit or through-lane during peak period conditions. After implementation, the study saw that the average ramp delay reduced from over 20 minutes to less than 5, and decreased total crashes by 30% from the previous year. One aspect this study did not address, however, is whether any other factors were implemented or played a role in this reduction figure, or if the data acquired specifically shows that the dynamic junction control was the primary cause. Still, figures such as this do show promise that such ATM methods have a positive effect on driver safety (Moinuddin, 2012).

5.4. Dynamic Signing and Re-Routing

A variation of active traffic management intended to more effectively direct traffic is dynamic signing and re-routing. Dynamic signing serves to alert drivers to irregular traffic conditions and attempt to provide directions to a more optimal route. These are placed in such a way that, in response to an event such as non-recurring congestion, signs are installed at critical locations to provide sufficient notice to drivers, warning them of approaching conditions and providing an alternate route that will help to better maintain traffic flow. These are often deployed in conjunction with other ATM strategies such as speed harmonization and hard shoulder running and can be connected to traffic management centers that coordinate alternate route information. Dynamic signing can also be used in relation to a local community, giving advance notice to drivers less familiar with the area of special events or other potential delays (Nezamuddin et al, 2011). Related to dynamic signing, lane use control signs, in addition to re-routing traffic when necessary, have safety effects on the general public outside of crash reduction. In some studies, law enforcement or first responders have noted that the use of lane control signals can help to slow traffic or move it away from blocked lanes while responding to an incident, allowing for a better response time while still maintaining traffic flow (NCHRP 2014).

Unfortunately for this ATM method, determining its effect on driver safety is difficult. Given that this method is meant to warn drivers of adverse conditions or determine an alternate route, the actual safety effects tend to be inferred at best. This method has been shown to reduce travel times for those re-routed compared to those in the congested or adverse conditions, as well as reduce congestion levels overall, but concrete data regarding the effect on safety seen by dynamic signing is severely lacking. Instead, there is simply an implied benefit to driver safety, based on the improvement to driver conditions overall.

5.5. Queue Warning Systems

Queue warning systems are another ATM strategy meant to provide advance notice to drivers of approaching congestion conditions. These are frequently deployed alongside road construction work, since construction or maintenance work performed on a roadway often requires at least one lane along the travel way to be closed to traffic, greatly increasing the potential for congestion to occur. Typically, a queue warning system consists of a series of traffic sensors that relay information to an ITS, which is able to detect the current traffic conditions in real-time that then connects to a variable message sign that changes its displayed message accordingly based on a set of pre-defined criteria. For instance, the system may be set to initially display the message “Road Work Ahead” when as much as a minor delay is detected. As traffic slows or even comes to a near stop, the message sign will then be set to a message akin to “Slowed”

or “Stopped Traffic, 2 miles”, depending on where the detectors determine the back of the queue presently is (Ullman et al. 2016).

General studies of queue warning systems have shown that they primarily decrease rear-end type crashes by providing drivers with advanced warnings and allowing them to have a greater reaction time. One study, in particular, cited that around 60% of rear-end crashes could be prevented if drivers had an extra half-second to react to slower traffic. This same study also cited that in general, queue warning systems have been found to reduce rear-end crash frequency between 14% and 44% (Khazraeian et al. 2017). According to a synthesis of ATM effects in European countries, one study of queue warning systems along an autobahn in Germany found that crashes were reduced by 20% with queue warning systems in place, while crashes increased by 10% on a similar roadway without this same warning system (Brinckerhoff, 2010). A case study that found highly promising results regarding queue warning systems’ effects on safety analyzed a freeway construction project along I-35 in Texas. This project spanned over 96 miles of roadway in total, widening the freeway from four to six lanes. In addition to the queue warning system used during construction hours, this project also used portable rumble strips, meant to provide a more auditory and tactile signal to drivers, though they did not have a major effect on vehicle speeds. Ultimately, this study recorded over 200 nights both with and without queue warning systems deployed, and with this data were able to estimate the total crashes were reduced 44% while deployment was active. Additionally, in a monetary analysis, the total reduction in crashes during deployment translated to a reduction in crash costs of approximately $1.36 million, an average of over $6000 per night. However, these figures may not be fully representative of the safety effects seen by queue warning systems, as it was not directly correlated to actual traffic conditions, meaning that though queues were expected for every recorded night, it was not determined whether or not queues actually formed (Ullman et al. 2016).

5.6. ATM Strategy Combinations

Though there have been numerous studies that were able to clearly discern specific ATM strategies’ effects on roadway safety, it is often not feasible to study the effects of a single method in particular. Many transportation agencies will tend to implement several ATM strategies at once rather than introduce one at a time in different phases and study the effects, as this would not be the safest approach. It instead keeps the roadway safer in many cases to implement as many strategies as deemed necessary in as close a time frame as possible, but unfortunately for research purposes, this limits the relevancy of data pertaining to traffic safety, as it causes the safety effects of one ATM method to be indistinguishable from the effects of the system as a whole. Instead, for such cases an individual effect can only be inferred or modeled at best, and may not be entirely representative of actual conditions.

However, numerous studies have been performed that analyze the overall safety effects of a combination of ATM strategies on a given roadway. One such study focused on the effects of multiple ATM strategies along 7.5 miles of Oregon Route 217 in 2016, which at the time of the study had seen traffic volumes more than double over the last three decades, and are expected to increase by a further 30% by 2025. As a result, the corridor's safety and reliability continued to decline, as it was often operating at or above capacity. Due to limited funding as well, major infrastructure changes were not feasible, and so ATM was implemented for a relatively lower cost safety and efficiency improvement to the roadway beginning in 2014. Ultimately, this roadway utilized ATM strategies such as queue warning, congestion-related variable speed limits, weather-responsive variable speed limits, dynamic ramp metering, and curve warning. Across the entire corridor, the collected crash data saw a reduction in total crashes by 21%, with a nearly 60% reduction in typical crash severity. Primarily, the kinds of crashes that were reduced were those due to congestion conditions such as rear-end and side-swipe crashes, which accounted for 86% of the total crash reduction. One aspect of note is that wet or icy surface condition crashes did increase by 17.5% after ATM implementation, but the study saw that total days with rain increased from 51 days prior to this project to 63 days and a nearly 55% increase in overall precipitation levels over the same period of time. This study also noted that in one particularly volatile section of roadway, a variable message sign that alerted drivers to hazardous curves decreased total crashes between 40 and 60% and crash severity by 70 to 92%. While this is an encouraging figure, it is worth noting again that these locations, in particular, were historically volatile, and so are not necessarily representative of the safety effects as a whole. But, while it is somewhat an overstatement of the safety benefits seen by this particular ATM method, it does still demonstrate an undeniable safety improvement.

Other safety benefits of combinations of ATM systems were recorded in an FHWA report (Nuedorff and McCabe, 2015), which gave brief summaries of a variety of different safety analyses. One such study analyzed a before-after study of a 7-mile corridor of Interstate-5 near Seattle, Washington, which implemented dynamic speed limits, dynamic lane assignment, and queue warning along the entire stretch in addition to previous management such as ramp metering and a "robust" traveler information system. What this study saw was that during the total 6 years of before-after analysis, the total crashes decreased by 4.1% along the ATM segment, and actually saw a 4.4% increase in crash rate where ATM strategies were not implemented (WSDOT, 2014). Another study based in Minneapolis, Minnesota, along I-35 West analyzed the effects of dynamic speed limits, dynamic lane assignment, queue warning, and dynamic shoulder lane use as high-occupancy toll lanes. This study focuses on the 6-month post-deployment period of the ATM methods, which saw 17% less congestion, largely credited to the dynamic speed limit use, as well as a total reduction in fatal plus injury type crashes of 9% as well as over a 20% reduction in property damage only (PDO)

crashes (Nuedorff and McCabe, 2015). A study based in the UK along Motorway M25 utilized dynamic speed limits and dynamic lane assignment showed promising results relating to safety and congestion, as the data showed a reduction in typically shockwaves per morning rush hour from 7 to 5 after implementation, as well as a reduction in injury type crashes of 10% and a reduction in PDO crashes by 30% (Harbord et al. 2007). Another UK-based study that analyzed M24 utilized dynamic speed limits, dynamic lane assignment, and dynamic shoulder lanes, found that after implementation, the PDO crash rate decreased by 30% and injury crash rates decreased from approximately 5.2 per month to 1.5 per month. Additionally, the maximum speed was increased from 55 to 60 mph with shoulder lanes, and average travel times were decreased by 4% with no adverse safety effects (Department for Transport, 2008).

5.7. Crash Modification Factors

In addition to directly determining crash rates and severity, another method used to determine the safety of different ATM methods is through crash modification factors (CMFs), which are used to compute the expected number of crashes after implementing a particular countermeasure. Simply put, multiplying current crash counts by the appropriate CMF will provide an estimation of what future crash counts will be, and thus give insight into the safety effect of the countermeasure (Clearinghouse).

For instance, as found in values published within CMF Clearinghouse, a promising CMF for the installation of variable speed limits is 0.71 for an urban environment. This particular CMF was obtained from a study that analyzed all crash types and severity levels through before-after empirical Bayes analysis of a 7.23 mile roadway segment in Washington. This study period ranged from 2007 to 2012, with 1175 crashes recorded in the before period, and 599 after (Pu et al. 2017).

Relating to installation of ramp meters, an analysis in California found a CMF through simple before-after analysis of 0.64. This study analyzed all crash types and severities on a two-way freeway. This finding was based on 19 sites and 57 sight-years before and after. The before period showed 219 crashes and the after 137 (Liu and Wang, 2013).

A CMF regarding changeable signs, specifically curve speed warning signs, analyzed all crash types and severities for a rural, principal arterial. Through simple before-after analysis, an ultimate CMF of 1.13 for this ATM method was found, which does indicate that during the after period the crash rate actually increased (Tribbet et al. 2000). However, from the published Clearinghouse values, though this CMF was ranked at the top of its category it is still ranked overall as “poor”, indicating that its actual effect on safety is significantly different.

Finally, after a meta-analysis of urban principal arterials in the UK, for installation of a queue warning system, a CMF of 0.84 was found for injury-type crashes. Specifically, this value was determined for rear-end type crashes. For property damage only crashes,

however, from this same source the CMF value was 1.16 (Elvik and Vaa, 2004). This value does make logical sense, however, as queue warning installation can still increase the overall rate of rear-end type collisions, even if in most cases they tend to decrease. Given that from this source injury type crashes decreased from queue warning, it is likely that overall crashes could have increased slightly, while they primarily decreased in severity.

6. Summary and conclusions

This report documents the findings from a multi-institutional effort to enhance our capability of analyzing and improving freeway travel time reliability.

In Chapter 2, we have investigated the effect of incidents on freeway segment capacity. The main objective was to develop methods to enable the calibration and validation of the emergent travel time distribution for a baseline condition of a freeway facility, using existing probe data sources. A portion of WB I-540 in Raleigh, NC, was selected as the study area in which the proposed method was tested. Between January 2014 and December 2018, the team identified 22 isolated incidents (away from the recurring congestion period) that closed one or two lanes of traffic, creating a distinct congestion pattern. By applying a genetic algorithm calibration method on each incident day and calibrating the incident CAFs, optimal time-dependent CAFs were derived that best represented the impact of incidents on the freeway segment capacity. By analyzing the optimal CAFs, the strongest relationship was revealed to be between the optimal time-dependent CAF and the temporal progression of the incident. A regression model was developed to represent this behavior. This was formulated in a manner that can directly adjust the current HCM's fixed CAF values (for a specific lane closure configuration) for modeling incidents both in a single day, seed file application, or for an entire year reliability analysis.

In Chapter 3, a unified framework for assessing the freeway travel time reliability was presented. This framework is based on a novel Lagrangian formulation of a traffic flow model, making it capable of efficiently investigating the relation between the travel time reliability and individualized vehicle control. Additionally, a novel control strategy for travel time reliability is proposed. This strategy controls each vehicle's headway based on connected vehicle data. The effectiveness of the new strategy as well as conventional methods, namely, travel demand management and variable speed limit, was investigated by the proposed framework. The headway normalization strategy tends to realize smaller effective travel time compared to conventional strategies. The headway normalization strategy was effective even if the intervention was mild; it implies that the strategy may be accepted by the traveling public.

In Chapter 4, we found the DTA solutions for different types of road networks, through both analytical analysis and simulation. System optimum assignment saves much travel time compared to the user equilibrium assignment.

In Chapter 5, it was noted that directly measuring the impact of ATM strategies on safety along a roadway is difficult or even impossible in many cases. ATM strategies are also commonly used in conjunction with other safety measures, so isolating the effect of one in particular out of a system of traffic management methods becomes unfeasible. In many studies, active traffic management is assumed to correlate to a direct benefit to

roadway safety, but due to the nature of these devices, the degree to which they benefit safety is more difficult to determine. That is not to say there are no accounts of how ATM approaches directly affect safety, as many studies have been able to analyze either isolated systems or combined systems through means such as modeling or before-after analysis to demonstrate how conditions are made safer.

7. RECOMMENDATIONS

Specific recommendations from each task are as follows. It is recommended to extend the work in Chapter 2 beyond one- and two-lane closure incidents and to potentially incorporate additional explanatory variables to improve on its predictive ability (current combined data model R^2= 0.544). This effort will require a significant amount of data collection as higher severity incidents are quite rare and the need to isolate the effect of the incident from other factors makes it difficult to achieve a statistically meaningful sample size. Further research is needed to confirm the results of this study for freeway with a different number of lanes than our generally three-lane study did. Finally, additional work is needed to extend the recurring congestion calibration efforts to other segment types beyond basic segments, such as merge, diverge and weaving segments. In Chapter 3, a unified framework was proposed to assess travel time reliability. It is recommended to conduct in-depth research on the behavioral response to the headway normalization strategy. This is because the effectiveness of the strategy inherently depends on how drivers adjust their headway according to individualized control. The simulation-based platform, reported in Chapter 4, needs to be further enhanced to achieve its ultimate goal, i.e., conducting simulation-based dynamic traffic assignments to assess ATM strategies in a timely fashion for realistic networks.

This project has laid a foundation for developing tools for analyzing and optimizing system reliability on freeways. We recommend furthering the investigation. The end product of this series of research would include analytical and simulation frameworks for the optimization and near real-time performance forecast of ATM systems. The strategies will include local and/or system-wide adaptive ramp metering, integrated ramp-metering and variable speed limit control, hard shoulder running, speed harmonization, dynamic pricing of express lanes, optimized traffic diversions and efficient incident response and management. ATM deployment is a means to meet specific reliability goals below a desirable agency specified threshold. Ultimately, we aim to develop a novel integrative process of system modeling that will select and optimize appropriate strategies from the ATM toolbox to meet reliability goals.

Future research also includes field implementation and testing, and developing guidelines on the implementation of the proposed ATM strategies. It will also develop a scheme to optimally select the various ATM strategies available at a given facility, with consideration of their user benefits and implementation costs.

8. REFERENCE LIST

1. Aghdashi, S., N. Rouphail, and A. Hajbabaie. (2013). Estimation of Incident Propensity for Reliability Analysis in the Highway Capacity Manual. Transportation Research Record: Journal of the Transportation Research Board, 2013. 2395: 123-131.
2. Astarita, V., Bertini, R. L., d'Elia, S., Guido, G., 2006. Motorway traffic parameter estimation from mobile phone counts. European Journal of Operational Research 175 (3), 1435–1446.
3. Bekiaris-Liberis, N., Roncoli, C., Papageorgiou, M., 2016. Highway traffic state estimation with mixed connected and conventional vehicles. IEEE Transactions on Intelligent Transportation Systems 17 (12), 3484–3497.
4. Caliper. TransModeler Traffic Simulation Software. https://www.caliper.com/transmodeler/default.htm. Accessed July 15, 2019.
5. CMF Clearinghouse. "About CMFs", US Department of Transportation Federal Highway Administration. www.cmfclearinghouse.org/about.cfm.
6. Cohen, S. "Using the Hard Shoulder and Narrowing Lanes to Reduce Congestion. Some Lessons from an Experience on the Paris Motorway Network", The 12th IEE Conference on Road Transport Information and Control, London, UK. 149-15. 2004.
7. Daganzo, C. F., 2006. On the variational theory of traffic flow: well-posedness, duality and applications. Networks and Heterogeneous Media 1 (4), 601–619.
8. Daganzo, C.F. The cell transmission model: A dynamic representation of highway traffic consistent with the hydrodynamic theory. Transportation Research Part B: Methodological, 1994. 28: 269-287.
9. Daganzo, C.F. The cell transmission model, part II: network traffic. Transportation Research Part B: Methodological, 1995. 29: 79-93.
10. Department for Transport. "Advanced Motorway Signaling and Traffic Management Feasibility Study", A report to the Secretary of State for Transport, London, United Kingdom. March 2008.
11. Edie, L. C., 1963. Discussion of traffic stream measurements and definitions. In: Almond, J. (Ed.), Proceedings of the 2nd International Symposium on the Theory of Traffic Flow. pp. 139–154.
12. Elvik, R. and T. Vaa, "Handbook of Road Safety Measures", Oxford, United Kingdom, Elsevier. 2004.
13. Farradyne, P. Traffic Incident Management Handbook. Prepared for Federal Highway Administration, Office of Travel Management, 2000.
14. Federal Highway Administration. "Synthesis of Active Traffic Management Experiences in Europe and the United States", FHWA-HOP-10-031. US Department of Transportation, Washington D.C. May 2010.
15. Federal Highway Administration. "A Field Test and Evaluation of Variable Speed Limits in Work Zones", US Department of Transportation, Washington, D.C. 2004.
16. Federal Register 2016-08014. National Performance Management Measures; Assessing 17 Performance of the National Highway System, Freight Movement on the Interstate System, 18 and Congestion Mitigation and Air Quality Improvement Program. Federal Highway Administration, U.S. Department of Transportation.
17. Fosgerau, M., Karlström, A., 2010. The value of reliability. Transportation Research Part B: Methodological 44 (1), 38–49.

18. Harbord, B. “M25 Controlled Motorway: Results of the First Two Years”, Proc 9th Int. Conference on Road Transport Information and Control, Institution of Electrical Engineers, 21-23. London, UK, 149-154. April 1998.
19. Harbord, B. and J. Jones. “Camera Enforcement of Traffic Regulations (Digest No: 1996/252)”, IEE Colloquium on Volume 18, 5/1 - 5/4. 1996.
20. Harbord, B., J. White, K. McCabe, A. Riley, and S. Tarry. “Calmed and Controlled – Improving Efficiency, Safety, and Emissions”, Traffic Technology International pp. 100-105. 2007.
21. Hadi, M., Y. Xiao, T. Wang, P. Hu, J. Jia, R. Edelstein, and A. Lopez. Pilot Testing of SHRP 2 Reliability Data and Analytical Products: Florida. The National Academies Press, Washington, D.C., 2014. https://doi.org/10.17226/22331.
22. Hall, F.L., L. Bloomberg, N.M. Rouphail, B. Eads, and A.D. May. Validation results for four models of oversaturated freeway facilities. Transportation Research Record: Journal of the Transportation Research Board, 2000. 1710: 161-170.
23. HERE. https://www.here.com/. Accessed July 20, 2019.
24. Holland, J. H. Adaptation in natural and artificial systems: an introductory analysis with applications to biology, control, and artificial intelligence. University of Michigan Press, Ann Arbor, Michigan, 1975.
25. Institute of Transportation Engineers. Traffic Management Data Dictionary (TMDD) and Message Sets for External Traffic Management Center Communications (MS/ETMCC). http://www.ite.org/tmdd. (undated)
26. INRIX. http://inrix.com/. Accessed July 20, 2019.
27. Jabari, S. E., Zheng, F., Liu, H., Filipovska, M., 2018. Stochastic Lagrangian modeling of traffic dynamics. In: Transporation Research Board 97th Annual Meeting.
28. Jones, J., M. Knopp, K. Fitzpatrick, M. Doctor, C. Howard, G. Laragan, J. Rosenow, B. Struve, B. Thrasher, and E. Young. “Freeway Geometric Design for Active Traffic Management in Europe”, FHWA-PL-11-004. US Department of Transportation, Washington D.C. March 2011.
29. Karmakar, N., S. Aghdashi, N.M. Rouphail, and B.M. Williams. Validation and Calibration of Freeway Reliability Methodology in the Highway Capacity Manual: Method and Case Studies. Transportation Research Record: Journal of the Transportation Research Board, 2018. 2672: 93-104.
30. Kleinbaum, D.G., L.L. Kupper, A. Nizam, and K.E. Muller. Dummy Variables in Regression. In Applied Regression Analysis and Other Multivariate Methods. Duxbury Press: Belmont, CA, 2008, pp. 217-233.
31. Kellermann, G. “Experience of Using Hard Shoulder to Improve Traffic Flow.” Traffic Engineering and Control 41, 412-414. 2000.
32. Khazraeian S., H. Mohammed, and Y. Xiao, “Safety Impacts of Queue Warning in a Connected Vehicle Environment”, Transportation Research Board. January 2017.
33. Kondyli, A., B. St. George, L. Elefteriadou, G. Bonyani, “Defining, Measuring, and Modeling Capacity for the Highway Capacity Manual” ASCE *Journal of Transportation Engineering, Part A: Systems*, Vol 143(3), March 2017. (10.1061/JTEPBS.0000017)
34. Kuwahara, M., 2007. A theory and implications on dynamic marginal cost. Transportation Research Part A: Policy and Practice 41 (7), 627–643.
35. Lam, T. C., Small, K. A., 2001. The value of time and reliability: measurement from a value pricing experiment. Transportation Research Part E: Logistics and Transportation Review 37 (2), 231–251.

36. Lagrangian traffic state estimator for freeways. IEEE Transactions on Intelligent Transportation Systems 13 (1), 59–70. 19.
37. Laval, J. A., Leclercq, L., 2013. The Hamilton–Jacobi partial differential equation and the three representations of traffic flow. Transportation Research Part B: Methodological 52, 17–30.
38. Lee, C., B. Hellinga and F. Saccomanno. “Evaluation of Variable Speed Limits to Improve Traffic Safety”, Transportation Research Part C 14, 213-228. 2006.
39. Levinson, D., K. Harder, J. Bloomfield, and K. Winiarcyzk. “Ramp Meter Delays, Freeway Congestion, and Driver Acceptance”, University of Minnesota Center for Transportation Studies Report CTS 05-02. 2005.
40. Liu, C. and Z. Wang, "Ramp Metering Influence on Freeway Operational Safety near On-ramp Exits", International Journal of Transportation Science and Technology, Vol.2, No.2, Multi Science Publishing, pp.87-94. 2013.
41. Leclercq, L., Laval, J. A., 2009. A multiclass car-following rule based on the LWR model. In: Traffic and Granular Flow’ 07. Springer, pp. 151–160.
42. Leclercq, L., Laval, J. A., Chevallier, E., 2007. The Lagrangian coordinates and what it means for first order traffic flow models. In: Allsop, R., Bell, M., Heydecker, B. (Eds.), Transportation and Traffic Theory 2007. Elsevier, pp. 735–753.
43. Lighthill, M. J., Whitham, G. B., 1955. On kinematic waves. II. a theory of traffic flow on long crowded roads. Proceedings of the Royal Society of London. Series A. Mathematical and Physical Sciences 229 (1178), 317–345.
44. Laval J A (2009). Graphical Solution and Continuum Approximation for the Single Destination Dynamic User Equilibrium Problem. Transportation Research Part B, 43 (1): 108-118
45. Lo, H. K., Luo, X., Siu, B. W., 2006. Degradable transport network: travel time budget of travelers with heterogeneous risk aversion. Transportation Research Part B: Methodological 40 (9), 792–806.
46. Muñoz J C and Laval, J A (2006). System optimum dynamic traffic assignment graphical solution method for a congested freeway and one destination. Transportation Research Part B, 40 (1): 1-15.
47. Metz, N., H. Schlichter, and H. Schellenberg. “Positive Effects of a Traffic Control System on Fuel Consumption and Exhaust Emissions on the German A9 Autobahn.” Int. J. of Vehicle Design 18 (Special Issue), 354-367. 1997.
48. Mitchell, D., “Doing More With Less”, Traffic and Transit, Roads and Bridges. October 7, 2016.
49. Moinuddin, S., “Dynamic Lane Management – An ITS Solution to Enhance Safety and Mobility: NB SR 110 to NB I-5 Connector”, California Department of Transportation. July 2012.
50. Nezamuddin N., N. Jiang, T. Zhang, T. Waller, and D. Sun, “Traffic Operations and Safety Benefits of Active Traffic Strategies on TxDOT Freeways”, Texas Department of Transportation, Austin, TX, October 2011.
51. Nisbet, J., D. Bremmer, S. Yan, D. Murshed, Y. Wang, Y. Zou, W. Zhu, M. Dunlap, B. Wright, T. Zhu, and Y. Zhang. Pilot Testing of SHRP 2 Reliability Data and Analytical Products: Washington. The National Academies Press, Washington, D.C., 2014. https://doi.org/10.17226/22254.
52. Newell, G. F., 1993a. A simplified theory of kinematic waves in highway traffic, part I: General theory. Transportation Research Part B: Methodological 27 (4), 281–287.

53. Newell, G. F., 1993b. A simplified theory of kinematic waves in highway traffic, part II: Queueing at freeway bottlenecks. Transportation Research Part B: Methodological 27 (4), 289–303.
54. Newell, G. F., 1993c. A simplified theory of kinematic waves in highway traffic, part III: Multi-destination flows. Transportation Research Part B: Methodological 27 (4), 305–313.
55. Newell, G. F., 2002. A simplified car-following theory: a lower order model. Transportation Research Part B: Methodological 36 (3), 195–205.
56. Nuedorff, L., and K. McCabe, "Active Traffic Management (ATM) Feasibility and Screening Guide", FHWA HOP-14-019. US Department of Transportation, Washington D.C. May 2015.
57. North Carolina Department of Transportation. Drive NC. https://drivenc.gov/. Accessed July 20, 2019.
58. North Carolina Department of Transportation. Connect NC. https://connect.ncdot.gov/resources/State-Mapping/Pages/Traffic-Volume-Maps.aspx. Accessed August 2018.
59. North Carolina Department of Transportation. Traveler Information Management System. https://tims.ncdot.gov/tims/. Accessed March 2019.
60. Ozbay, K., Bartin, B., Yanmaz-Tuzel, O., Berechman, J., 2007. Alternative methods for estimating full marginal costs of highway transportation. Transportation Research Part A: Policy and Practice 41 (8), 768–786.
61. Papageorgiou, M., Kosmatopoulos, E., Papamichail, I., 2008. Effects of variable speed limits on motorway traffic flow. Transportation Research Record: Journal of the Transportation Research Board (2047), 37–48.
62. PTV group. PTV Vissim. http://vision-traffic.ptvgroup.com/en-us/products/ptv-vissim/. Accessed July 15, 2019.
63. Pu, Z., Z. Li., W. Zhu, Z. Cui, and Y. Wang. "Evaluating Safety Effects of Variable Speed Limit System using Empirical Bayesian Before-After Analysis", Presented at the 96th Annual Meeting of the Transportation Research Board, Paper No. 17-05863, Washington, D.C. 2017.
64. Rama, P. "Effects of Weather-Controlled Variable Speed Limits and Warning Signs on Driver Behavior", Transportation Research Record 1689, 53-59. 1999.
65. Riegelhuth, G. and A. Pilz. "Temporary Hard Shoulder Use in Hessen: Experiences and Strategic Planning". Technical Session 3.3: ERP achievements and results in Traffic Management. 2007.
66. Richards, P. I., 1956. Shock waves on the highway. Operations Research 4 (1), 42–51.
67. Seo, T., Bayen, A. M., Kusakabe, T., Asakura, Y., 2017. Traffic state estimation on highway: A comprehensive survey. Annual Reviews in Control 43, 128–151.
68. Seo, T., Kusakabe, T., 2015. Probe vehicle-based traffic state estimation method with spacing information and conservation law. Transportation Research Part C: Emerging Technologies 59, 391–403.
69. Sorrell, C., Texas A&M Transportation Institute, Battelle, and Kimley-Horn and Associates Inc. "Planning and Evaluating Active Traffic Management Strategies", NCHRP Project 03-114. National Cooperative Highway Research Program. September 2014.
70. Tribbet, L., P. McGowen, and J. Mounce, "An Evaluation of Dynamic Curve Warning Systems in the Sacramento River Canyon", Sacramento, California Department of Transportation. 2000.
71. Takayasu, A., Hara, Y.,Wada, K., Kuwahara, M., 2016. Traffic state estimation considering stochasticity of input data based on variational theory. In: Proceedings of the 21st International Conference of Hong Kong Society for Transportation Studies.

72. Trask, J. L. Optimization Methods for Calibration and Analysis of Congested Freeway Facilities. North Carolina State University, Operations Research PhD Dissertation, 2017.
73. Trask, J.L., S. Aghdashi, J. Baugh, and N.M. Rouphail. Capacity Calibration for Freeway Facilities Methodology in the HCM: A Metaheuristic Approach. Transportation Research Board, Washington, D.C., 2017.
74. The Center for Advanced Transportation Technology Laboratory. Regional Integrated Transportation Information System. University of Maryland, College Park, M.D. https://ritis.org/. Accessed September 2018.
75. Transportation Research Board. Highway Capacity Manual. Sixth Edition. Transportation Research Board, National Research Council, 21 Washington, D.C., 2016.
76. US Department of Commerce. National Oceanic and Atmospheric Administration. https://www.noaa.gov/. Accessed September 2018.
77. USDOT, 2006. NGSIM—Next Generation Simulation. http://ops.fhwa.dot.gov/trafficanalysistools/ngsim.htm.
78. Ullman, G., V. Iragavarapu, and R. Brydia, "Safety Effects of Portable End-of-Queue Warning System Deployments at Texas Work Zones", Transportation Research Board, Washington D.C. January 10, 2016.
79. Washington State Department of Transportation (WSDOT). "2014 Corridor Capacity Report", Thirteenth edition of the Annual Congestion Report. October 2014.
80. Wada, K., Seo, T., Kusakabe, T., in preparation. An analysis of stochastic kinematic wave models in Eulerian and Lagrangian coordinates.
81. Wada, K., Usui, K., Takigawa, T., Kuwahara, M., 2018. An optimization modeling of coordinated traffic signal control based on the variational theory and its stochastic extension. Transportation Research Part B: Methodological.
82. Williges, C., B. McCullough, Y.Y. Chu, N. Amatya, R. Kuo, M. Lin, and L. Chu. Pilot Testing of SHRP 2 Reliability Data and Analytical Products: Southern California. The National Academies Press, Washington, D.C., 2014. https://doi.org/10.17226/22332.
83. Sobolewski, M., T. Polum, P. Morris, R. Loos, and K. Anderson. Pilot Testing of SHRP 2 Reliability Data and Analytical Products: Minnesota. The National Academies Press, Washington, D.C., 2014. https://doi.org/10.17226/22255.
84. Samander, M.S., B.M. Williams, I. Ahmed, and N. Rouphail. Validation of Highway Capacity Manual's Freeway Travel Time Reliability Prediction using Probe and Sensor Data. Transportation Research Board, Washington, D.C., 2019.
85. Yang, H., Huang, H.-J., 2005. Mathematical and Economic Theory of Road Pricing. Emerald. Yuan, Y., van Lint, J. W. C., Wilson, R. E., van Wageningen-Kessels, F., Hoogendoorn, S. P., 2012. Real-time.
86. Zegeer, J., J. Bonneson, R. Dowling, P. Ryus, M. Vandehey, W. Kittelson, N. Rouphail, B. Schroeder, A. Hajbabaie, B. Aghdashi, T. Chase, S. Sajjadi, R. Margiotta, and L. Elefteriadou. Incorporating Travel Time Reliability in the Highway Capacity Manual. SHRP 2 Report S2-L08-RW-1. Transportation Research Board, Washington, D.C., 2014.

APPENDICES

Appendix A – Details of the Selected Daily Incident Data

General Incident Information

1 Lane Closure:

TABLE A-1: 2/27/2014 INCIDENT DATA

Incident Date:	2/27/2014	Weekday:	Thursday
Incident Start Time:	9:19 EST	Incident End Time:	10:19 EST
Approx. Queue length:	13,274 ft	Weather Condition:	Clear/Normal
Incident Severity:	One Lane Closure	# of Freeway lanes:	3
Incident Description (from TIMS):	Left median reopened near Exit 11, Six Forks Road		

TABLE A-2: 3/14/2014 INCIDENT DATA

Incident Date:	3/14/2014	Weekday:	Friday
Incident Start Time:	16:08	Incident End Time:	16:41
Approx. Queue length:	17717 ft	Weather Condition:	Clear/Normal
Incident Severity:	One Lane Closure	# of Freeway lanes:	3
Incident Description (from TIMS):	All Lanes Open		

TABLE A-3: 5/5/2014 INCIDENT DATA

Incident Date:	5/5/2014	Weekday:	Monday
Incident Start Time:	9:42	Incident End Time:	9:52
Approx. Queue length:	10964 ft	Weather Condition:	Clear/Normal
Incident Severity:	One Lane Closure	# of Freeway lanes:	3
Incident Description (from TIMS):	All lanes have re-opened at NC-50.		

TABLE A-4: 6/24/2014 INCIDENT DATA

Incident Date:	6/24/2014	Weekday:	Tuesday
Incident Start Time:	9:01	Incident End Time:	9:54
Approx. Queue length:	8984 ft	Weather Condition:	Clear/Normal
Incident Severity:	One Lane Closure	# of Freeway lanes:	3
Incident Description (from TIMS):	All lanes are now open near Creedmoor Rd.		

TABLE A-5: 7/15/2014 INCIDENT DATA

Incident Date:	7/15/2014	Weekday:	Tuesday
Incident Start Time:	13:05	Incident End Time:	13:38
Approx. Queue length:	13875 ft	Weather Condition:	Clear/Normal
Incident Severity:	One Lane Closure	# of Freeway lanes:	3
Incident Description (from TIMS):	The right lane has reopened near US-1 (Capital Blvd).		

TABLE A-6: 2/5/2015 INCIDENT DATA

Incident Date:	2/5/2015	Weekday:	Thursday

Incident Start Time:	17:30	Incident End Time:	18:05
Approx. Queue length:	10809 ft	Weather Condition:	Clear/Normal
Incident Severity:	One Lane Closure	# of Freeway lanes:	3
Incident Description (from TIMS):	The right lane has reopened near US-70.		

TABLE A-7: 3/27/2015 INCIDENT DATA

Incident Date:	3/27/2015	Weekday:	Friday
Incident Start Time:	5:09	Incident End Time:	5:33
Approx. Queue length:	9311 ft	Weather Condition:	Clear/Normal
Incident Severity:	One Lane Closure	# of Freeway lanes:	3
Incident Description (from TIMS):	All lanes are now open.		

TABLE A-8: 4/7/2015 INCIDENT DATA

Incident Date:	4/7/2015	Weekday:	Tuesday
Incident Start Time:	4:59	Incident End Time:	5:08
Approx. Queue length:	10809 ft	Weather Condition:	Clear/Normal
Incident Severity:	One Lane Closure	# of Freeway lanes:	3
Incident Description (from TIMS):	The right lane has reopened near I-40.		

TABLE A-9: 8/5/2015 INCIDENT DATA

Incident Date:	8/5/2015	Weekday:	Wednesday
Incident Start Time:	21:06	Incident End Time:	21:16
Approx. Queue length:	10809 ft	Weather Condition:	Clear/Normal
Incident Severity:	One Lane Closure	# of Freeway lanes:	4
Incident Description (from TIMS):	The left lane has reopened east of Glenwood Avenue.		

TABLE A-10: 4/5/2016 INCIDENT DATA

Incident Date:	4/5/2016	Weekday:	Tuesday
Incident Start Time:	17:35	Incident End Time:	17:47
Approx. Queue length:	13875 ft	Weather Condition:	Clear/Normal
Incident Severity:	One Lane Closure	# of Freeway lanes:	3
Incident Description (from TIMS):	The right lane has reopened near Exit 14 (Falls of the Neuse Rd).		

TABLE A-11: 4/26/2016 INCIDENT DATA

Incident Date:	4/26/2016	Weekday:	Tuesday
Incident Start Time:	16:28	Incident End Time:	17:02
Approx. Queue length:	10964 ft	Weather Condition:	Clear/Normal
Incident Severity:	One Lane Closure	# of Freeway lanes:	3
Incident Description (from TIMS):	All lanes are open.		

TABLE A-12: 6/10/2016 INCIDENT DATA

Incident Date:	6/10/2016	Weekday:	Friday
Incident Start Time:	6:14	Incident End Time:	6:39
Approx. Queue length:	9680 ft	Weather Condition:	Clear/Normal
Incident Severity:	One Lane Closure	# of Freeway lanes:	2

Incident Description (from TIMS):	The right lane has reopened near Exit 16 (US-1).

TABLE A-13: 9/6/2016 INCIDENT DATA

Incident Date:	9/6/2016	Weekday:	Tuesday
Incident Start Time:	14:59	Incident End Time:	16:16
Approx. Queue length:	13274 ft	Weather Condition:	Clear/Normal
Incident Severity:	One Lane Closure	# of Freeway lanes:	3
Incident Description (from TIMS):	The right lane has reopened near Exit 11, Six Forks Road.		

TABLE A-14: 11/8/2016 INCIDENT DATA

Incident Date:	11/8/2016	Weekday:	Tuesday
Incident Start Time:	8:36	Incident End Time:	9:01
Approx. Queue length:	13875 ft	Weather Condition:	Clear/Normal
Incident Severity:	One Lane Closure	# of Freeway lanes:	3
Incident Description (from TIMS):	The shoulder reopened near Exit 14 (Falls of Neuse Road).		

TABLE A-15: 5/4/2018 INCIDENT DATA

Incident Date:	5/4/2018	Weekday:	Friday
Incident Start Time:	6:26	Incident End Time:	7:23
Approx. Queue length:	23555 ft	Weather Condition:	Clear/Normal
Incident Severity:	One Lane Closure	# of Freeway lanes:	3
Incident Description (from TIMS):	The right lane reopened near Exit 14 (Falls of Neuse).		

TABLE A-16: 6/18/2018 INCIDENT DATA

Incident Date:	6/18/2018	Weekday:	Monday
Incident Start Time:	17:08	Incident End Time:	17:41
Approx. Queue length:	3112 ft	Weather Condition:	Clear/Normal
Incident Severity:	One Lane Closure	# of Freeway lanes:	3
Incident Description (from TIMS):	The right lane has reopened near Exit 18 (US-401)		

2 Lane Closure:

TABLE A-17: 2/25/2015 INCIDENT DATA

Incident Date:	2/25/2015	Weekday:	Wednesday
Incident Start Time:	7:05	Incident End Time:	7:59
Approx. Queue length:	17387 ft	Weather Condition:	Clear/Normal
Incident Severity:	Two Lane Closure	# of Freeway lanes:	4
Incident Description (from TIMS):	The right lane and ramp lane are open at US-70.		

TABLE A-18: 4/22/2015 INCIDENT DATA

Incident Date:	4/22/2015	Weekday:	Wednesday
Incident Start Time:	12:52	Incident End Time:	13:28
Approx. Queue length:	13274 ft	Weather Condition:	Clear/Normal
Incident Severity:	Two Lane Closure	# of Freeway lanes:	3
Incident Description (from TIMS):	All lanes have reopened near Six Forks Road.		

TABLE A-19: 4/29/2015 INCIDENT DATA

Incident Date:	4/29/2015	Weekday:	Wednesday
Incident Start Time:	20:33	Incident End Time:	21:11
Approx. Queue length:	12375 ft	Weather Condition:	Clear/Normal
Incident Severity:	Two Lane Closure	# of Freeway lanes:	3
Incident Description (from TIMS):	All lanes are open near Falls of Neuse Road.		

TABLE A-20: 12/15/2015 INCIDENT DATA

Incident Date:	12/15/2015	Weekday:	Tuesday
Incident Start Time:	9:13	Incident End Time:	9:49
Approx. Queue length:	15701 ft	Weather Condition:	Clear/Normal
Incident Severity:	Two Lane Closure	# of Freeway lanes:	3
Incident Description (from TIMS):	The shoulder has reopened near Exit 14 (Falls of Neuse Road).		

TABLE A-21: 11/7/2016 INCIDENT DATA

Incident Date:	11/7/2016	Weekday:	Monday
Incident Start Time:	9:35	Incident End Time:	10:05
Approx. Queue length:	36829 ft	Weather Condition:	Clear/Normal
Incident Severity:	Two Lane Closure	# of Freeway lanes:	3
Incident Description (from TIMS):	The left lanes have reopened west of Exit 14 (Falls of Neuse Road).		

TABLE A-22: 6/19/2018 INCIDENT DATA

Incident Date:	6/19/2018	Weekday:	Tuesday
Incident Start Time:	12:06	Incident End Time:	12:32
Approx. Queue length:	3112 ft	Weather Condition:	Clear/Normal
Incident Severity:	Two Lane Closure	# of Freeway lanes:	3
Incident Description (from TIMS):	The two right lanes have reopened near Exit 18 (US-401).		

Daily Speed Contours

1 Lane Closure:

TABLE A-23: 2/27/2014 SPEED CONTOUR

FREEVAL Seg #:	Seg. 13	Seg. 14	Seg. 15	Seg. 16
Segment type:	On Ramp	Basic	Off Ramp	Basic
Segment length (ft):	1500	7640	1500	2634
INRIX / TARGET Speeds				
9:15 - 9:30	53.0	21.0	21.0	44.5
9:30 - 9:45	22.2	8.8	8.8	37.9
9:45 - 10:00	10.9	8.2	8.2	36.1
10:00 - 10:15	17.7	12.2	12.2	38.0
10:15 - 10:30	48.3	34.5	34.5	49.1
FREEVAL - Time-Dependent CAF				
9:15 - 9:30	63.9	26.5	6.3	1.2
9:30 - 9:45	27.7	1.6	1.2	1.0
9:45 - 10:00	4.8	8.0	9.9	9.0
10:00 - 10:15	16.1	14.2	14.1	11.4
10:15 - 10:30	43.6	39.0	32.9	23.3
FREEVAL - Average CAF				
9:15 - 9:30	63.9	70.0	65.7	17.1
9:30 - 9:45	64.4	70.0	66.1	13.4
9:45 - 10:00	64.4	70.0	66.2	22.3
10:00 - 10:15	64.6	70.0	66.6	56.9
10:15 - 10:30	64.9	70.0	66.7	69.9
FREEVAL - HCM CAF				
9:15 - 9:30	63.9	70.0	65.7	17.3
9:30 - 9:45	64.4	70.0	66.1	13.7
9:45 - 10:00	64.4	70.0	66.2	23.6
10:00 - 10:15	64.6	70.0	66.6	60.2
10:15 - 10:30	64.9	70.0	66.7	69.9
FREEVAL - Unadjusted CAF				
9:15 - 9:30	63.9	70.0	65.7	69.8
9:30 - 9:45	64.4	70.0	66.1	69.9
9:45 - 10:00	64.4	70.0	66.2	69.9
10:00 - 10:15	64.6	70.0	66.6	69.9
10:15 - 10:30	64.9	70.0	66.7	69.9

TABLE A-24: 3/14/2014 SPEED CONTOUR

FREEVAL Seg #:	Seg. 6	Seg. 7	Seg. 8	Seg. 9	Seg. 10	Seg. 11	Seg. 12
Segment type:	Basic	On Ramp	Basic	On Ramp	Basic	Off Ramp	Basic
Segment length (ft):	2016	1500	326	1500	9230	1500	1645
INRIX / TARGET Speeds							
16:00 - 16:15	58.1	37.8	37.8	33.3	22.1	22.1	38.4
16:15 - 16:30	39.3	7.5	7.5	10.6	18.5	18.5	35.4
16:30 - 16:45	44.5	12.5	12.5	14.9	21.1	21.1	36.1
16:45 - 17:00	52.0	28.7	28.7	29.9	33.0	33.0	43.3
FREEVAL - Time-Dependent CAF							
16:00 - 16:15	70.0	62.2	68.2	67.7	45.8	5.8	1.2
16:15 - 16:30	70.0	62.1	68.2	67.7	2.6	1.2	1.0
16:30 - 16:45	70.0	55.3	44.1	16.7	9.1	9.6	9.1
16:45 - 17:00	70.0	48.7	38.9	25.7	33.5	33.6	25.2
FREEVAL - Average CAF							
16:00 - 16:15	70.0	62.2	68.2	67.7	70.0	64.5	69.6
16:15 - 16:30	70.0	62.1	68.2	67.7	70.0	64.7	69.6
16:30 - 16:45	70.0	61.9	68.2	67.4	70.0	64.8	69.6
16:45 - 17:00	70.0	61.9	68.1	67.4	70.0	64.7	69.6
FREEVAL - HCM CAF							
16:00 - 16:15	70.0	62.2	68.2	67.7	70.0	64.5	69.6
16:15 - 16:30	70.0	62.1	68.2	67.7	70.0	64.7	69.6
16:30 - 16:45	70.0	61.9	68.2	67.4	70.0	64.8	69.6
16:45 - 17:00	70.0	61.9	68.1	67.4	70.0	64.7	69.6
FREEVAL - Unadjusted CAF							
16:00 - 16:15	70.0	62.2	68.2	67.7	70.0	64.5	69.6
16:15 - 16:30	70.0	62.1	68.2	67.7	70.0	64.7	69.6
16:30 - 16:45	70.0	61.9	68.2	67.4	70.0	64.8	69.6
16:45 - 17:00	70.0	61.9	68.1	67.4	70.0	64.7	69.6

TABLE A-25: 5/5/2014 SPEED CONTOUR

FREEVAL Seg #:	Seg. 17	Seg. 18	Seg. 19	Seg. 20	Seg. 21
Segment type:	On Ramp	Basic	Off Ramp	Basic	On Ramp
Segment length (ft):	1500	3350	1500	3114	1500
INRIX / TARGET Speeds					
9:30 - 9:45	19.9	12.4	12.4	18.8	28.9
9:45 - 10:00	34.3	16.0	16.0	23.3	34.0
FREEVAL - Time-Dependent CAF					
9:30 - 9:45	66.7	69.9	38.5	3.0	1.4
9:45 - 10:00	55.8	32.9	18.6	22.6	35.2
FREEVAL - Average CAF					
9:30 - 9:45	66.7	69.9	64.1	69.9	65.3
9:45 - 10:00	66.5	69.9	64.5	69.9	65.0
FREEVAL - HCM CAF					
9:30 - 9:45	66.7	69.9	64.1	69.9	65.3
9:45 - 10:00	66.5	69.9	64.5	69.9	65.0
FREEVAL - Unadjusted CAF					
9:30 - 9:45	66.7	69.9	64.1	69.9	65.3
9:45 - 10:00	66.5	69.9	64.5	69.9	65.0

TABLE A-26: 6/24/2014 SPEED CONTOUR

FREEVAL Seg #:	Seg. 16	Seg. 17	Seg. 18	Seg. 19
Segment type:	Basic	On Ramp	Basic	Off Ramp
Segment length (ft):	2634	1500	3350	1500
INRIX / TARGET Speeds				
9:00 - 9:15	48.6	29.8	30.1	30.1
9:15 - 9:30	32.1	10.4	14.8	14.8
9:30 - 9:45	37.2	21.4	26.3	26.3
FREEVAL - Time-Dependent CAF				
9:00 - 9:15	68.4	25.2	13.6	11.3
9:15 - 9:30	30.5	10.5	9.4	9.1
9:30 - 9:45	34.0	24.8	27.7	26.4
FREEVAL - Average CAF				
9:00 - 9:15	69.8	32.7	14.3	12.0
9:15 - 9:30	65.2	33.8	13.5	12.9
9:30 - 9:45	69.9	66.7	43.5	22.7
FREEVAL - HCM CAF				
9:00 - 9:15	47.4	19.3	11.9	9.7
9:15 - 9:30	14.5	11.0	10.5	10.4
9:30 - 9:45	29.5	19.5	12.6	11.8
FREEVAL - Unadjusted CAF				
9:00 - 9:15	69.8	64.4	66.1	64.2
9:15 - 9:30	69.8	65.9	69.9	64.6
9:30 - 9:45	69.9	66.7	69.9	64.1

TABLE A-27: 7/15/2014 SPEED CONTOUR

FREEVAL Seg #:	Seg. 9	Seg. 10	Seg. 11	Seg. 12
Segment type:	On Ramp	Basic	Off Ramp	Basic
Segment length (ft):	1500	9230	1500	1645
INRIX / TARGET Speeds				
13:15 - 13:30	48.6	33.9	33.9	45.6
13:30 - 13:45	49.8	30.6	30.6	42.2
FREEVAL - Time-Dependent CAF				
9:00 - 9:15	67.9	70.0	32.9	3.0
9:30 - 9:45	67.9	69.5	37.6	38.7
FREEVAL - Average CAF				
9:00 - 9:15	67.9	70.0	64.5	69.6
9:30 - 9:45	67.9	70.0	64.5	69.6
FREEVAL - HCM CAF				
9:00 - 9:15	67.9	70.0	64.5	69.6
9:30 - 9:45	67.9	70.0	64.5	69.6
FREEVAL - Unadjusted CAF				
9:00 - 9:15	67.9	70.0	64.5	69.6
9:30 - 9:45	67.9	70.0	64.5	69.6

TABLE A-28: 2/5/2015 SPEED CONTOUR

FREEVAL Seg #:	Seg. 26	Seg. 27	Seg. 28
Segment type:	Basic	Off Ramp	Off Ramp
Segment length (ft):	7957	1500	1352
INRIX / TARGET Speeds			
17:30 - 17:45	42.8	42.8	43.4
17:45 - 18:00	27.0	27.0	27.9
18:00 - 18:15	25.1	25.1	26.0
FREEVAL - Time-Dependent CAF			
17:30 - 17:45	70.0	38.3	3.9
17:45 - 18:00	27.7	3.1	1.6
18:00 - 18:15	43.6	25.8	18.4
FREEVAL - Average CAF			
17:30 - 17:45	70.0	66.3	69.6
17:45 - 18:00	70.0	65.6	69.6
18:00 - 18:15	70.0	66.2	69.6
FREEVAL - HCM CAF			
17:30 - 17:45	70.0	66.3	69.6
17:45 - 18:00	70.0	65.6	69.6
18:00 - 18:15	70.0	66.2	69.6
FREEVAL - Unadjusted CAF			
17:30 - 17:45	70.0	66.3	69.6
17:45 - 18:00	70.0	65.6	69.6
18:00 - 18:15	70.0	66.2	69.6

TABLE A-29: 3/27/2015 SPEED CONTOUR

	FREEVAL Seg #:	Seg. 22	Seg. 23
	Segment type:	Basic	Off Ramp
	Segment length (ft):	7811	1500
INRIX / TARGET Speeds			
	5:45 - 6:00	40.9	40.9
	6:00 - 6:15	41.1	41.1
FREEVAL - Time-Dependent CAF			
	5:45 - 6:00	36.1	7.6
	6:00 - 6:15	53.7	39.9
FREEVAL - Average CAF			
	5:45 - 6:00	70.0	64.9
	6:00 - 6:15	69.9	64.5
FREEVAL - HCM CAF			
	5:45 - 6:00	70.0	64.9
	6:00 - 6:15	69.9	64.5
FREEVAL - Unadjusted CAF			
	5:45 - 6:00	70.0	64.9
	6:00 - 6:15	69.9	64.5

TABLE A-30: 4/7/2015 SPEED CONTOUR

FREEVAL Seg #:	Seg. 26	Seg. 27	Seg. 28
Segment type:	Basic	Off Ramp	Off Ramp
Segment length (ft):	7957	1500	1352
INRIX / TARGET Speeds			
17:00 - 17:15	36.3	36.3	37.1
17:15 - 17:30	46.7	46.7	47.2
FREEVAL - Time-Dependent CAF			
17:00 - 17:15	41.0	6.5	1.6
17:15 - 17:30	42.6	36.1	31.8
FREEVAL - Average CAF			
17:00 - 17:15	69.8	65.9	69.6
17:15 - 17:30	70.0	65.3	69.5
FREEVAL - HCM CAF			
17:00 - 17:15	69.8	65.9	69.6
17:15 - 17:30	70.0	65.3	69.5
FREEVAL - Unadjusted CAF			
17:00 - 17:15	69.8	65.9	69.6
17:15 - 17:30	70.0	65.3	69.5

TABLE A-31: 8/5/2015 SPEED CONTOUR

FREEVAL Seg #:	Seg. 26	Seg. 27	Seg. 28
Segment type:	Basic	Off Ramp	Off Ramp
Segment length (ft):	7957	1500	1352
INRIX / TARGET Speeds			
20:45 - 21:00	43.9	43.9	44.5
FREEVAL - Time-Dependent CAF			
20:45 - 21:00	70.0	67.0	69.7
FREEVAL - Average CAF			
20:45 - 21:00	70.0	67.0	69.7
FREEVAL - HCM CAF			
20:45 - 21:00	70.0	67.0	69.7
FREEVAL - Unadjusted CAF			
20:45 - 21:00	70.0	67.0	69.7

TABLE A-32: 4/5/2016 SPEED CONTOUR

FREEVAL Seg #:	Seg. 10	Seg. 11	Seg. 12	Seg. 13
Segment type:	Basic	Off Ramp	Basic	On Ramp
Segment length (ft):	9230	1500	1645	1500
INRIX / TARGET Speeds				
17:30 - 17:45	42.5	42.5	42.5	49.0
17:45 - 18:00	34.3	34.3	34.3	43.3
FREEVAL - Time-Dependent CAF				
17:30 - 17:45	58.0	8.4	1.5	1.8
17:45 - 18:00	36.3	20.7	25.9	43.2
FREEVAL - Average CAF				
17:30 - 17:45	70.0	64.5	69.6	64.3
17:45 - 18:00	70.0	64.5	69.6	64.5
FREEVAL - HCM CAF				
17:30 - 17:45	70.0	64.5	69.6	64.3
17:45 - 18:00	70.0	64.5	69.6	64.5
FREEVAL - Unadjusted CAF				
17:30 - 17:45	70.0	64.5	69.6	64.3
17:45 - 18:00	70.0	64.5	69.6	64.5

TABLE A-33: 4/26/2016 SPEED CONTOUR

FREEVAL Seg #:	Seg. 17	Seg. 18	Seg. 19	Seg. 20	Seg. 21
Segment type:	On Ramp	Basic	Off Ramp	Basic	On Ramp
Segment length (ft):	1500	3350	1500	3114	1500
INRIX / TARGET Speeds					
16:15 - 16:30	46.9	19.9	19.9	19.9	27.4
16:30 - 16:45	37.9	19.6	19.6	19.6	26.7
16:45 - 17:00	37.7	22.2	22.2	22.2	29.1
FREEVAL - Time-Dependent CAF					
16:15 - 16:30	66.6	69.6	21.7	2.4	1.3
16:30 - 16:45	27.7	9.4	8.3	8.9	12.3
16:45 - 17:00	39.0	29.7	32.7	22.3	26.2
FREEVAL - Average CAF					
16:15 - 16:30	66.6	69.9	64.5	69.9	65.1
16:30 - 16:45	66.1	69.9	64.7	69.9	64.7
16:45 - 17:00	66.1	69.9	64.5	69.9	64.6
FREEVAL - HCM CAF					
16:15 - 16:30	66.6	69.9	64.5	69.9	65.1
16:30 - 16:45	66.1	69.9	64.7	69.9	14.5
16:45 - 17:00	66.1	69.9	64.5	20.1	8.4
FREEVAL - Unadjusted CAF					
16:15 - 16:30	66.6	69.9	64.5	69.9	65.1
16:30 - 16:45	66.1	69.9	64.7	69.9	64.7
16:45 - 17:00	66.1	69.9	64.5	69.9	64.6

TABLE A-34: 6/10/2016 SPEED CONTOUR

FREEVAL Seg #:	Seg. 3	Seg. 4	Seg. 5	Seg. 6	Seg. 7	Seg. 8	Seg. 9
Segment type:	Basic	Off Ramp	Off Ramp	Basic	On Ramp	Basic	On Ramp
Segment length (ft):	1116	1500	1722	2016	1500	326	1500
HERE / TARGET Speeds							
6:15-6:30	72.7	72.7	72.7	72.7	72.7	72.7	72.2
6:30-6:45	74.2	74.2	74.2	74.2	74.2	74.2	74.0
6:45-7:00	44.6	44.6	44.6	44.6	44.6	44.6	51.7
7:00-7:15	70.0	62.2	68.2	67.7	45.8	5.8	1.2
7:15-7:30	70.0	62.1	68.2	67.7	2.6	1.2	1.0
7:30-7:45	14.0	14.0	14.0	14.0	14.0	14.0	29.2
7:45-8:00	21.7	21.7	21.7	21.7	21.7	21.7	34.3
FREEVAL - Time-Dependent CAF							
6:15-6:30	69.6	65.3	28.6	10.6	6.9	5.8	5.4
6:30-6:45	13.0	9.1	7.2	10.0	12.6	13.4	13.6
6:45-7:00	18.1	18.3	14.7	21.5	28.2	30.8	28.6
7:00-7:15	25.7	28.3	18.6	21.4	25.1	25.0	24.3
7:15-7:30	25.0	22.9	17.5	28.6	34.2	36.2	35.8
7:30-7:45	21.5	20.4	16.4	25.8	30.2	30.6	32.6
7:45-8:00	34.2	32.6	18.3	28.0	41.5	43.3	41.3
FREEVAL - Average CAF							
6:15-6:30	69.6	65.3	69.7	69.8	60.9	67.9	66.4
6:30-6:45	69.5	65.2	69.6	69.6	60.7	67.9	66.0
6:45-7:00	68.6	65.1	69.1	67.0	58.6	65.5	63.1
7:00-7:15	68.1	65.0	68.8	67.2	58.6	65.6	62.2
7:15-7:30	67.2	65.0	45.4	26.8	23.5	21.9	22.0
7:30-7:45	19.7	18.0	11.0	14.2	17.3	17.2	20.5
7:45-8:00	19.5	17.7	12.5	17.6	19.8	19.6	20.6
FREEVAL - HCM CAF							
6:15-6:30	69.6	65.3	69.7	63.9	24.1	16.9	10.6
6:30-6:45	69.5	37.9	12.1	6.6	6.8	6.8	8.4
6:45-7:00	4.4	3.6	3.3	3.6	4.4	4.4	8.4
7:00-7:15	2.7	2.7	2.6	2.9	3.8	3.8	8.4
7:15-7:30	2.5	2.4	2.4	2.7	3.8	3.8	8.4
7:30-7:45	2.2	2.1	2.2	2.6	3.8	3.8	8.4
7:45-8:00	2.9	2.8	3.0	3.6	4.6	4.6	8.4
FREEVAL - Unadjusted CAF							
6:15-6:30	69.6	65.3	69.7	69.8	60.9	67.9	66.4
6:30-6:45	69.5	65.2	69.6	69.6	60.7	67.9	66.0
6:45-7:00	68.6	65.1	69.1	67.0	58.6	65.5	63.1
7:00-7:15	68.1	65.0	68.8	67.2	58.6	65.6	62.2
7:15-7:30	67.2	65.0	68.0	64.0	56.0	61.3	60.8
7:30-7:45	66.8	65.0	67.7	63.0	54.9	55.1	54.0
7:45-8:00	68.6	65.0	69.2	58.5	52.5	60.6	62.6

TABLE A-35: 9/6/2016 SPEED CONTOUR

FREEVAL Seg #:	Seg. 14	Seg. 15	Seg. 16	Seg. 17
Segment type:	Basic	Off Ramp	Basic	On Ramp
Segment length (ft):	7640	1500	2634	1500
HERE / TARGET Speeds				
15:00 - 15:15	34.0	34.0	34.0	42.0
15:15 - 15:30	11.9	11.9	11.9	24.8
15:30 - 15:45	15.6	15.6	15.6	27.9
15:45 - 16:00	20.8	20.8	20.8	31.3
16:00 - 16:15	47.4	47.4	47.4	52.1
FREEVAL - Time-Dependent CAF				
15:00 - 15:15	70.0	46.6	3.2	1.4
15:15 - 15:30	10.0	2.0	1.8	2.9
15:30 - 15:45	5.2	4.2	3.8	5.4
15:45 - 16:00	17.4	19.9	17.2	24.3
16:00 - 16:15	70.0	47.8	47.4	50.3
FREEVAL - Average CAF				
15:00 - 15:15	70.0	66.7	69.9	67.0
15:15 - 15:30	70.0	66.6	69.9	66.8
15:30 - 15:45	70.0	66.5	69.9	66.7
15:45 - 16:00	70.0	66.4	69.9	66.7
16:00 - 16:15	70.0	66.3	69.9	66.6
FREEVAL - HCM CAF				
15:00 - 15:15	70.0	66.7	69.9	67.0
15:15 - 15:30	70.0	66.6	69.9	66.8
15:30 - 15:45	70.0	66.5	69.9	66.7
15:45 - 16:00	70.0	66.4	69.9	66.7
16:00 - 16:15	70.0	66.3	69.9	66.6
FREEVAL - Unadjusted CAF				
15:00 - 15:15	70.0	66.7	69.9	67.0
15:15 - 15:30	70.0	66.6	69.9	66.8
15:30 - 15:45	70.0	66.5	69.9	66.7
15:45 - 16:00	70.0	66.4	69.9	66.7
16:00 - 16:15	70.0	66.3	69.9	66.6

TABLE A-36: 11/8/2016 SPEED CONTOUR

FREEVAL Seg #:	Seg. 10	Seg. 11	Seg. 12	Seg. 13
Segment type:	Basic	Off Ramp	Basic	On Ramp
Segment length (ft):	9230	1500	1645	1500
HERE / TARGET Speeds				
8:30 - 8:45	23.7	23.7	23.7	30.8
8:45 - 9:00	10.8	10.8	10.8	25.2
9:00 - 9:15	36.9	36.9	36.9	44.0
FREEVAL - Time-Dependent CAF				
8:30 - 8:45	25.4	9.5	5.1	7.6
8:45 - 9:00	13.1	13.2	11.3	20.5
9:00 - 9:15	36.7	35.3	22.2	39.2
FREEVAL - Average CAF				
8:30 - 8:45	67.3	51.1	16.6	18.7
8:45 - 9:00	50.3	14.3	10.8	17.9
9:00 - 9:15	55.9	14.5	10.9	17.9
FREEVAL - HCM CAF				
8:30 - 8:45	29.9	11.1	6.0	8.7
8:45 - 9:00	6.1	5.4	4.5	8.4
9:00 - 9:15	5.4	5.5	4.5	8.4
FREEVAL - Unadjusted CAF				
8:30 - 8:45	67.3	64.1	69.2	54.7
8:45 - 9:00	68.0	64.4	69.4	55.3
9:00 - 9:15	69.9	64.7	69.6	62.4

TABLE A-37: 5/4/2018 SPEED CONTOUR

FREEVAL Seg #:	Seg. 3	Seg. 4	Seg. 5	Seg. 6	Seg. 7	Seg. 8	Seg. 9	Seg. 10	Seg. 11	Seg. 12	Seg. 13
Segment type:	Basic	Off Ramp	Off Ramp	Basic	On Ramp	Basic	On Ramp	Basic	Off Ramp	Basic	On Ramp
Segment length (ft):	1116	1500	1722	2016	1500	326	1500	9230	1500	1645	1500
HERE / TARGET Speeds											
6:30 - 6:45	22.1	22.1	22.1	22.1	22.1	22.1	20.5	16.4	16.4	16.4	31.1
6:45 - 7:00	7.6	7.6	7.6	7.6	7.6	7.6	10.6	18.1	18.1	18.1	32.4
7:00 - 7:15	8.8	8.8	8.8	8.8	8.8	8.8	11.5	18.4	18.4	18.4	32.3
7:15 - 7:30	8.2	8.2	8.2	8.2	8.2	8.2	13.4	26.7	26.7	26.7	37.8
FREEVAL - Time-Dependent CAF											
6:30 - 6:45	69.5	65.2	69.6	69.6	60.7	67.9	66.0	14.4	4.0	1.1	2.5
6:45 - 7:00	68.6	40.1	17.8	10.2	9.9	9.8	9.0	10.0	13.1	12.1	23.6
7:00 - 7:15	6.8	8.0	8.6	13.4	13.7	16.4	19.6	17.6	15.9	11.5	18.9
7:15 - 7:30	7.0	7.3	6.3	8.0	11.8	15.1	18.4	25.0	23.4	17.0	29.5
FREEVAL - Average CAF											
6:30 - 6:45	69.5	65.2	69.6	69.6	60.7	67.9	66.0	69.3	64.1	40.7	18.3
6:45 - 7:00	68.6	65.1	69.1	67.0	58.6	65.5	63.1	31.3	13.8	8.9	14.8
7:00 - 7:15	68.1	65.0	62.9	47.8	31.9	27.0	19.7	12.1	11.3	8.7	14.7
7:15 - 7:30	18.5	12.6	9.1	9.1	9.6	11.7	10.8	11.2	11.1	8.6	14.8
FREEVAL - HCM CAF											
6:30 - 6:45	69.5	65.2	69.6	69.6	60.7	67.9	66.0	56.9	17.6	7.4	9.1
6:45 - 7:00	68.6	65.1	69.1	66.8	44.6	37.4	23.9	6.6	5.2	4.4	8.4
7:00 - 7:15	17.0	11.8	6.8	4.7	4.9	6.0	4.9	5.2	5.3	4.5	8.4
7:15 - 7:30	3.5	3.4	3.7	3.9	5.2	5.8	4.9	5.3	5.4	4.4	8.4
FREEVAL - Unadjusted CAF											
6:30 - 6:45	69.5	65.2	69.6	69.6	60.7	67.9	66.0	69.3	64.1	69.5	61.5
6:45 - 7:00	68.6	65.1	69.1	67.0	58.6	65.5	63.1	65.2	64.1	67.9	58.4
7:00 - 7:15	68.1	65.0	68.8	67.2	58.6	65.6	62.2	64.3	63.7	67.9	57.3
7:15 - 7:30	67.2	65.0	68.0	64.0	56.0	61.3	60.8	61.6	61.6	66.0	51.9

TABLE A-38: 6/18/2018 SPEED CONTOUR

	FREEVAL Seg #:	Seg. 1	Seg. 2
	Segment type:	Basic	On Ramp
	Segment length (ft):	1612	1500
HERE / TARGET Speeds			
	17:00 - 17:15	34.9	42.6
	17:15 - 17:30	45.6	51.4
FREEVAL - Time-Dependent CAF			
	17:00 - 17:15	48.9	8.4
	17:15 - 17:30	50.2	52.0
FREEVAL - Average CAF			
	17:00 - 17:15	70.0	67.1
	17:15 - 17:30	70.0	67.6
FREEVAL - HCM CAF			
	17:00 - 17:15	70.0	67.1
	17:15 - 17:30	70.0	67.6
FREEVAL - Unadjusted CAF			
	17:00 - 17:15	70.0	67.1
	17:15 - 17:30	70.0	67.6

2 Lane Closure:

TABLE A-39: 2/25/2015 SPEED CONTOUR

FREEVAL Seg #:	Seg 25	Seg 26	Seg 27	Seg 28	Seg 29	Seg 30
Segment type:	On Ramp	Basic	Off Ramp	Off Ramp	Basic	Weaving
Segment length (ft):	1500	7957	1500	1352	2301	2777
INRIX / TARGET Speeds						
7:30-7:45	53.1	26.1	26.1	26.2	31.6	39.8
7:45-8:00	33.1	15.5	15.5	15.9	35.4	43.9
8:00-8:15	17.7	16.0	16.0	16.4	35.5	43.4
8:15-8:30	20.4	23.8	23.8	24.0	34.7	44.0
8:30-8:45	29.4	27.8	27.8	28.0	36.4	43.9
FREEVAL - Time-Dependent CAF						
7:30-7:45	57.4	55.1	32.2	14.9	10.1	2.4
7:45-8:00	16.2	13.2	7.6	6.1	9.8	6.3
8:00-8:15	17.6	27.0	11.1	6.5	8.6	4.9
8:15-8:30	17.4	26.3	11.0	6.5	8.5	4.9
8:30-8:45	29.0	41.1	25.3	19.7	38.2	39.4
FREEVAL - Average CAF						
7:30-7:45	57.4	57.7	64.9	69.5	66.9	12.6
7:45-8:00	57.6	57.7	64.6	48.8	20.4	6.6
8:00-8:15	57.5	48.7	19.4	8.8	11.8	6.5
8:15-8:30	37.7	46.0	21.1	9.0	12.5	6.6
8:30-8:45	47.4	45.2	15.7	8.5	12.1	6.6
FREEVAL - HCM CAF						
7:30-7:45	57.4	57.7	52.8	23.5	15.1	3.7
7:45-8:00	14.4	13.3	4.3	3.0	4.0	2.8
8:00-8:15	7.8	7.6	4.0	2.9	3.8	2.8
8:15-8:30	8.4	9.1	4.7	3.2	4.2	2.8
8:30-8:45	6.3	7.1	4.8	3.0	4.0	2.8
FREEVAL - Unadjusted CAF						
7:30-7:45	57.4	57.7	64.9	69.5	66.9	55.6
7:45-8:00	57.6	57.7	64.6	69.5	67.4	56.4
8:00-8:15	57.5	57.7	64.5	69.5	67.7	55.7
8:15-8:30	57.5	57.7	63.2	69.3	69.0	58.5
8:30-8:45	57.7	57.7	63.7	69.4	68.5	58.2

TABLE A-40: 4/22/2015 SPEED CONTOUR

FREEVAL Seg #:	Seg 14	Seg 15	Seg 16	Seg 17
Segment type:	Basic	Off Ramp	Basic	On Ramp
Segment length (ft):	7640	1500	2634	1500
INRIX / TARGET Speeds				
13:00-13:15	26.6	26.6	31.9	44.0
13:15-13:30	20.9	20.9	34.3	50.2
FREEVAL - Time-Dependent CAF				
13:00-13:15	70.0	28.6	2.0	1.0
13:15-13:30	46.5	15.4	23.6	41.6
FREEVAL - Average CAF				
13:00-13:15	70.0	66.8	69.9	67.0
13:15-13:30	70.0	66.7	69.9	66.9
FREEVAL - HCM CAF				
13:00-13:15	70.0	66.8	7.3	2.6
13:15-13:30	20.3	2.5	1.2	2.2
FREEVAL - Unadjusted CAF				
13:00-13:15	70.0	66.8	69.9	67.0
13:15-13:30	70.0	66.7	69.9	66.9

TABLE A-41: 4/29/2015 SPEED CONTOUR

FREEVAL Seg #:	Seg 10	Seg 11	Seg 12
Segment type:	Basic	Off Ramp	Basic
Segment length (ft):	9230	1500	1645
INRIX / TARGET Speeds			
20:30-20:45	48.0	48.0	54.6
20:45-21:00	27.1	27.1	32.0
21:00-21:15	28.9	28.9	42.2
FREEVAL - Time-Dependent CAF			
20:30-20:45	70.0	64.5	4.5
20:45-21:00	70.0	19.9	1.0
21:00-21:15	70.0	32.4	29.3
FREEVAL - Average CAF			
20:30-20:45	70.0	64.5	69.6
20:45-21:00	70.0	64.5	69.6
21:00-21:15	70.0	64.3	69.6
FREEVAL - HCM CAF			
20:30-20:45	70.0	64.5	69.6
20:45-21:00	70.0	64.5	69.6
21:00-21:15	70.0	64.3	69.6
FREEVAL - Unadjusted CAF			
20:30-20:45	70.0	64.5	69.6
20:45-21:00	70.0	64.5	69.6
21:00-21:15	70.0	64.3	69.6

TABLE A-42: 12/15/2015 SPEED CONTOUR

FREEVAL Seg #:	Seg 7	Seg 8	Seg 9	Seg 10	Seg 11	Seg 12
Segment type:	On Ramp	Basic	On Ramp	Basic	Off Ramp	Basic
Segment length (ft):	1500	326	1500	9230	1500	1645
INRIX / TARGET Speeds						
9:15-9:30	38.8	38.8	28.8	3.7	3.7	19.9
9:30-9:45	10.7	10.7	9.7	7.1	7.1	18.9
9:45-10:00	19.4	19.4	20.0	21.6	21.6	32.3
FREEVAL - Time-Dependent CAF						
9:15-9:30	61.5	68.1	67.1	16.6	3.0	1.0
9:30-9:45	62.2	68.2	67.7	1.7	1.3	1.1
9:45-10:00	23.7	19.2	12.1	16.1	25.2	20.7
FREEVAL - Average CAF						
9:15-9:30	61.5	68.1	67.1	70.0	32.2	6.4
9:30-9:45	62.2	68.2	67.7	70.0	8.4	4.5
9:45-10:00	62.0	68.2	67.6	56.6	5.9	4.5
FREEVAL - HCM CAF						
9:15-9:30	61.5	68.1	67.1	32.1	5.9	2.0
9:30-9:45	62.2	68.2	67.7	4.2	2.1	1.8
9:45-10:00	62.0	68.2	21.2	2.3	2.1	1.8
FREEVAL - Unadjusted CAF						
9:15-9:30	61.5	68.1	67.1	70.0	64.7	69.6
9:30-9:45	62.2	68.2	67.7	70.0	64.4	69.6
9:45-10:00	62.0	68.2	67.6	70.0	64.5	69.6

TABLE A-43: 11/7/2018 SPEED CONTOUR

FREEVAL Seg #:	Seg 3	Seg 4	Seg 5	Seg 6	Seg 7	Seg 8	Seg 9	Seg 10	Seg 11	Seg 12	Seg 13	Seg 14	Seg 15	Seg 16	Seg 17
Segment type:	Basic	Off Ramp	Off Ramp	Basic	On Ramp	Basic	On Ramp	Basic	Off Ramp	Basic	On Ramp	Basic	Off Ramp	Basic	On Ramp
Segment length (ft):	1116	1500	1722	2016	1500	3226	1500	9230	1500	1645	1500	7640	1500	2634	1500
INRIX / TARGET Speeds															
9:45-10:00	21.2	21.2	21.2	21.2	21.2	21.2	16.5	4.6	4.6	4.6	9.3	22.1	22.1	22.1	32.3
10:00-10:15	12.5	12.5	12.5	12.5	12.5	12.5	11.7	9.7	9.7	9.7	14.7	28.3	28.3	28.3	38.2
10:15-10:30	23.5	23.5	23.5	23.5	23.5	23.5	20.5	13.2	13.2	13.2	22.8	49.0	49.0	49.0	53.4
FREEVAL - Time-Dependent CAF															
9:45-10:00	69.7	65.1	69.6	70.0	62.0	68.2	67.6	70.0	64.5	69.6	64.4	54.7	11.0	1.5	1.0
10:00-10:15	69.7	65.0	69.6	70.0	62.3	68.2	67.8	70.0	64.4	69.6	49.9	24.7	17.9	25.7	38.0
10:15-10:30	69.7	65.0	69.6	70.0	62.4	68.3	68.0	70.0	64.4	69.6	64.9	70.0	66.7	69.9	67.1
FREEVAL - Average CAF															
9:45-10:00	69.7	65.1	69.6	70.0	62.0	68.2	67.6	70.0	64.5	69.6	64.4	70.0	66.2	69.9	66.5
10:00-10:15	69.7	65.0	69.6	70.0	62.3	68.2	67.8	70.0	64.4	69.6	64.6	70.0	66.6	69.9	66.8
10:15-10:30	69.7	65.0	69.6	70.0	62.4	68.3	68.0	70.0	64.4	69.6	64.9	70.0	66.7	69.9	67.1
FREEVAL - HCM CAF															
9:45-10:00	69.7	65.1	69.6	70.0	62.0	68.2	67.6	70.0	64.5	69.6	64.4	70.0	25.9	3.7	2.4
10:00-10:15	69.7	65.0	69.6	70.0	62.3	68.2	67.8	70.0	64.4	69.6	64.6	4.8	1.5	1.3	2.2
10:15-10:30	69.7	65.0	69.6	70.0	62.4	68.3	68.0	70.0	64.4	69.6	36.9	1.9	1.6	1.4	2.2
FREEVAL - Unadjusted CAF															
9:45-10:00	69.7	65.1	69.6	70.0	62.0	68.2	67.6	70.0	64.5	69.6	64.4	70.0	66.2	69.9	66.5
10:00-10:15	69.7	65.0	69.6	70.0	62.3	68.2	67.8	70.0	64.4	69.6	64.6	70.0	66.6	69.9	66.8
10:15-10:30	69.7	65.0	69.6	70.0	62.4	68.3	68.0	70.0	64.4	69.6	64.9	70.0	66.7	69.9	67.1

TABLE A-44: 6/19/2018 SPEED CONTOUR

FREEVAL Seg #:	Seg 1	Seg 2
Segment type:	Basic	On Ramp
Segment length (ft):	1612	1500
HERE / TARGET Speeds		
12:15-12:30	15.7	29.4
12:30-12:45	21.1	33.3
FREEVAL - Time-Dependent CAF		
12:15-12:30	13.7	2.5
12:30-12:45	26.3	33.2
FREEVAL - Average CAF		
12:15-12:30	70.0	67.8
12:30-12:45	70.0	67.8
FREEVAL - HCM CAF		
12:15-12:30	30.7	3.3
12:30-12:45	1.5	2.2
FREEVAL - Unadjusted CAF		
12:15-12:30	70.0	67.8
12:30-12:45	70.0	67.8

Daily Incident Modeling Scenarios and Results

1 Lane Closure:

TABLE A-45: 2/27/2014 CAF RESULTS

Scenario		Time-Dependent	Average	HCM	Unadjusted
Bottleneck Location (TMC Segment)		125-05080			
FREEVAL Segment # and Type		Seg17, On Ramp			
Objective Function Domain		TMCs 125-05081 to 125N05081, HCM Segments 13 to 16			
Resulting time-based CAFs at bottleneck segment	9:15-9:30	0.10	0.46	0.49	1.00
	9:30-9:45	0.10	0.46	0.49	1.00
	9:45-10:00	0.62	0.46	0.49	1.00
	10:00-10:15	0.71	0.46	0.49	1.00
	10:15-10:30	0.91	0.46	0.49	1.00
Resulting CAFs -- Statistics	Average	0.38	0.46	0.49	1.00
	Median	0.36	0.46	0.49	1.00
	Standard Deviation	0.33	0.00	0.00	0.00
Error Function		4712	15755	15784	16518

TABLE A-46: 3/14/2014 CAF RESULTS

Scenario		Time-Dependent	Average	HCM	Unadjusted
Bottleneck Location (TMC Segment)		125-05081			
FREEVAL Segment # and Type		Seg13, On Ramp			
Objective Function Domain		TMCs 125N05083 to 125-05081, HCM Segments 6 to 12			
Resulting time-based CAFs at bottleneck segment	16:00-16:15	0.10	0.49	0.49	1.00
	16:15-16:30	0.10	0.49	0.49	1.00
	16:30-16:45	0.62	0.49	0.49	1.00
	16:45-17:00	1.00	0.49	0.49	1.00
Resulting CAFs -- Statistics	Average	0.46	0.49	0.49	1.00
	Median	0.36	0.49	0.49	1.00
	Standard Deviation	0.44	0.00	0.00	0.00
Error Function		13414	21757	21757	21757

TABLE A-47: 5/5/2014 CAF RESULTS

Scenario		Time-Dependent	Average	HCM	Unadjusted
Bottleneck Location (TMC Segment)		125-05079			
FREEVAL Segment # and Type		Seg22, Basic			
Objective Function Domain		TMCs 125-05080 to 125-05079, HCM Segments 17 to 21			
Resulting time-based CAFs at bottleneck segment	9:30-9:45	0.10	0.52	0.49	1.00
	9:45-10:00	0.94	0.52	0.49	1.00
Resulting CAFs -- Statistics	Average	0.52	0.52	0.49	1.00
	Median	0.52	0.52	0.49	1.00
	Standard Deviation	0.60	0.00	0.00	0.00
Error Function		4328	9114	9114	9114

TABLE A-48: 6/24/2014 CAF RESULTS

Scenario		Time-Dependent	Average	HCM	Unadjusted
Bottleneck Location (TMC Segment)		125N05080			
FREEVAL Segment # and Type		Seg20, Basic			
Objective Function Domain		TMCs 125N05081 to 125N05080, HCM Segments 16 to 19			
Resulting time-based CAFs at bottleneck segment	9:00-9:15	0.54	0.55	0.49	1.00
	9:15-9:30	0.45	0.55	0.49	1.00
	9:30-9:45	0.68	0.55	0.49	1.00
Resulting CAFs -- Statistics	Average	0.55	0.55	0.49	1.00
	Median	0.54	0.55	0.49	1.00
	Standard Deviation	0.12	0.00	0.00	0.00
Error Function		1605	4331	2298	9672

TABLE A-49: 7/15/2014 CAF RESULTS

Scenario		Time-Dependent	Average	HCM	Unadjusted
Bottleneck Location (TMC Segment)		125-05081			
FREEVAL Segment # and Type		Seg13, On Ramp			
Objective Function Domain		TMCs 125-05082 to 125-05081, HCM Segments 9 to 12			
Resulting time-based CAFs at bottleneck segment	13:15-13:30	0.19	0.59	0.49	1.00
	13:30-13:45	1.00	0.59	0.49	1.00
Resulting CAFs -- Statistics	Average	0.59	0.59	0.49	1.00
	Median	0.59	0.59	0.49	1.00
	Standard Deviation	0.57	0.00	0.00	0.00
Error Function		3330	4573	4573	4573

TABLE A-50: 2/5/2015 CAF RESULTS

Scenario		Time-Dependent	Average	HCM	Unadjusted
Bottleneck Location (TMC Segment)		125-04898			
FREEVAL Segment # and Type		Seg29, Basic			
Objective Function Domain		TMCs 125-04899 to 125N04899, HCM Segments 26 to 28			
Resulting time-based CAFs at bottleneck segment	17:30-17:45	0.25	0.41	0.49	1.00
	17:45-18:00	0.16	0.41	0.49	1.00
	18:00-18:15	0.83	0.41	0.49	1.00
Resulting CAFs -- Statistics	Average	0.41	0.41	0.49	1.00
	Median	0.25	0.41	0.49	1.00
	Standard Deviation	0.36	0.00	0.00	0.00
Error Function		2979	6604	6604	6604

TABLE A-51: 3/27/2015 CAF RESULTS

Scenario		Time-Dependent	Average	HCM	Unadjusted
Bottleneck Location (TMC Segment)		125-04899			
FREEVAL Segment # and Type		Seg24, Basic			
Objective Function Domain		TMCs 125-05079 to 125N05079, HCM Segments 22 to 23			
Resulting time-based CAFs at bottleneck segment	5:45-6:00	0.36	0.59	0.49	1.00
	6:00-6:15	0.83	0.59	0.49	1.00
Resulting CAFs -- Statistics	Average	0.59	0.59	0.49	1.00
	Median	0.59	0.59	0.49	1.00
	Standard Deviation	0.33	0.00	0.00	0.00
Error Function		1039	2106	2106	2106

TABLE A-52: 4/7/2015 CAF RESULTS

Scenario		Time-Dependent	Average	HCM	Unadjusted
Bottleneck Location (TMC Segment)		125-04898			
FREEVAL Segment # and Type		Seg29, Basic			
Objective Function Domain		TMCs 125-04899 to 125N04899, HCM Segments 26 to 28			
Resulting time-based CAFs at bottleneck segment	17:00-17:15	0.13	0.56	0.49	1.00
	17:15-17:30	1.00	0.56	0.49	1.00
Resulting CAFs -- Statistics	Average	0.56	0.56	0.49	1.00
	Median	0.56	0.56	0.49	1.00
	Standard Deviation	0.62	0.00	0.00	0.00
Error Function		2003	3199	3199	3199

TABLE A-53: 8/5/2015 CAF RESULTS

Scenario		Time-Dependent	Average	HCM	Unadjusted
Bottleneck Location (TMC Segment)		125-04898			
FREEVAL Segment # and Type		Seg29, Basic			
Objective Function Domain		TMCs 125-04899 to 125N04899, HCM Segments 26 to 28			
Resulting time-based CAFs at bottleneck segment	20:45-21:00	0.59	0.59	0.49	1.00
Resulting CAFs -- Statistics	Average	0.59	0.59	0.49	1.00
	Median	0.59	0.59	0.49	1.00
	Standard Deviation	N/A	N/A	N/A	N/A
Error Function		1488	1488	1488	1488

TABLE A-54: 4/5/2016 CAF RESULTS

Scenario		Time-Dependent	Average	HCM	Unadjusted
Bottleneck Location (TMC Segment)		125-05081			
FREEVAL Segment # and Type		Seg14, Basic			
Objective Function Domain		TMCs 125-05082 to 125-05081, HMC Segments 10 to 13			
Resulting time-based CAFs at bottleneck segment	17:30-17:45	0.13	0.56	0.49	1.00
	17:45-18:00	1.00	0.56	0.49	1.00
Resulting CAFs -- Statistics	Average	0.56	0.56	0.49	1.00
	Median	0.56	0.56	0.49	1.00
	Standard Deviation	0.62	0.00	0.00	0.00
Error Function		3240	4287	4287	4287

TABLE A-55: 4/26/2016 CAF RESULTS

Scenario		Time-Dependent	Average	HCM	Unadjusted
Bottleneck Location (TMC Segment)		125-05079			
FREEVAL Segment # and Type		Seg22, Basic			
Objective Function Domain		TMCs 125-05080 to 125-05079, HCM Segments 17 to 21			
Resulting time-based CAFs at bottleneck segment	16:15 - 16:30	0.10	0.53	0.49	1.00
	16:30 - 16:45	0.62	0.53	0.49	1.00
	16:45 - 17:00	0.85	0.53	0.49	1.00
Resulting CAFs -- Statistics	Average	0.53	0.53	0.49	1.00
	Median	0.62	0.53	0.49	1.00
	Standard Deviation	0.39	0.00	0.00	0.00
Error Function		3876	12311	10589	12311

TABLE A-56: 6/10/2016 CAF RESULTS

Scenario		Time-Dependent	Average	HCM	Unadjusted
Bottleneck Location (TMC Segment)		125-05082			
FREEVAL Segment # and Type		Seg10, Basic			
Objective Function Domain		TMCs 125-05083 to 125-05082, HCM Segments 3 to 9			
Resulting time-based CAFs at bottleneck segment	6:15-6:30	0.33	0.80	0.49	1.00
	6:30-6:45	0.65	0.80	0.49	1.00
	6:45-7:00	0.88	0.80	0.49	1.00
	7:00-7:15	0.85	0.80	0.49	1.00
	7:15-7:30	0.97	0.80	0.49	1.00
	7:30-7:45	0.94	0.80	0.49	1.00
	7:45-8:00	0.94	0.53	0.49	1.00
Resulting CAFs -- Statistics	Average	0.80	0.76	0.49	1.00
	Median	0.88	0.80	0.49	1.00
	Standard Deviation	0.23	0.10	0.00	0.00
Error Function		8983	28750	23335	34401

TABLE A-57: 9/6/2016 CAF RESULTS

Scenario		Time-Dependent	Average	HCM	Unadjusted
Bottleneck Location (TMC Segment)		125-05080			
FREEVAL Segment # and Type		Seg18, Basic			
Objective Function Domain		TMCs 125-05081 to 125-05080, HCM Segments 14 to 17			
Resulting time-based CAFs at bottleneck segment	15:00-15:15	0.10	0.50	0.49	1.00
	15:15-15:30	0.22	0.50	0.49	1.00
	15:30-15:45	0.36	0.50	0.49	1.00
	15:45-16:00	0.85	0.50	0.49	1.00
	16:00-16:15	0.97	0.50	0.49	1.00
Resulting CAFs -- Statistics	Average	0.50	0.50	0.49	1.00
	Median	0.36	0.50	0.49	1.00
	Standard Deviation	0.39	0.00	0.00	0.00
Error Function		5197	15963	15963	15963

TABLE A-58: 11/8/2016 CAF RESULTS

Scenario		Time-Dependent	Average	HCM	Unadjusted
Bottleneck Location (TMC Segment)		125-05081			
FREEVAL Segment # and Type		Seg14, Basic			
Objective Function Domain		TMCs 125-05082 to 125-05081, HCM Segments 10 to 13			
Resulting time-based CAFs at bottleneck segment	8:30-8:45	0.45	0.75	0.49	1.00
	8:45-9:00	0.80	0.75	0.49	1.00
	9:00-9:15	1.00	0.75	0.49	1.00
Resulting CAFs -- Statistics	Average	0.75	0.75	0.49	1.00
	Median	0.80	0.75	0.49	1.00
	Standard Deviation	0.28	0.00	0.00	0.00
Error Function		1776	4677	4448	9299

TABLE A-59: 5/4/2018 CAF RESULTS

Scenario		Time-Dependent	Average	HCM	Unadjusted
Bottleneck Location (TMC Segment)		125-05081			
FREEVAL Segment # and Type		Seg14, Basic			
Objective Function Domain		TMCs 125-05083 to 125-05081, HCM Segments 3 to 13			
Resulting time-based CAFs at bottleneck segment	6:30-6:45	0.19	0.68	0.49	1.00
	6:45-7:00	0.85	0.68	0.49	1.00
	7:00-7:15	0.77	0.68	0.49	1.00
	7:15-7:30	0.91	0.68	0.49	1.00
Resulting CAFs -- Statistics	Average	0.68	0.68	0.49	1.00
	Median	0.81	0.68	0.49	1.00
	Standard Deviation	0.33	0.00	0.00	0.00
Error Function		12172	25874	19817	42586

TABLE A-60: 6/18/2018 CAF RESULTS

Scenario		Time-Dependent	Average	HCM	Unadjusted
Bottleneck Location (TMC Segment)		125-05083			
FREEVAL Segment # and Type		Seg3, Basic			
Objective Function Domain		TMC 125-05083, HCM Segments 1 to 2			
Resulting time-based CAFs at bottleneck segment	17:00-17:15	0.36	0.64	0.49	1.00
	17:15-17:30	0.91	0.64	0.49	1.00
Resulting CAFs -- Statistics	Average	0.64	0.64	0.49	1.00
	Median	0.64	0.64	0.49	1.00
	Standard Deviation	0.39	0.00	0.00	0.00
Error Function		1068	2005	2005	2005

2 Lane Closure:

TABLE A-61: 2/25/2015 CAF RESULTS

Scenario		Time-Dependent	Average	HCM	Unadjusted
Bottleneck Location (TMC Segment)		125-05083			
FREEVAL Segment # and Type		Seg3, Basic			
Objective Function Domain		TMC 125-05083 to 125-05083, HCM Segments 1 to 2			
Resulting time-based CAFs at bottleneck segment	7:30-7:45	0.17	0.48	0.25	1.00
	7:45-8:00	0.48	0.48	0.25	1.00
	8:00-8:15	0.39	0.48	0.25	1.00
	8:15-8:30	0.39	0.48	0.25	1.00
	8:30-8:45	0.97	0.48	0.25	1.00
Resulting CAFs -- Statistics	Average	0.48	0.48	0.25	1.00
	Median	0.39	0.48	0.25	1.00
	Standard Deviation	0.30	0.00	0.00	0.00
Error Function		8656	15417	13098	19930

TABLE A-62: 4/22/2015 CAF RESULTS

Scenario		Time-Dependent	Average	HCM	Unadjusted
Bottleneck Location (TMC Segment)		125-05080			
FREEVAL Segment # and Type		Seg18, Basic			
Objective Function Domain		TMCs 125-05081 to 125-05080, HCM Segments 14 to 17			
Resulting time-based CAFs at bottleneck segment	13:00-13:15	0.05	0.53	0.17	1.00
	13:15-13:30	1.00	0.53	0.17	1.00
Resulting CAFs -- Statistics	Average	0.53	0.53	0.17	1.00
	Median	0.53	0.53	0.17	1.00
	Standard Deviation	0.67	0.00	0.00	0.00
Error Function		3376	5833	4998	5833

TABLE A-63: 4/29/2015 CAF RESULTS

Scenario		Time-Dependent	Average	HCM	Unadjusted
Bottleneck Location (TMC Segment)		125-05081			
FREEVAL Segment # and Type		Seg13, On Ramp			
Objective Function Domain		TMCs 125-05082 to 125-05081, HCM Segments 10 to 12			
Resulting time-based CAFs at bottleneck segment	20:30-20:45	0.11	0.37	0.17	1.00
	20:45-21:00	0.05	0.37	0.17	1.00
	21:00-21:15	0.94	0.37	0.17	1.00
Resulting CAFs -- Statistics	Average	0.37	0.37	0.17	1.00
	Median	0.11	0.37	0.17	1.00
	Standard Deviation	0.50	0.00	0.00	0.00
Error Function		4545	5502	5502	5502

TABLE A-64: 12/15/2015 CAF RESULTS

Scenario		Time-Dependent	Average	HCM	Unadjusted
Bottleneck Location (TMC Segment)		125-05081			
FREEVAL Segment # and Type		Seg13, On Ramp			
Objective Function Domain		TMCs 125N05083 to 125-05081, HCM Segments 7 to 12			
Resulting time-based CAFs at bottleneck segment	9:15-9:30	0.05	0.38	0.17	1.00
	9:30-9:45	0.11	0.38	0.17	1.00
	9:45-10:00	0.97	0.38	0.17	1.00
Resulting CAFs -- Statistics	Average	0.38	0.38	0.17	1.00
	Median	0.11	0.38	0.17	1.00
	Standard Deviation	0.51	0.00	0.00	0.00
Error Function		7037	13235	9853	17460

TABLE A-65: 11/7/2016 CAF RESULTS

Scenario		Time-Dependent	Average	HCM	Unadjusted
Bottleneck Location (TMC Segment)		125-05080			
FREEVAL Segment # and Type		Seg18, Basic			
Objective Function Domain		TMCs 125-05083 to 125-05080, HCM Segments 3 to 17			
Resulting time-based CAFs at bottleneck segment	9:45-10:00	0.05	0.60	0.17	1.00
	10:00-10:15	1.00	0.60	0.17	1.00
	10:15-10:30	0.75	0.60	0.17	1.00
Resulting CAFs -- Statistics	Average	0.60	0.60	0.17	1.00
	Median	0.75	0.60	0.17	1.00
	Standard Deviation	0.49	0.00	0.00	0.00
Error Function		37480	42010	41639	42010

TABLE A-66: 6/19/2018 CAF RESULTS

Scenario		Time-Dependent	Average	HCM	Unadjusted
Bottleneck Location (TMC Segment)		125-05083			
FREEVAL Segment # and Type		Seg3, Basic			
Objective Function Domain		TMC 125-05083 to 125-05083, HCM Segments 1 to 2			
Resulting time-based CAFs at bottleneck segment	12:15-12:30	0.14	0.46	0.17	1.00
	12:30-12:45	0.79	0.46	0.17	1.00
Resulting CAFs -- Statistics	Average	0.46	0.46	0.17	1.00
	Median	0.46	0.46	0.17	1.00
	Standard Deviation	0.46	0.00	0.00	0.00
Error Function		685	3519	3519	1837

Recurring Congestion Result

TABLE A0-67: CAF RESULTS OF RECURRING CONGESTION

Incident Date	CAF 1	CAF 2	CAF 3	CAF 4	CAF 5	CAF 6	CAF 7	CAF 8	Average CAF
2/27/2014	0.922581	0.877419	0.870968	0.877419	0.83871	0.980645			0.89
5/5/2014	0.806452	0.806452	0.8	0.806452	0.806452				0.81
6/24/2014	0.993548	0.96129	0.948387						0.97
4/22/2015	0.941936	0.980645	0.832258	0.883871	0.935484	0.948387			0.92
8/5/2015	0.941936	0.96129	0.948387	0.825806	0.948387	0.806452			0.91
8/11/2015	0.922581	0.987097	0.941936	0.974194	0.974194				0.96
4/5/2016	0.890323	0.864516	0.83871	0.877419	0.941936				0.88
4/26/2016	0.896774	0.929032	0.864516	0.8	0.974194	0.83871	0.974194		0.90
6/10/2016	0.922581	0.993548	0.806452	0.812903	0.806452				0.87
9/6/2016	0.825806	0.845161	0.916129	0.877419	0.987097				0.89
4/3/2017	0.974194	0.96129	0.980645	0.993548	0.974194				0.98
4/5/2017	0.980645	0.909677	0.948387	0.851613	0.967742	0.812903	0.987097		0.92
4/6/2017	0.954839	0.974194	0.825806	0.922581	0.896774	0.993548	0.987097		0.94
4/7/2017	1	0.993548	0.993548						1.00
4/10/2017	0.941936	1	0.993548	0.929032	0.883871	0.870968			0.94
4/11/2017	0.832258	0.851613	0.935484	0.851613					0.87
4/12/2017	0.993548	0.974194	1	0.974194	0.967742				0.98
4/13/2017	0.980645	0.896774							0.94
4/17/2017	0.954839	0.883871	0.967742	0.83871	0.993548	0.993548			0.94
4/21/2017	0.916129	0.8							0.86
4/26/2017	0.870968	0.851613	0.883871	0.877419	0.83871	0.845161	0.819355	0.812903	0.85
4/27/2017	0.987097	0.903226	0.980645	0.812903	0.980645	0.980645	0.864516	0.929032	0.93
3/26/2018	0.890323	0.870968	0.909677	0.851613	0.890323	0.980645			0.90
5/4/2018	0.870968	0.974194	0.896774	0.941936	0.929032	1			0.94
6/18/2018	0.896774	0.877419	0.83871	0.909677	0.993548	0.974194			0.92
6/19/2018	0.954839	0.896774	0.948387	0.993548	0.974194				0.95